Technical Report GL-98-16
August 1998

US Army Corps of Engineers
Waterways Experiment Station

Geophysical Site Characterization for UXO Background Studies: Fort Carson, Colorado; Fort A. P. Hill, Virginia; and Jefferson Proving Ground, Indiana

by Janet E. Simms, José L. Llopis, Dwain K. Butler, Lawson M. Smith

Prepared for Defense Advanced Research Projects Agency
U.S. Army Environmental Center

Technical Report GL-98-16
August 1998

Geophysical Site Characterization for UXO Background Studies: Fort Carson, Colorado; Fort A. P. Hill, Virginia; and Jefferson Proving Ground, Indiana

by Janet E. Simms, José L. Llopis, Dwain K. Butler, Lawson M. Smith

U.S. Army Corps of Engineers
Waterways Experiment Station
3909 Halls Ferry Road
Vicksburg, MS 39180-6199

Final report

Approved for public release; distribution is unlimited

Prepared for Defense Advanced Research Projects Agency
Arlington, VA 22202

U.S. Army Environmental Center
Aberdeen, MD 21010

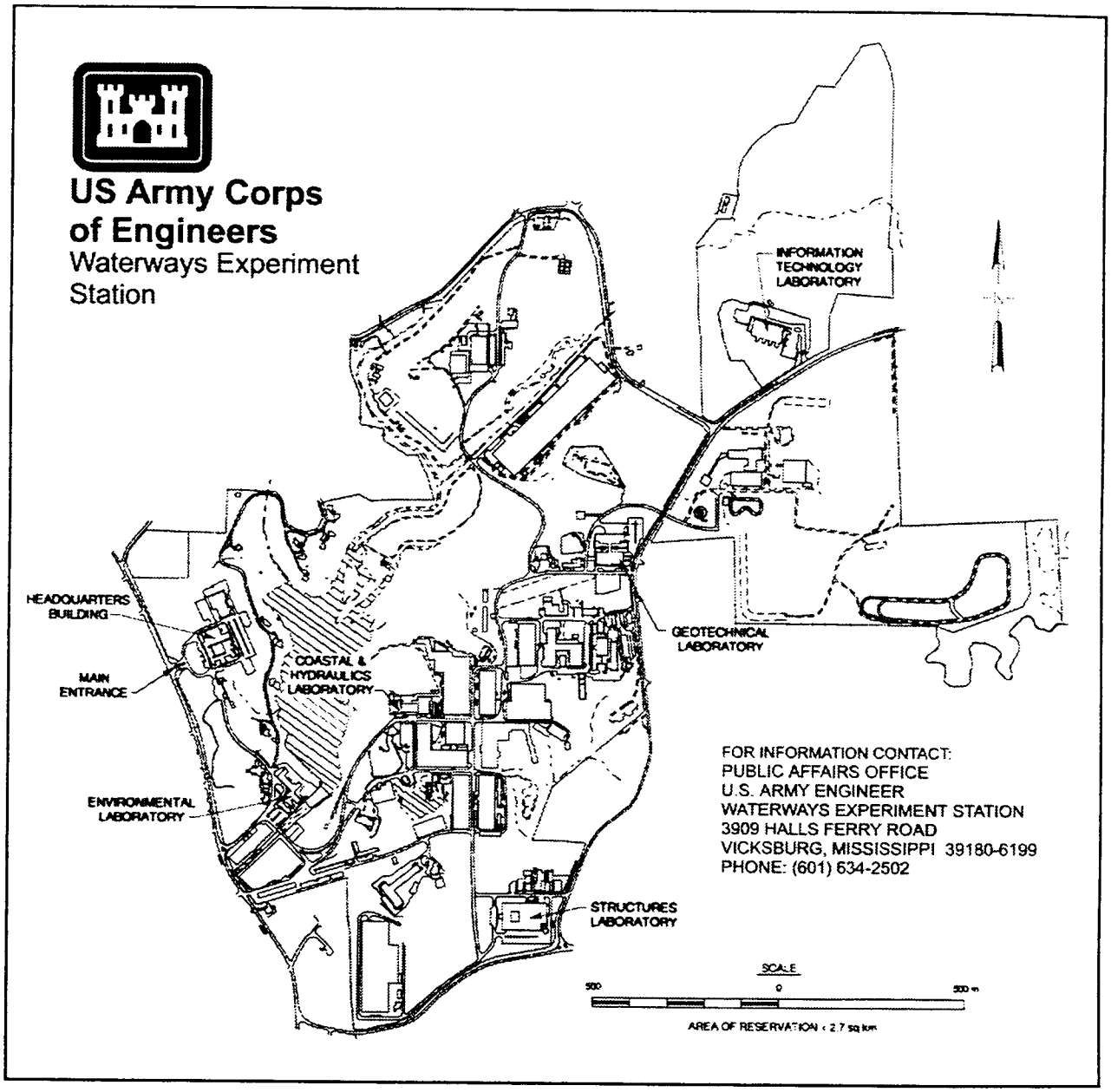

Waterways Experiment Station Cataloging-in-Publication Data

Geophysical site characterization for UXO background studies : Fort Carson, Colorado; Fort A.P. Hill, Virginia; and Jefferson Proving Ground, Indiana / by Janet E. Simms ... [et al.] ; prepared for Defense Advanced Research Projects Agency and U.S. Army Environmental Center.
489 p. : ill. ; 28 cm. — (Technical report ; GL-98-16)
Includes bibliographic references.

1. Land mines. 2. Mines (Military explosives) 3. Geophysics. 4. Ground penetrating radar — Military applications. I. Simms, Janet E. II. United States. Army. Corps of Engineers. III. U.S. Army Engineer Waterways Experiment Station. IV. Geotechnical Laboratory (U.S. Army Engineer Waterways Experiment Station) V. United States. Defense Advanced Research Projects Agency. VI. U.S. Army Environmental Center. VII. Series: Technical report (U.S. Army Engineer Waterways Experiment Station) ; GL-98-16.
TA7 W34 no.GL-98-16

Contents

Preface

Site characterization investigations were conducted at Fort Carson, Colorado; Fort A. P. Hill, Virginia; and Jefferson Proving Ground (JPG), Indiana, by personnel of the Geotechnical Laboratory (GL) and Environmental Laboratory (EL), U.S. Army Engineer Waterways Experiment Station (WES). The site characterizations were conducted over a 2-year period, 1996-1998. The investigations included measurements and surveys to determine geological, geophysical, and environmental parameters or properties and their variation with depth, lateral dimension, and time. The investigations at Fort Carson and Fort A. P. Hill were conducted for the Defense Advanced Research Projects Agency (DARPA), Arlington, VA, whereas those at JPG were part of the Science and Technology Program, Unexploded Ordnance (UXO) Technology Demonstration Phase IV Study overseen by the U.S. Army Environmental Center (USACE), Aberdeen Proving Ground, MD. The purpose of the study was to characterize the sites for comparison with other UXO/landmine test sites and to provide presite disturbance assessments of site heterogeneity (variability) and the presence of buried cultural features. Drs. Dwain K. Butler and Ernesto R. Cespedes were the WES Principal Investigators. Dr. Regina Dugan was the DARPA Program Manager. Ms. Kelly Rigano and Mr. George Robitaille were USACE Program Managers.

This report was prepared by Drs. Dwain K. Butler, Janet E. Simms, and Lawson M. Smith and Mr. José L. Llopis, Earthquake Engineering and Geosciences Division (EEGD), GL. Preliminary geologic evaluation of the DARPA sites was provided by Dr. Smith; geophysical field work was performed by Dr. Simms and Mr. Llopis; and soil samples were collected by GL and EL personnel. Soils testing and analysis were conducted by the Soil and Rock Mechanics Division, GL. Geophysical data analysis was performed by Drs. Butler and Simms and Mr. Llopis; and geologic interpretation (DARPA sites) was provided by Dr. Smith. The work was performed under the direct supervision of Mr. Joseph R. Curro, Jr., DARPA sites, and Dr. Mary Ellen Hynes, JPG site, Chiefs, Engineering Geophysics Branch, EEGD; and the general supervision of Drs. A. G. Franklin, DARPA sites, Chief, EEGD, Lillian Wakeley, JPG site, Acting Chief, EEGD, and William F. Marcuson III, Director, GL.

At the time of publication of this report, Director of WES was Dr. Robert W. Whalin. Commander was COL Robin R. Cababa, EN.

Conversion Factors, Non-SI to SI Units of Measurement

Non-SI units of measurement used in this report can be converted to SI units as follows:

Multiply	By	To Obtain
acres	4,046.873	square meters
feet	0.3048	meters
feet per second	0.3048	meters per second
gamma	1.0	nanotesla
miles (U.S. statute)	1.609347	kilometers
millimho per foot	3.28	millisiemen per meter

1 Introduction

Background Information

Location of buried landmines and unexploded ordnance (UXO) requires the application of surface geophysical techniques and/or very low-level airborne geophysical techniques to detect anomalies or signatures of the objects against a background. The geophysical techniques include magnetic methods, electromagnetic induction methods, ground penetrating radar (GPR) methods (wave propagation electromagnetic methods), microgravity methods, and various multi-spectral and infrared (IR) remote imaging methods. Since each of the detection methods listed respond to contrasts, changes or variations of physical properties or features, a multitude of geophysical sensor responses are a result of site characteristics. Site characteristics which produce sensor responses are called the background. The background is both site and time dependent and includes the effects of site geology, site physiography, vegetation, climatic variables, and any surface and buried cultural debris or engineered structures. Often, much of the surface and buried cultural debris will be the metallic remains of ordnance that has performed successfully (i.e., detonated as designed). The background at a site may be such that the geophysical signatures of landmines and UXO cannot be discriminated or detected against the background signature complex. Also, particular features of the background may produce signatures that are interpreted as caused by landmines or UXO, thus producing false alarms. For example, buried metallic debris can produce magnetic and electromagnetic signatures that look similar to the signatures of UXO. Also, buried metallic debris, tree roots, and large cobbles can produce GPR signatures that look similar to UXO.

For UXO remediation/cleanup based on geophysical surveys for UXO detection and location, the current levels of false alarms are a major limiting factor in cleanup effort and cost. Recent Technology Demonstrations (TDs) at Jefferson Proving Ground (JPG), Indiana, demonstrated the problems caused by the site background and associated false alarms in degrading the capability for landmine and UXO detection (Altshuler et al. 1995; Sparrow, Andrews, and Dugan 1995). In JPG TD Phase I (Sparrow, Andrews, and Dugan 1995), only one demonstrator had an ordnance detection ratio in excess of 60 percent (considering only the portion of the 40 acre area actually surveyed). Performance by demonstrators in JPG TD Phase II improved somewhat, with seven demonstrators having ordnance detection ratios in excess of 60 percent. The best performance in terms of ordnance detection ratio in Phase II was 85 percent, but that demonstrator had 4.7 false alarms per ordnance item detected. Even the best performer in terms of false alarms had 3.4 false alarms

per ordnance item detected. Much of the improved performance from Phase I to Phase II can be attributed to repeat demonstrators' improved knowledge of site conditions and generally improved positioning capability. Magnetic and electromagnetic induction systems were the most successful at JPG. GPR systems performed extremely poorly at JPG, both in terms of poor ordnance detection rates and high false alarm rates. Airborne systems were totally ineffective at JPG for both Phases I and II, with ordnance detection results statistically indistinguishable from random anomaly location (Altshuler et al. 1995).

The variability of soils, high soil moisture content, rough surface conditions, and large amounts of buried metallic debris at JPG provided a background against which ordnance detection and discrimination by the geophysical systems was difficult. Climatic variables, such as temperature and soil moisture content, and site surface condition variations (e.g., due to traffic or vegetation) are time-dependent background variables which can effect ordnance detection and false alarm rates. The site-(geologic and cultural components of background) and time-(climatic and surface condition changes) dependent background will vary from site to site. For a given site, while the geology is fixed, the geologic component of the background will have both fixed and time varying aspects, since the properties of geologic materials vary with moisture content and temperature. Site geology can be determined by geological investigations and geophysical surveys, and the impact of time varying properties, particularly of the very near-surface region, can be estimated or predicted. The cultural component of background, e.g., buried metallic debris, will depend on prior site use and may not be easily determined or predicted except by analogy with similarly used nearby sites.

In the context of classical radar target detection and other types of remote imagery, the background against which targets are detected is sometimes called "clutter." For problems such as detecting targets through a tree canopy or through atmospheric conditions with varying density and water content, empirical, analytical, and statistical clutter models have been developed which sometimes allow feature extraction and target discrimination against the clutter or background (e.g., Kreithen and Crooks 1990; Brown 1990). While the geophysical signatures of landmines and UXO can be predicted or modeled using analytical or numerical modeling procedures, there has been little study directed toward the development of background or clutter models to aid in reducing or mitigating the impact of false alarms in UXO and landmine detection and mapping efforts. The goal of the present effort is to begin to fill this void by collecting geophysical data at well documented test sites and investigating the feasibility of developing site clutter or background models, perhaps similar to clutter models used in remote imagery or to geostatistical models of heterogeneity and scale commonly used in the geosciences. This report documents the site selection criteria and geophysical site characterization.

Defense Advanced Research Project Agency (DARPA) Background Characterization Program

The present program was developed by DARPA in an effort to collect background or clutter data at test sites in a variety of geologic and geographic

settings. Data collection efforts are to involve all the geophysical methods and sensors commonly used or proposed for use for UXO and landmine detection. The program involves the following key aspects:

a. A criteria guided site selection process.

b. Thorough geologic, geophysical, and environmental characterization of the sites prior to any site disturbance.

c. Careful and accurate site layout to include a central portion for background/clutter measurements and sidebar areas for installation of landmine and UXO targets.

d. Well documented burial of registration targets, calibration targets, and landmine and UXO targets.

e. Development of a detailed data collection test plan, monitoring site, and target conditions (temperature, soil moisture, meteorological data) (George 1996).

f. Carefully documented and supervised data collection efforts by contractors using a single geophysical system at a time on each site.

g. Submittal of data in a standard and consistent format (George 1997).

h. Subsequent analysis of the data using advanced data processing and analysis tools.

Phase I of this program called for the selection of four 1-hectare (1 hectare = 100 × 100 m) sites at two locations in the U.S. (two sites at each of two locations). The site selection, site layout, site characterization, target acquisition and emplacement, and sensor navigation/location aspects of the program were managed for DARPA by the U.S. Army Engineer Waterways Experiment Station (WES), Vicksburg, MS, and the U.S. Army Night Vision Electronic Sensors Directorate (NVESD), Fort Belvoir, VA. WES and NVESD also managed contractor proposal evaluations and contract awards for three to four contractors each.

General and Logistical Site Selection Criteria

The following criteria guided the initial phase for site selection of four sites at two locations. These criteria address key issues of geology, physiography, and accessibility. While no known hazardous, toxic and radiological wastes (HTRW) and UXO should be on or buried at the sites, small amounts of buried cultural debris (metallic or otherwise) are acceptable as part of the background. The following criteria were viewed as guidelines rather than rigorous requirements:

DARPA Background Program
Site Selection Criteria

- Thick, relatively homogeneous soil (≅ 5 m)
- Minimal known ground disturbance
- Groundwater table at least 3 m deep
- Surface slopes < 5 percent
- No trees or other obstacles
- At least 120 × 120 m
- Readily accessible by all-weather road
- Area available for vehicle parking

– No known or suspected HTRW or UXO
– No large gullies, depressions, or water bodies
– No large vehicle traffic
– No overhead or underground utilities
– No metal fences, buildings, or other cultural features within 50 m

Site Selection Process

It was determined early in this program that one location for two of the test sites would be Fort A. P. Hill, Virginia. The soils at Fort A. P. Hill are well-drained sands (sandy loam) and, with an average of 107 cm (43 in.) precipitation yearly, the location is classified as "moist." Considering a simple site classification scheme that includes sand and clay as generic particle size and soil type classifiers and moist and dry as the soil moisture and climatic classifiers, military installations were considered for the remaining two test sites that would (a) provide contrasting site conditions to the Fort A. P. Hill site and (b) satisfy the general site selection criteria. Among the installations considered were Fort Hood, Texas, Fort Leonard Wood, Missouri, and Fort Carson, Colorado. Fort Hood was eliminated for logistical reasons. The following simple site classification diagram (Figure 1) guided the selection of Fort Carson, Colorado, for location of the remaining two sites.

SAND	**Fort A. P. Hill, VA**	**Fort Carson, CO**
CLAY	**Fort Leonard Wood, MO** **Jefferson Proving Ground, IN**	**Fort Carson, CO**
	MOIST	**DRY**

Figure 1. Selection considerations for research sites

As noted in the preceding diagram, both sand and clay sites can be found at Fort Carson and, with an average annual precipitation of 41 cm (16 in.), Fort Carson is classified as a dry location. JPG is indicated in the diagram (matrix) as a moist, clay location, and Fort Leonard Wood generally duplicates the conditions at JPG. Thus, for the simple classification scheme of moist or dry and sand or clay described above, the selections of appropriate sites at Fort A. P. Hill and Fort Carson complements the JPG TD sites and "fills in" the classification matrix. However, this assertion does not imply that the simple classification scheme includes the complete range of geologic variability and complexity likely to be encountered at UXO sites. Locations with possible UXO contamination exist that would be classified as "wet," such as Fort Polk, Louisiana, and as "very dry (arid)," such as Fort Irwin, California. Also, soil types exist at military facilities over the full range of gravels, sands, silts, clays, and mixtures. There are complex alluvial sites at Fort Carson, for example, with interfingered gravels, sands, and clays and isolated cobble-sized rocks in the soil. Sites with more extreme climatic conditions and complex geologies may be used for future background characterization studies.

The 1-hectare (ha) test site at JPG was established subsequent to the DARPA sites and following the TD Phase I-III studies at JPG. A thorough characterization of the 40- and 80-acre sites at JPG was not performed prior to UXO emplacement at these sites (PRC Environmental Management, Inc. 1996). Since additional UXO backgrounds characterization studies were to be conducted at JPG, it was deemed beneficial to establish a 1-ha test site at JPG similar to the DARPA sites. The basic guidelines and procedures used to establish the DARPA sites were followed at the JPG 1-ha site.

Site Characterization Objectives and Approach

This report documents the site characterization efforts at the four sites selected for the DARPA Background Characterization Program and the JPG 1-ha test site. Site characterizations were performed to (a) provide qualitative information to compare and contrast the sites selected, (b) provide electromagnetic property information relevant to contractor GPR surveys, (c) provide information to complement later sensor data analyses, (d) benchmark site characteristics for comparison to past and future sensor performance tests, and (e) provide initial estimates of sensor results (magnetic, electromagnetic induction, and GPR) as a benchmark to compare to contractor sensor data. The general results of the site characterization were provided to all contractors involved in the program for their planning purposes and subsequent use for self-analyses of results. The site characterization work was performed prior to any disturbance of the sites by installation of buried registration targets, UXO, and landmines, and prior to any measurements by contractors.

General objectives of the site characterization efforts were to determine site-specific details of subsurface geology, determine geophysical parameters, assess general site heterogeneity and scale, and detect buried cultural features or objects. The approach to achieve these objectives included geologic investigations, soil sampling and analyses, and geophysical surveys. In addition to the geologic and geophysical investigations, topographic surveys, vegetation surveys, and environmental monitoring were conducted; this report will concentrate on results of the geologic and geophysical investigations.

Scope of Report

Review of the regional geology of the Fort A. P. Hill, Fort Carson, and JPG areas and site-specific geologic details of the test sites are presented in Chapter 2. Chapter 3 presents details of the site characterization plan, concepts of the geophysical methods, and field survey procedures. Results of the geophysical surveys are presented and interpreted in Chapter 4, and conclusions are outlined in Chapter 5. Data compilations of the soil sampling analyses and geophysical surveys are presented in Appendices A through O.

2 Geology

Introduction

The research goals of the project require that test sites be selected that are significantly different in terms of site characteristics which may influence the ability of various geophysical methods to detect and identify potential UXOs. The test sites should include sites that have predominantly sandy soils and those that have clayey soils. Additionally, the different sites should reflect the significance of the variation in climate (primarily moisture regime) and man-made contamination on the detection system performance. Consequently, it was determined that optimally there would be four sites (in addition to the JPG site), two each in humid and semi-arid settings. In each climatic setting, the two sites should reflect a sandy site and a clayey site.

After review of existing regional geologic and climatic data for Department of the Army (DA) installations in the U.S., two installations were chosen for the establishment of the four research sites. These installations are Fort Carson, Colorado, and Fort A. P. Hill, Virginia (Figure 1). The two sites at Fort Carson represent sandy and clayey soil sites in a semi-arid regime. The two sites at Fort A. P. Hill represent sandy soil sites in a humid climate region. These four sites complement the general soil-climate classification of Jefferson Proving Ground, which is "clayey" soil in a humid region.

Surface soil samples were collected at five locations, and soil samples at depths of 0, 0.5, and 1 m were collected at five other locations at both sites on Fort Carson and Fort A. P. Hill. Surface soil samples were not collected at JPG, however a sample was taken at 0 or 10 cm depth at all seven locations, and samples at depth collected at four of those locations. The locations of the soil samples were specified by DARPA and are listed below. The coordinate locations correspond to the individual grid sites, which are generally 125 x 100 m. The surface soil samples were classified based on the U.S. Department of Agriculture (USDA) soil classification procedure. The USDA textural classification diagram is reproduced in Figure 2. Moisture contents were measured for all samples. A sieve analysis was performed on the surface soil samples, and both a sieve analysis and hydrometer analysis were performed on two soil samples collected at each site within the center square (100 x 100 m area) at Fort Carson and Fort A. P. Hill. A sieve analysis was performed on all of the soil samples collected at JPG. The sieve analysis provides

Surface Soil Samples Fort Carson, Fort A. P. Hill	Soil Samples Collected at Depth Fort Carson, Fort A. P. Hill, JPG	Soil Samples at 10 cm JPG
(27.5E, 73N)	(0E, 60N) FP 20	(40E, 23N)
(40E, 23N)	(2E, 60N) FP22	(52.5E, 85.5N)
(52.5E, 85.5N)	(8E, 17N) Seabee, Turkey Creek	(77.5E, 60.5N)
(65E, 10.5N)	(27.5E, 73N)	
(77.5E, 60.5N)	(65E, 10.5N)	
	(122E, 8N)	
	(123E, 97N)	

gradation information on the coarse fraction (> 0.075 mm), whereas the hydrometer analysis evaluates the finer material. The soil gradation boundaries used in the sieve and hydrometer analysis are based on the Unified Soil Classification System (USCS) (Table 1). The USCS provides both gradation and plasticity information about a soil, and differs with the USDA system on the particle size boundaries used to classify a soil (for example, USDA: 0.05 mm $\leq$ sand $\leq$ 2.00 mm; USCS: 0.075 mm $\leq$ sand $\leq$ 4.75 mm). Tabulated results of the laboratory analyses and plots of the soil gradation curves are provided in Appendices A, D, G, J and M for the Fort Carson (Seabee and Turkey Creek), Fort A. P. Hill (Firing Point 20 and Firing Point 22) and JPG sites, respectively.

In the following paragraphs, a general description of the regional setting of Fort Carson, Fort A. P. Hill, and Jefferson Proving Ground is provided. Additionally, a detailed description of each of the sites at each installation is given.

Fort Carson Research Sites

Fort Carson is located at the foot of the Rocky Mountains in central Colorado. The complex geologic history of the area has resulted in the occurrence of a wide variety of geologic materials at and near the surface (Figure 3). The highly variable geologic conditions at provided an opportunity to look at many different "sandy" and "clayey" settings for potential research sites.

Much of the landscape of Fort Carson dips from west to east, consisting of large alluvial fans and eastward dipping bedrock foothill ramps. The alluvial fans consist of material eroded from the sedimentary and igneous rocks of the steep Rampart Range which rise in elevation from about 1830 meters Mean Sea Level (M.S.L.) to almost 3050 meters immediately west of the installation. The fans and alluvial channels are separated by erosional remnants of bedrock tilted up to the west as the Rocky Mountains were thrust upward, also creating topographic ramps down to the Great Plains east of the installation.

Landslides and earthflows on the steep slopes along the north-south trending mountain front, active mountain building and seismicity, and changes in climate have produced a landscape that is characterized by a number of large-scale geomorphic features. These processes, including rapid erosion and deposition, landslides, uplift and subsequent deep weathering of underlying sediments, have been important in creating the settings of the two research sites.

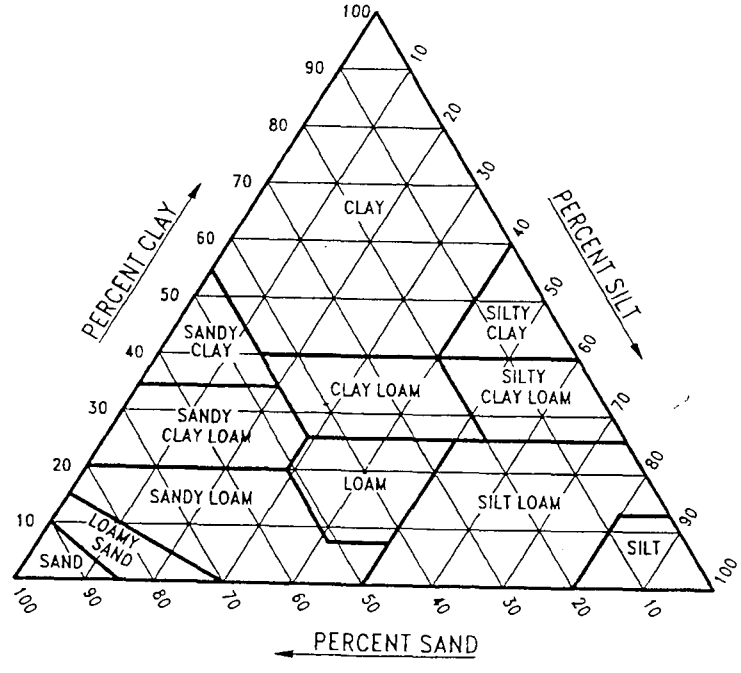

Figure 2. USDA soil classification diagram

Table 1
Unified Soil Classification System

Criteria for assigning soil symbols and descriptions				Soil Classification	
				Symbol	Description
Coarse grained soils, ≥ 50% retained on No. 200 sieve	Gravels, ≥ 50% coarse fraction retained on No. 4	< 5%* fines	$^{**}C_u \geq 4$ and $1 \leq {}^{***}C_c \leq 3$	GW	Well graded gravel
			$C_u < 4$ and/or $1 > C_c > 3$	GP	Poorly graded gravel
		> 12%* fines	Fines ML/MH	GM	Silty gravel
			Fines CL/CH	GC	Clayey gravel
	Sands, ≥ 50% coarse fraction passes No. 4	< 5%* fines	$C_u \geq 6$ and $1 \leq C_c \leq 3$	SW	Well graded sand
			$C_u < 6$ and/or $1 > C_c > 3$	SP	Poorly graded sand
		> 12%* fines	Fines ML/MH	SM	Silty sand
			Fines CL/CH	SC	Clayey sand
Fine grained soils, ≥ 50% passing No. 200 sieve	Silts and clays, LL ≤ 50	Inorganic	Above *A* line†	CL	Lean clay
			Below *A* line†	ML	Low compressibility silt
		Organic	$\frac{\text{Oven dried } LL}{\text{Original } LL} < 0.75$	OL	Organic silt or clay
	Silts and clays, LL ≥ 50	Inorganic	Above *A* line†	CH	Fat clay
			Below *A* line†	MH	High compressibility silt
		Organic	$\frac{\text{Oven dried } LL}{\text{Original } LL} < 0.75$	OH	Organic clay or silt
Highly organic soils		Dark, odorous organic matter		Pt	Peat

*5 to 12 percent, use dual symbol †Hatched zone, use dual symbol $^{**}C_u = D_{60} / D_{10}$ $^{***}C_c = (D_{30})^2 / (D_{10} \times D_{60})$

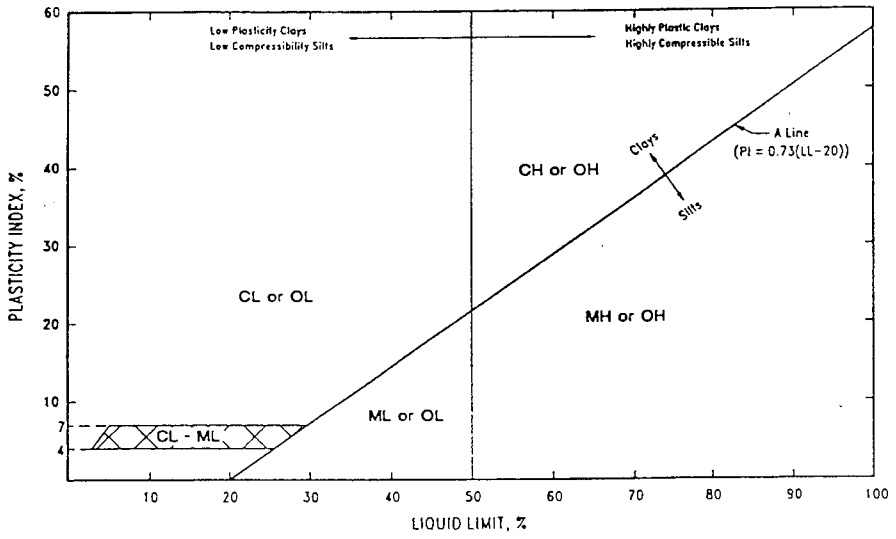

Plasticity chart.

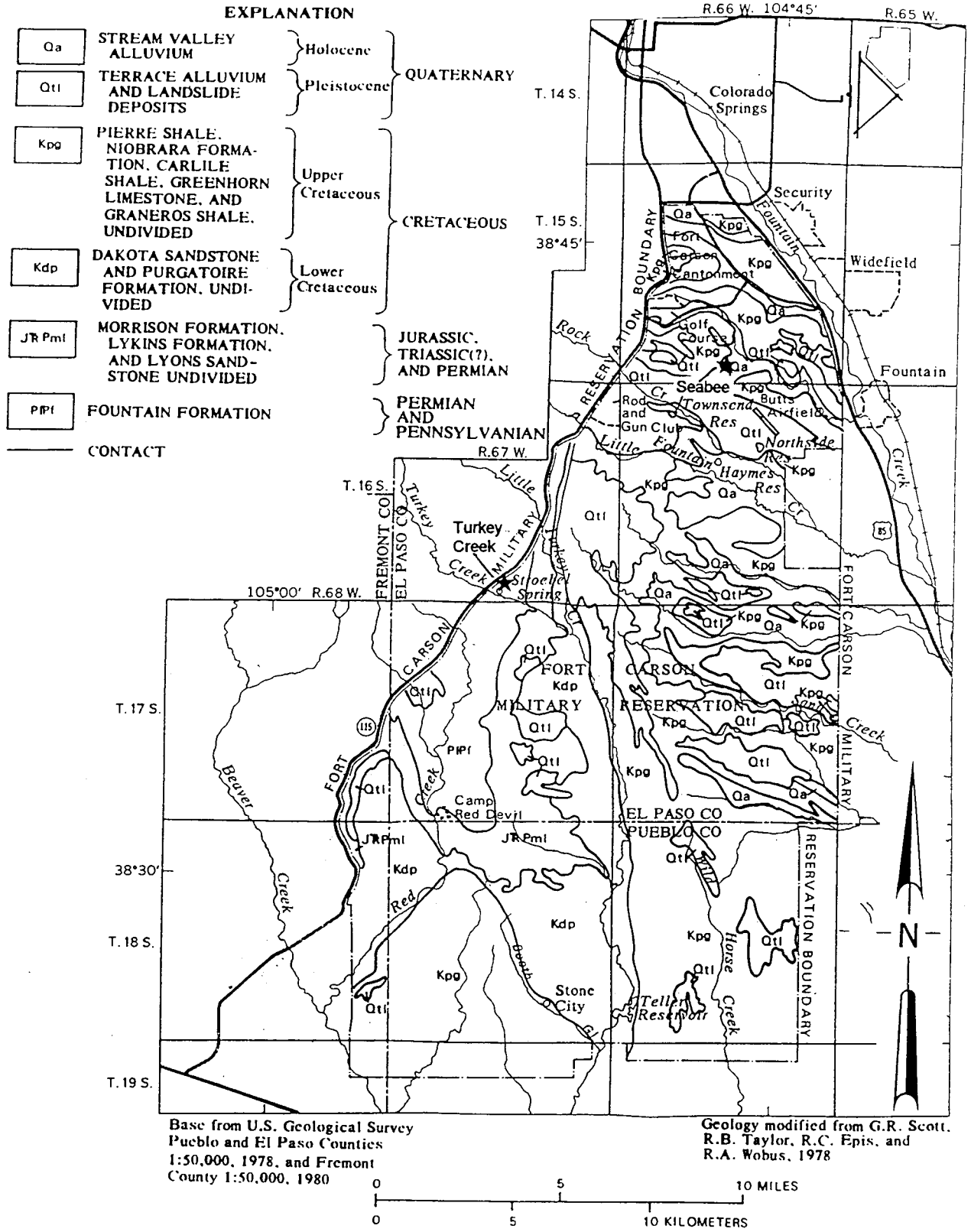

Figure 3. Generalized surficial geologic map, Fort Carson, Colorado (after Leonard 1984)

The age of surficial geologic units generally decreases from west to east across Fort Carson (Figure 4). The western boundary of the installation occurs on the eastern flank of the Rampart Range and consists primarily of the Paleozoic Fountain Formation. Outcropping sedimentary strata include Permian, Triassic, Jurassic, Cretaceous, and Quaternary age rocks, respectively to the east as these broad, deep formations are warped up and exposed on the eastern face and rampart of the Rockies. Draped across this west to east ramp are thick wedges of alluvial deposits In the form of alluvial fans and stream valleys.

Soils (pedogenic) of Fort Carson, a function of the complex geologic and climatic history of the area, are expectedly highly variable, but significantly related to underlying geologic units. Clayey soils occur primarily on outcrops of the Pierre Shale. Scattered clayey soils also occur on the clayey facies of the Morrison Formation (Jurassic) and overlying alluvial (stream) deposits, but are highly unpredictable. Sandy soils are found on most alluvial surfaces (fans, colluvial slopes, stream valleys, and landslide deposits) and on the Fountain (Pennsylvanian), Lyons (Permian), Lykins (Triassic), and Dakota (Lower Cretaceous) Formations (from west to east).

The climate of Fort Carson is typically semi-arid/temperate. Average annual precipitation is 400 millimeters (mm) with May usually the wettest month (mean May precipitation is 79 mm) and December the driest month (mean December precipitation is 7.6 mm). The Fort Carson area averages 110 days per year with measurable (0.25 mm) precipitation and 40 days per year with 25 mm or more snowfall. Annual average evaporation is approximately 1400 mm at Fort Carson.

Like the annual moisture regime, temperature is also highly variable through the year. July is the warmest month with a mean temperature of 28.9 degrees (Celcius) and January is the coldest month, averaging 5 degrees. The Fort Carson area averages about 200 days per year with freezing temperatures. Daily temperatures can fluctuate significantly (often more than 20 degrees), particularly in the fall and spring months. The area is often sunny, averaging more than 3000 hours of sunshine per year, with July being the sunniest month (300 hours) and December the cloudiest (170 hours sunshine).

Seabee site description

The Seabee site occurs on an upland surface of an outcrop of the upturned Pierre Shale. The site is located in the SE1/4, SE1/4, NE1/4, Section 33, Range 66 west, Township 15 south (map coordinate 193836 on the Mount Big Chief 1:50,000 Defense Mapping Agency (DMA) quadrangle) on a small eastward sloping shelf, surrounded by low hills eroded in the Cretaceous shale (Figures 5 and 6). The average elevation of the site is 1752 m M.S.L. (from the Cheyenne Mountain 1:24,000 U.S. Geological Survey (USGS) 7.5 minute quadrangle). Surface topographic features are few and almost imperceptible to casual inspection, since the site is covered by thick, tall grasses.

The shelf the site occupies appears to be the product of long term weathering of a surficial sandy clay-shale that is relatively resistant to erosion. Active geomorphic (land modifying) processes appear to be restricted to the slow weathering of the

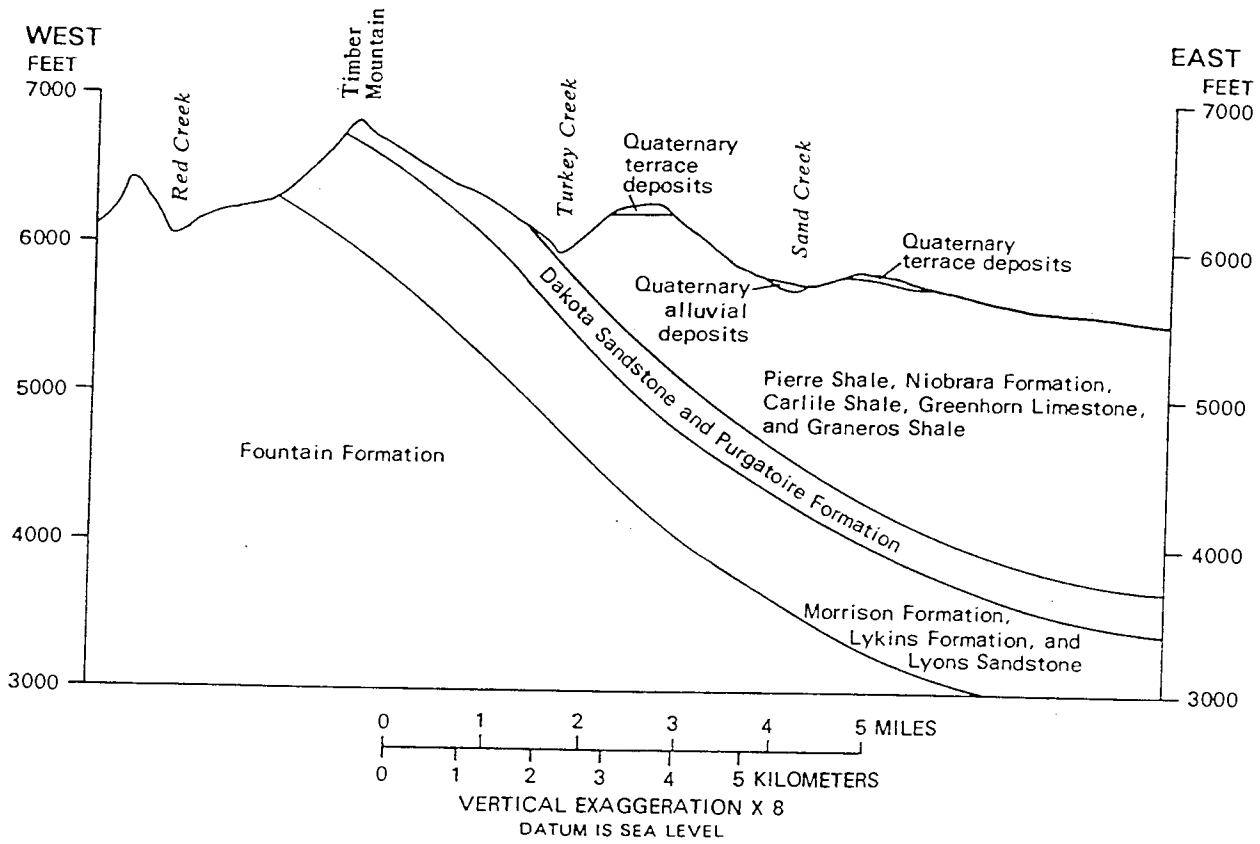

Figure 4. Generalized geologic section, Fort Carson, Colorado (after Leonard 1984)

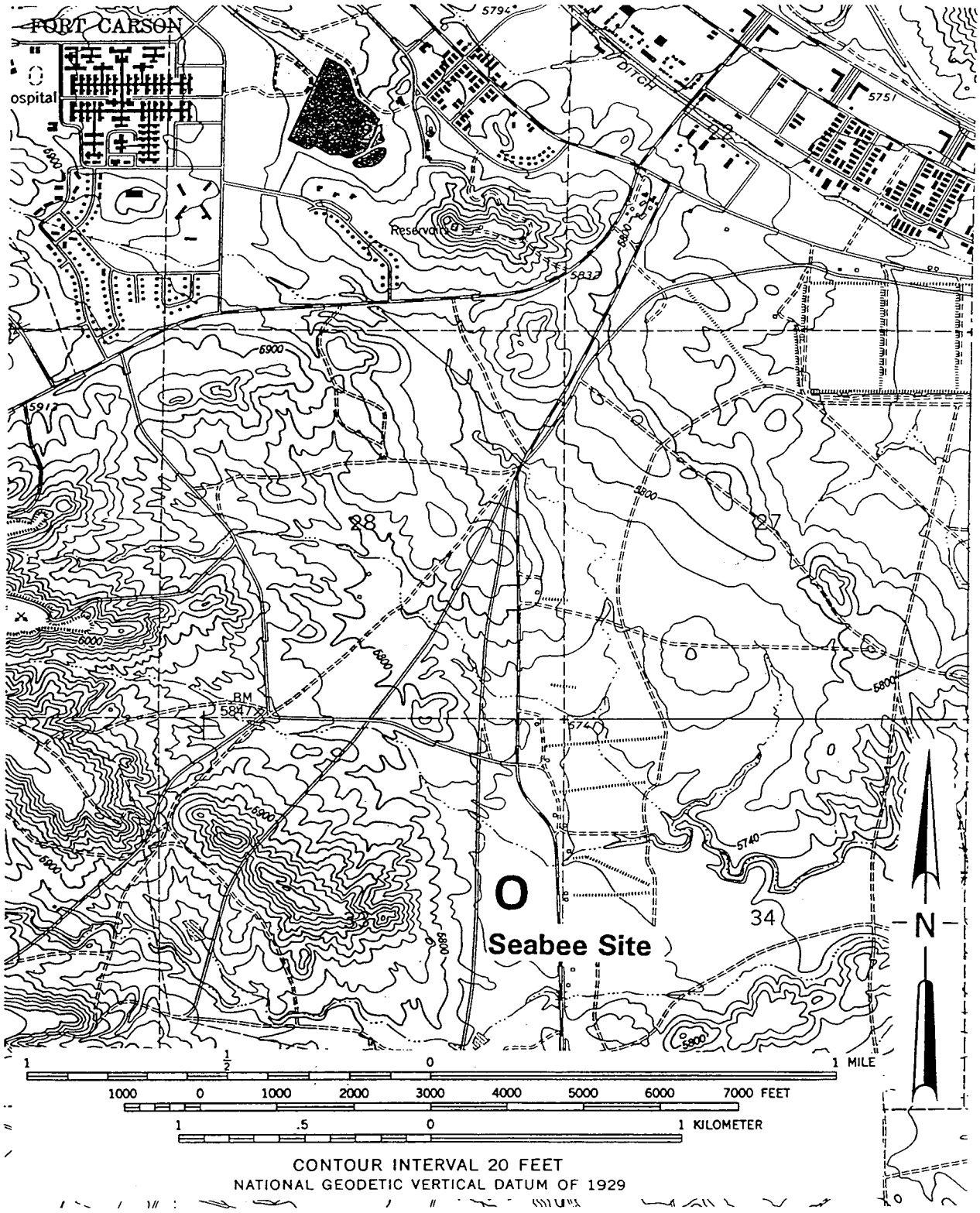

Figure 5. Location of the Seabee site, Fort Carson, Colorado (Mount Big Chief 1:50,000 DMA quadrangle)

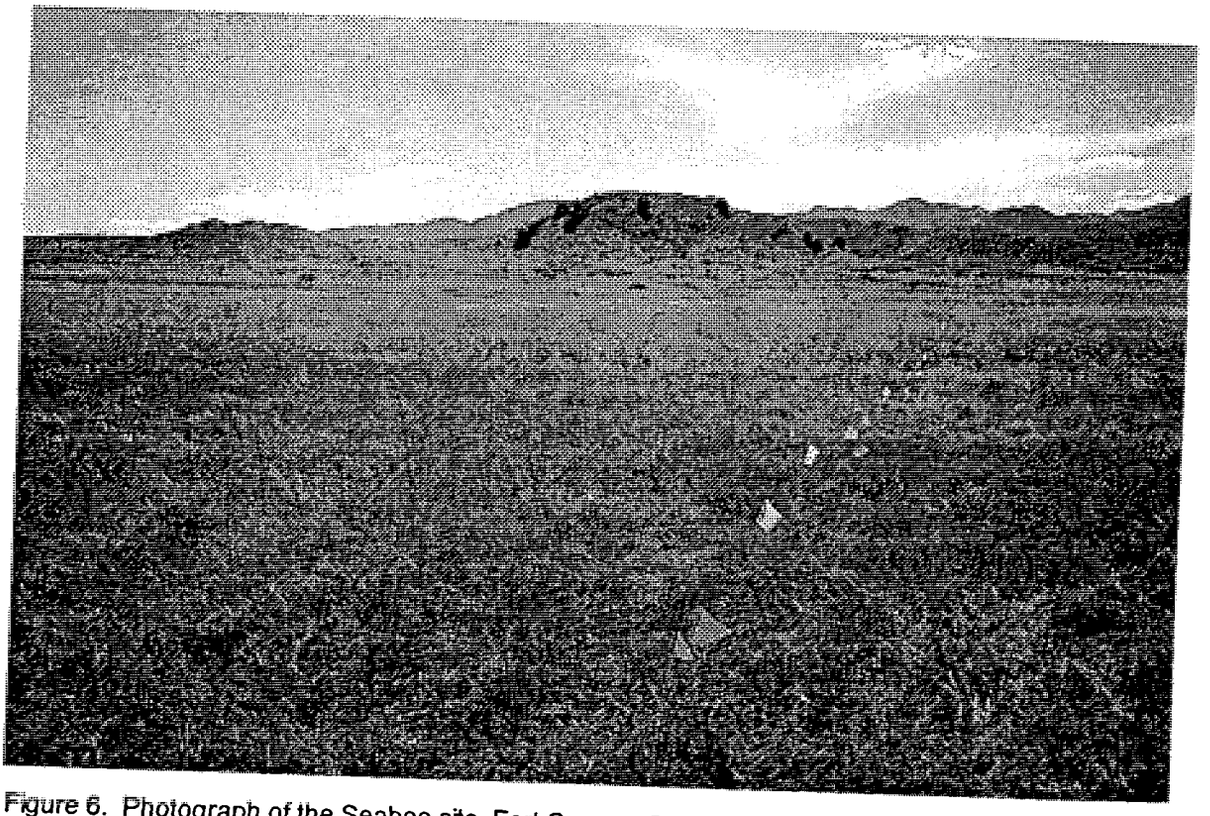

Figure 6. Photograph of the Seabee site, Fort Carson, Colorado

Pierre Shale with almost no deposition or surface soil erosion.

Weathering of the Pierre Shale at the Seabee site has produced a sandy clay soil (CL) which is fairly homogeneous both horizontally and vertically (up to one meter in depth) over the site (Table 2). Samples taken at several locations at depths of 0, 0.5, and 1.0 meters are consistently classified as a "CL" (clay, liquid limit < 50) by the Unified Soil Classification System (USCS) and a "silt-loam" (silt, with significant sand and clay) by the USDA soil classification system (Table 3). Field observations of the soil reveal that it is generally dense, dark grayish brown, moist to slightly moist (Table 4), and exhibits granular to subangular blocky to prismatic soil structure with depth. Stratigraphic units deeper than one meter were not sampled, so the actual thickness of the soil weathered from the underlying Pierre Shale is not known. Previous geologic (Leonard 1984; Jenkins 1964) and soil investigations (Soil Conservation Service 1981) state that residual soils developed in the Pierre Shale typically are 0.75 to 1.22 m deep above fractured sandy clay shale. The material beneath the weathered zone is usually a dark gray to blue sandy shale with calcareous concretions. Limestone "cores" on the order of 15 m in diameter occur in the uppermost part of the Pierre Shale. When the sandy shale around the cores erodes, small conical hills called "tepee buttes" are formed. There are no tepee buttes in the vicinity of the Seabee site, but there may be large limestone inclusions and concretions at depth in the Pierre Shale or overlying sediments that might give anomalous geophysical signatures. The thickness of the Pierre Shale at the Seabee site is approximately 830 m (Jenkins 1964).

Surface water drainage of the Seabee site is moderate to good where the surface slope is sufficient to provide expedient runoff. The permeability of the clayey soil is predictably very low and soil moisture drainage occurs primarily along discontinuities. The water table is probably greater than 15 m below the ground surface throughout the year.

Turkey Creek site description

The Turkey Creek site is about 13 kilometers southwest of the Seabee site on the western boundary of Fort Carson (Figures 7 and 8). The site is situated on the foot slopes of Mount Pittsburg of the Rampart Range which rises 550 m above the site. The foot slope is formed in the Pennsylvanian Fountain Formation which is sharply upturned to the west by the rising of the Rampart Range (Figure 4). The site is located in the SW1/4, SW1/4, NW1/4, Section 34, Range 67 west, Township 16 south (map coordinate 102739 on the Mount Big Chief 1:50,000 DMA quadrangle). The average elevation of the site is approximately 1950 m M.S.L. (from the Mount Pittsburg 1:24,000 USGS 7.5 minute quadrangle). Surface topographic features are minimal.

Landscape evolution at the Turkey Creek site appears to be the product of long term weathering of the underlying Fountain sandstone interrupted by occasional small landslides and earth flows. The scattered gravels that were found in the soil samples (Table 5) are most likely the result of down slope movement of colluvium from Mount Pittsburg. Steeper surface slopes at the site have also undoubtedly resulted in soil erosion as a product of agricultural disturbance of the soil during the historic period.

Table 2
Summary of Sieve Analysis, Seabee Site, Fort Carson, CO

Location	Depth (m)	Classification	Color	% Gravel	% Sand	% Fines	PI*	LL**	PL***	Moisture Content
27.5E, 73N (Reg. 1-1)	0	Sandy clay, CL	Gray	0	22.4	77.6	18	42	24	23.1
	0.5	Sandy clay, CL	Gray	0.1	14.9	84.9	23	38	15	17.8
	1	Sandy clay, CL	Gray	0	16.7	83.3	17	32	15	16.0
65E, 10.5N (Reg. 4-1)	0	Sandy clay, CL	Gray	0	2.5	97.5	16	38	22	24.5
	0.5	Sandy clay, CL	Gray	0	21.1	78.9	22	37	15	19.4
	1	Sandy clay, CL	Gray	0	18.5	81.5	18	33	15	17.9
27.5E, 73N	upper 10 cm	Sandy clay, CL	Gray	0	22.5	77.5	17	34	17	14.7
40E, 23N	upper 10 cm	Sandy clay, CL	Gray	0	25.7	74.3	17	33	17	17.6
52.5E, 85.5N	upper 10 cm	Sandy clay, CL	Gray	0	18.8	81.2	18	36	18	19.4
65E, 10.5N	upper 10 cm	Sandy clay, CL	Gray	0	29.9	70.1	15	35	20	21.2
77.5E, 60.5N	upper 10 cm	Sandy clay, CL	Gray	0	19.5	80.5	21	39	18	18.1

*Plasticity Index PI = LL - PL **Liquid Limit ***Plastic Limit

Table 3
USDA Soil Classification, Seabee Site, Fort Carson, CO

Location	Depth (m)	Texture	Munsell Color	Chroma & Hue
27.5E, 73N	Upper 10 cm	silt loam	dark grayish brown	2.5Y 4/2
40E, 23N	Upper 10 cm	silt loam	dark grayish brown	2.5Y 4/2
52.5E, 85.5N	Upper 10 cm	silty clay loam	dark grayish brown	2.5Y 4/2
65E, 10.5N	Upper 10 cm	silty clay loam, a few pebbles 1-2 cm diameter.	dark grayish brown	2.5YR 4/2
77.5E, 60.5N	Upper 10 cm	silty clay loam	dark grayish brown	2.5Y 4/2

Table 4
Soil Sample Moisture Contents, Seabee Site, Fort Carson, CO

Depth (m)	Location				
	8E, 17N (Red 6)	27.5E, 73N (Reg. 1-1)	65E, 10.5N (Reg. 4-1)	122E, 8N	123E, 97N
0	15.5	23.1	24.5	19.9	15.8
0.5	18	17.8	19.4	22.2	18.7
1	17.1	16	17.9	20.6	18.1

Unlike the homogeneous soils of the Seabee Site, the variation in thickness and lateral continuity of the soil texture at the Turkey Creek site is significant. This variability is due to the relatively high permeability and local heterogeneity of the underlying parent material, and the contribution of sediment to the site from up slope. Samples taken at several locations at depths of 0, 0.5, and 1.0 meters classify as a "CL" (clay, low liquid limits) or "SC" (sandy clay) by the USCS (Table 5) and a sandy loam or sandy clay loam in the USDA soil classification system (Table 6). Examination of the soil on the site reveal that it is primarily friable, reddish brown, slightly moist to dry (Table 7), and exhibits granular to subangular blocky soil structure with depth.

Like the Seabee site, stratigraphic units of the Turkey Creek site deeper than one meter were not sampled, so the actual thickness of the soil weathered from the underlying Fountain Formation is not known. Previous soil investigations (SCS 1981) in the immediate vicinity of the site show residual soils developed in the Fountain Formation in a similar landscape position are typically highly variable in thickness, ranging from 0.25 to 1.50 m. The material beneath the weathered (soil) zone is usually a red arkosic medium to coarse grained moderately indurated sandstone and/or conglomerate (McLaughlin 1947). The total thickness of the Fountain Formation beneath the Turkey Creek site is probably in excess of 600 m.

Surface water drainage of the Turkey Creek site is good to very good. The permeability of the sandy soil is moderate to high except in the areas where the

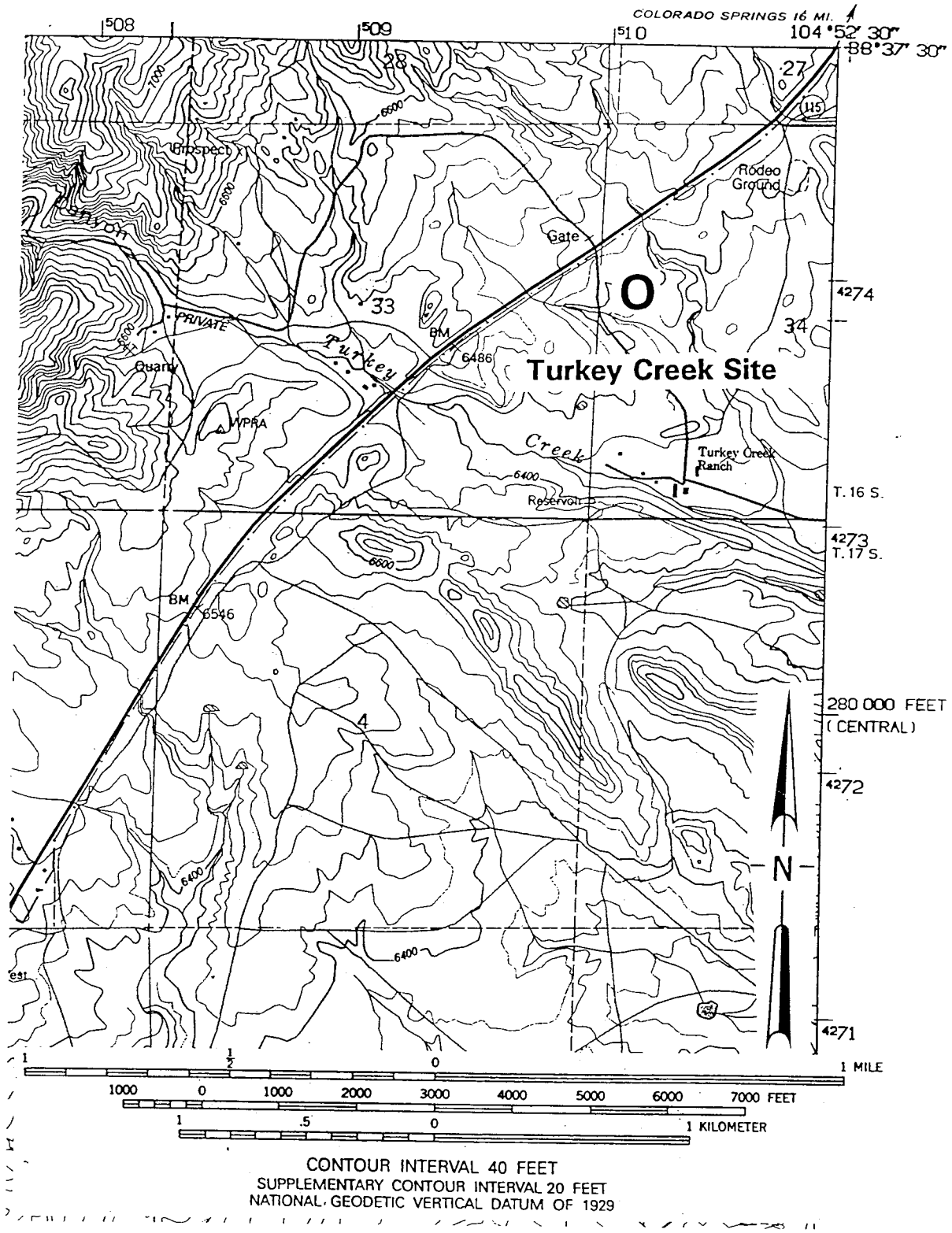

Figure 7. Location of the Turkey Creek site, Fort Carson, Colorado (Mount Big Chief 1:50,000 DMA quadrangle)

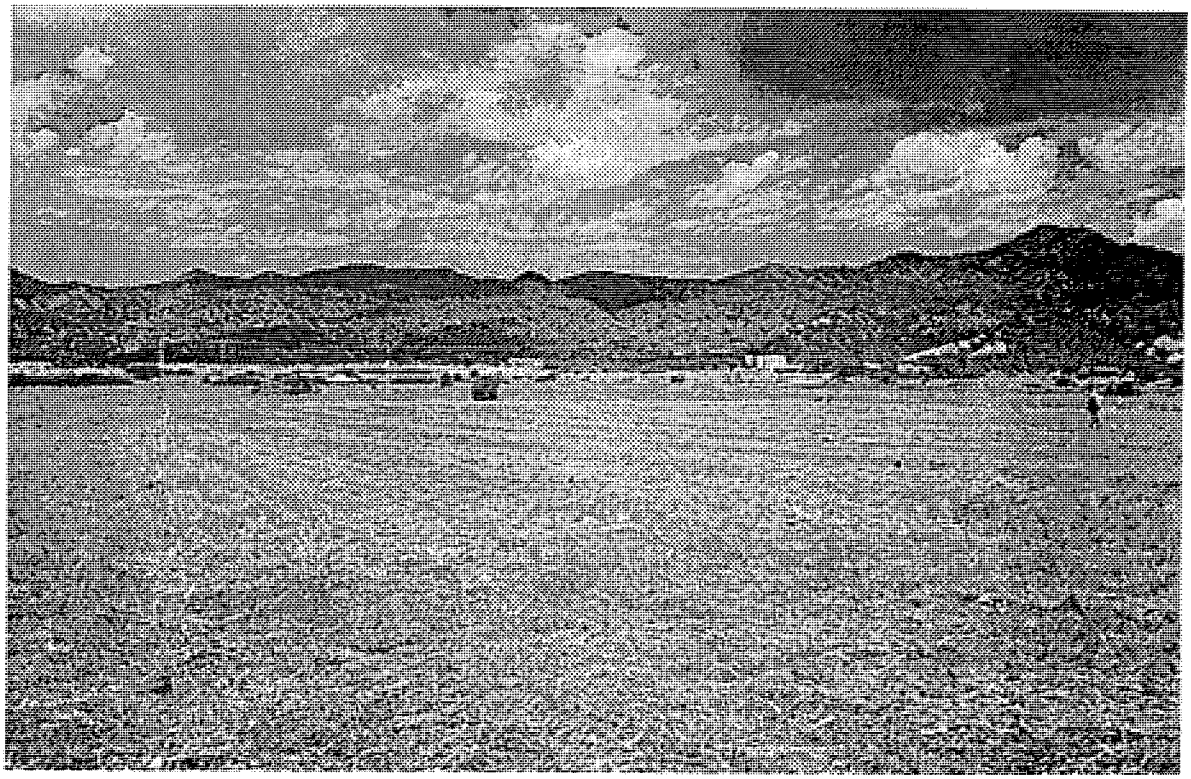

Figure 8. Photograph of the Turkey Creek site, Fort Carson, Colorado

Table 5
Summary of Sieve Analysis, Turkey Creek, Fort Carson, CO

Location	Depth (m)	Classification	Color	% Gravel	% Sand	% Fines	PI*	LL**	PL***	Moisture Content
27.5E, 73N (Reg. 1-1)	0	Sandy clay, CL	Brown	0.5	47.1	52.4	17	33	16	12.3
	0.5	Sandy clay, CL	Brown	0.7	27.9	71.5	23	40	17	17.4
	1	Sandy clay, CL	Brown	0.4	28	71.7	22	37	15	14.4
65E, 10.5N (Reg. 4-1)	0	Clayey sand w/ gravel SC	Brown	7.8	49.7	42.5	12	27	15	9
	0.5	Sandy clay, CL	Brown	0.4	28.9	70.7	23	39	16	16
	1	Sandy clay, CL	Brown	1.4	25.7	72.9	21	38	17	12.5
27.5E, 73N	upper 10 cm	Clayey sand, SC	Brown	0	56	44	13	29	16	7.4
40E, 23N	upper 10 cm	Clayey sand, SC	Brown	0	53.6	46.4	13	27	14	6.5
52.5E, 85.5N	upper 10 cm	Sandy clay, CL	Gray	0	38.5	61.5	12	28	16	9
65E, 10.5N	upper 10 cm	Clayey sand, SC	Brown	0	53.6	46.4	10	26	16	7.1
77.5E, 60.5N	upper 10 cm	Sandy clay, CL	Brown	0	40.5	59.9	14	30	16	10.4

*Plasticity Index PI = LL - PL **Liquid Limit ***Plastic Limit

Table 6
USDA Soil Classification, Turkey Creek, Fort Carson, CO

Location	Depth (m)	Texture	Munsell Color	Chroma & Hue
27.5E, 73N	upper 10 cm	sandy loam	dark reddish brown	5YR 3/4
40E, 23N	upper 10 cm	sandy loam, 1 pebble ~1 cm diameter	reddish brown	5YR 4/4
52.5E, 85.5N	upper 10 cm	sandy clay loam	reddish brown	5YR 4/4
65E, 10.5N	upper 10 cm	sandy loam, a few pebbles 1-2 cm diameter	reddish brown	5YR 4/4
77.5E, 60.5N	upper 10 cm	sandy loam	reddish brown	5YR 4/4

Table 7
Soil Sample Moisture Contents, Turkey Creek, Fort Carson, CO

Depth (m)	Location				
	8E, 17N (Red 6)	27.5E, 73N (Reg. 1-1)	65E, 10.5N (Reg. 4-1)	122E, 8N	123E, 97N
0	9.9	14.4	9	9.4	11.6
0.5	16.7	17.4	16	18.2	16.6
1	12.4	12.3	12.5	15.7	6

pedogenic clay units occur in the subsurface. The water table is greater than 15 m below the surface throughout most of the year but small localized perched groundwater lenses may occur in the upper 6 m.

Fort A. P. Hill Research Sites

General description

Fort A. P. Hill is situated on the Atlantic Coastal Plain of northeastern Virginia. The Atlantic Coastal Plain was formed over the last several tens of millions of years by the relative rise and fall of sea level and the subsequent transgression and regression of the Atlantic Ocean over the shelf of eastern Virginia. Unlike the rocky and steep ridges and valleys of central and western Virginia, the topography of the coastal plain may be described as undulating low hills separated by the floodplains of low gradient streams. The Atlantic Coastal Plain is dissected by several large rivers, one of which, the Rappahannock, is only 5.5 km north of the research sites. The Rappahannock flows into Chesapeake Bay approximately 100 km southeast of the research sites. Tidal influences on the Rappahannock extend upstream past the research sites.

The landscape of Fort A. P. Hill is relatively homogeneous, consisting primarily of low hills separated by small stream valleys (Figure 9). Hill crest elevations generally decrease from west to east, from a maximum of about 70 meters in the northeastern periphery to approximately 55 meters on the southeastern boundary. The generally sandy nature of surficial soils offer little resistance to erosion, a

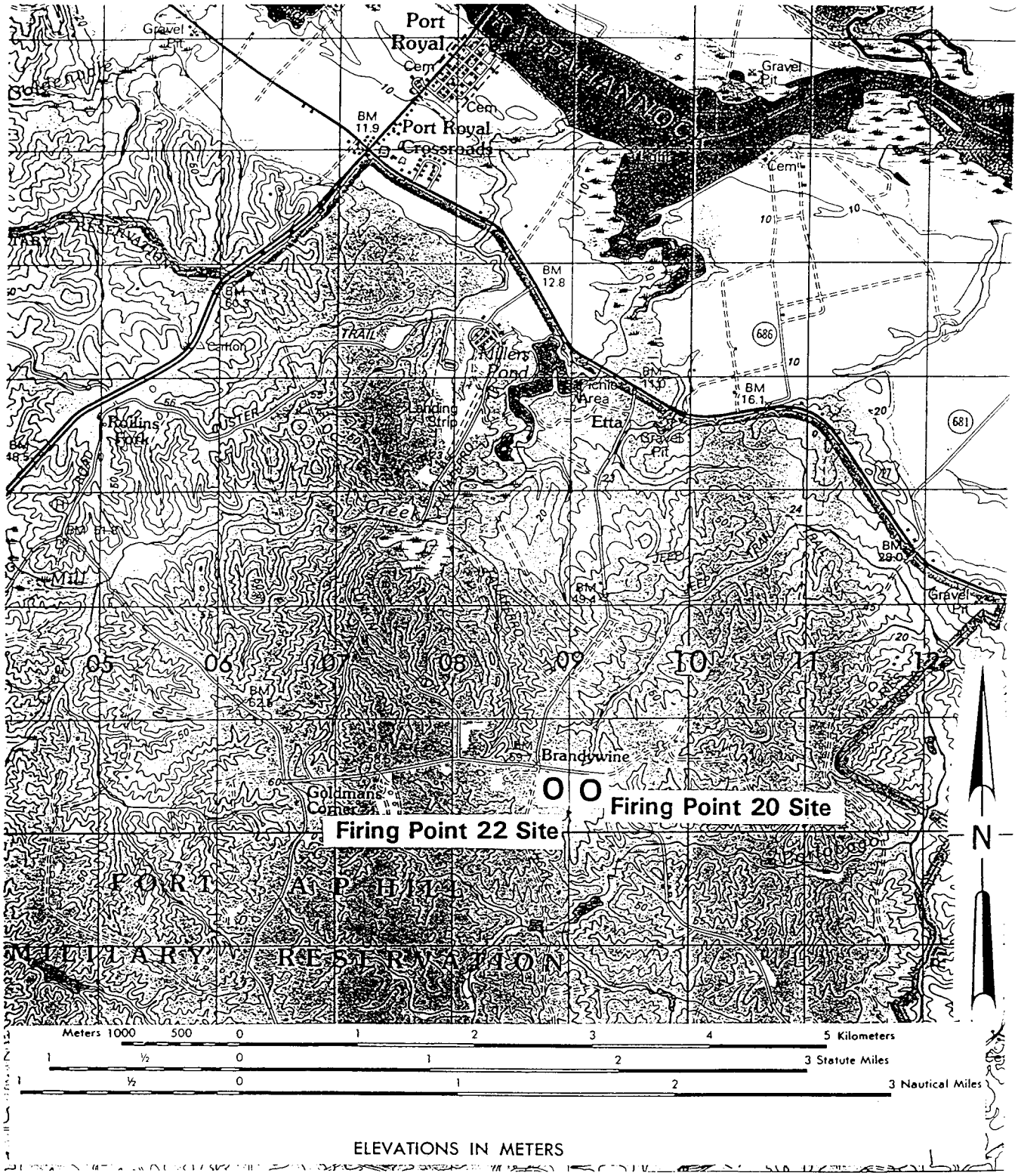

Figure 9. Location of the Firing Points 20 and 22 sites, Fort A.P. Hill, Virginia (Port Royal, VA, 1:50,000 DMA quadrangle)

process whose effectiveness is hindered only by the somewhat rapid rate of infiltration of the sandy soils.

Marine transgressions (sea level rise) across the Atlantic Coastal Plain have planed off the underlying bedrock to substantial depth, in excess of 120 meters at the research sites. Subsequent sea level fall and marine regressions have deposited weakly indurated sediments of sand, silt, clay, and marl on the coastal plain shelf in strata which generally thicken eastward (Figure 10). During low stands of sea level, the Atlantic Coastal Plain sediments have been reworked, eroded and transported by streams. The larger streams flowing out of the Appalachian Mountains (such as the Rappahannock) have added sand and gravel of a variety of rock types to the strata of the coastal plain. The surficial sandy strata covering much of Fort A. P. Hill were deposited by streams (most likely the ancestral Rappahannock River) during the Pleistocene Epoch (last 2 million years) (Wentworth 1930). In lower elevations near the northern boundary of Fort A. P. Hill, the underlying Calvert Formation clays of Miocene age and the Nanjemoy Formation glauconitic sands and clays (Upper Eocene) may be seen at or near the surface (Ward 1985).

Soils of Fort A. P. Hill are considerably more homogeneous and predictable than the soils of Fort Carson. Most of the hill crests and side slopes have deep, moderately weathered sandy soils derived from the sandy terrace deposits. Clay strata that occur in the sandy soils are of two origins. The clayey sandy soils near the surface are the product of pedogenesis (weathering) and may vary in thickness from 1 to 3 meters. These clayey soils somewhat impede infiltration and movement of soil moisture after precipitation events. Additional clay strata deposited by the stream that deposited the sands and gravels of the former floodplain may be found in the upper half of the terrace deposits of the uplands. These two different clayey strata may be differentiated on the basis of the nature of their boundaries with over and underlying soil strata. The upper pedogenic clays have gradational boundaries with underlying soils whereas the alluvial clay strata have sharp boundaries, indicating significant changes in the depositional environs.

The climate of Fort A. P. Hill is humid/temperate. Average annual precipitation is 1015 mm with August usually being the wettest month (mean August precipitation is 122 mm) and February the driest month (mean February precipitation is 64 mm). On the average, the Fort A. P. Hill area experiences 135 days per year with measurable precipitation and 5 days per year with 25 mm or more snowfall. Annual average evaporation is approximately 1120 mm. July is the warmest month with a mean temperature of 31.7 degrees Celcius. The coldest month is usually January, averaging 7.8 degrees Celcius. Typically, the temperature drops below freezing about 75 days during the year. Diurnal changes in temperatures are maximum in the fall and spring months and may reach 18 degrees. The Fort A. P. Hill area is not as sunny as the Fort Carson area, averaging about 2500 hours of sunshine per year. July is the sunniest month (280 hours) and January the cloudiest, averaging 140 hours of sunshine.

Firing Points 20 and 22 site description

The research sites at Fort A. P. Hill were established at the locations of Firing Points (FP) 20 (Figure 11) and 22 (Figure 12), at grid locations 092203 and

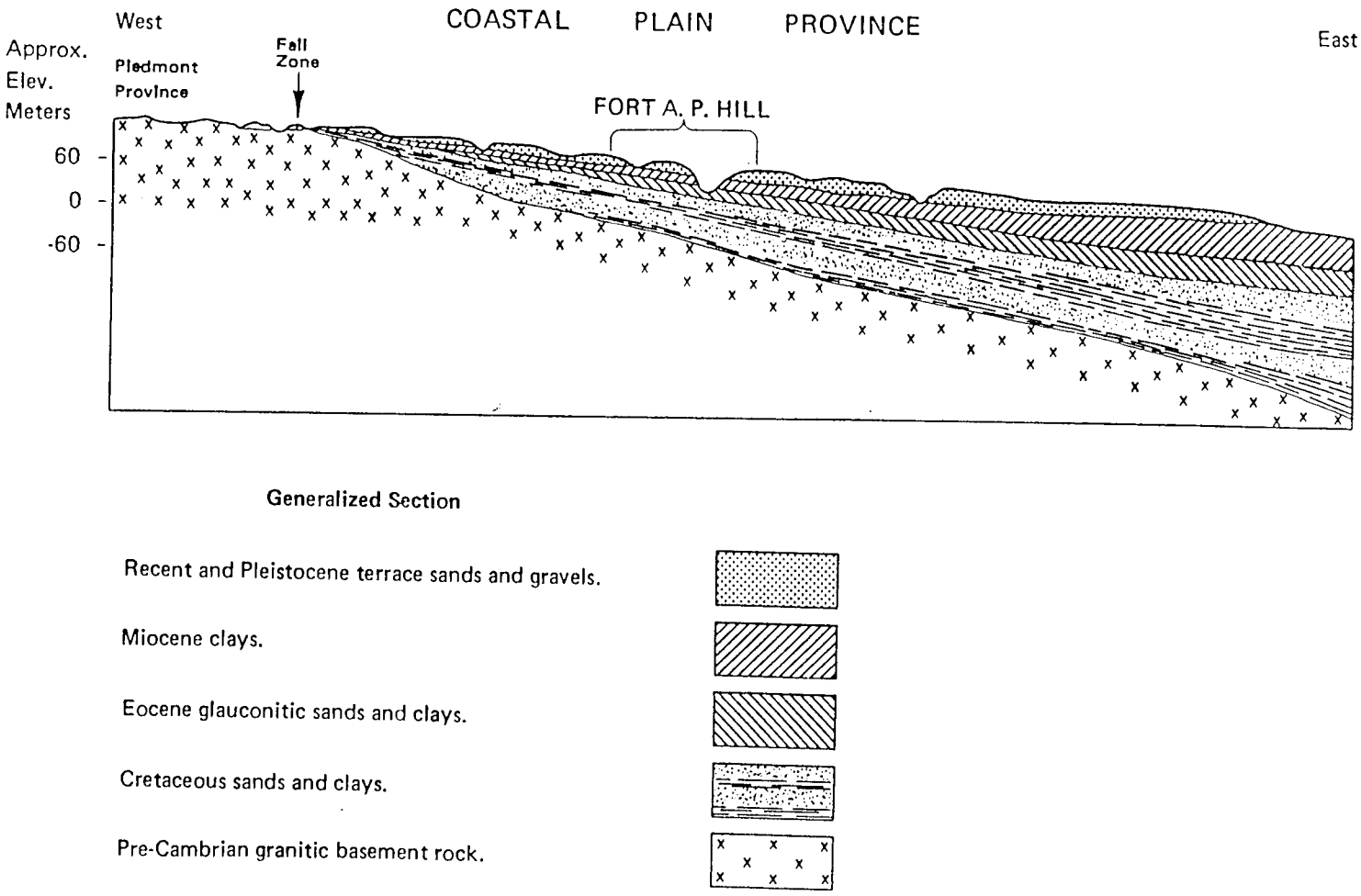

Figure 10. Generalized geologic section, Virginia Coastal Plain and Fort A. P. Hill (after Baker 1979)

Figure 11. Photograph of the Firing Point 20 site, Fort A.P. Hill, Virginia

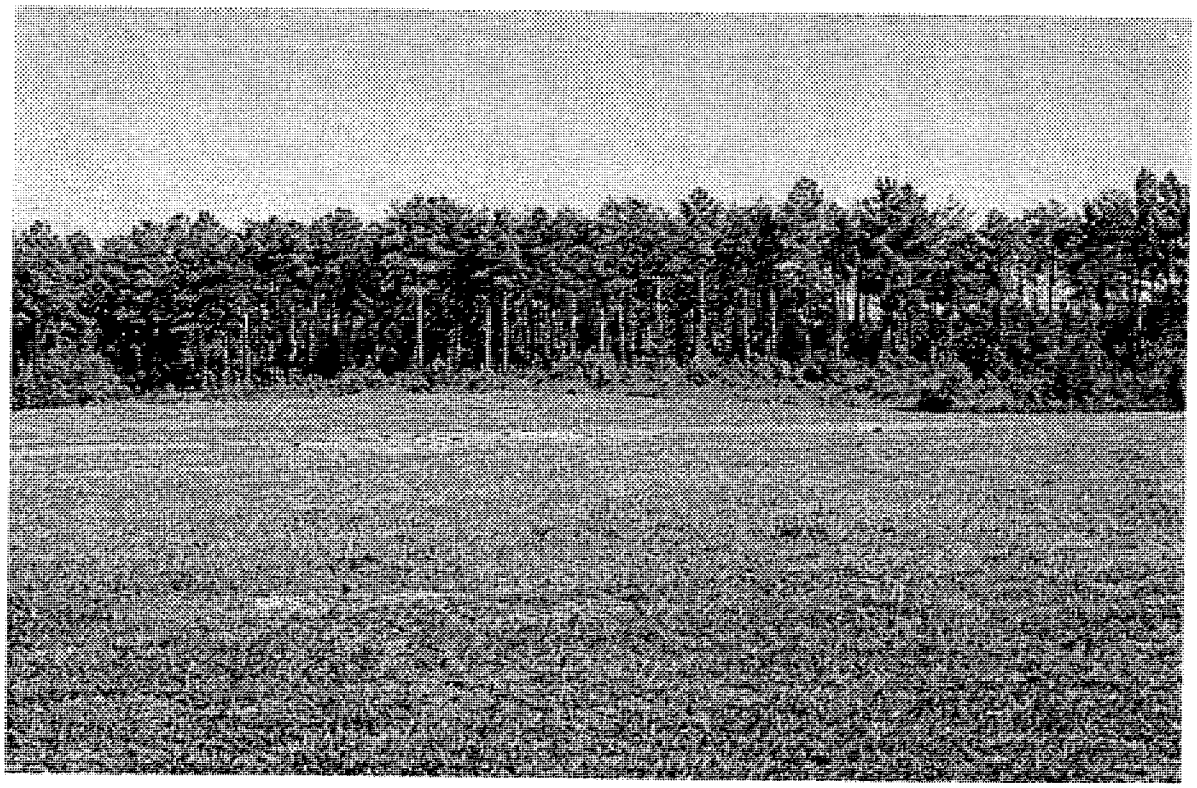

Figure 12. Photograph of the Firing Point 22 site, Fort A.P. Hill, Virginia

088203, respectively, on the Port Royal, VA, 1:50,000 DMA quadrangle. Since the two sites are in close proximity (about 400 meters apart) and essentially in the same landscape position, the sites will be discussed as one site, with the exception of differences in soils.

The two Fort A. P. Hill sites occur on the crest of an east-west trending low rounded ridge (Figure 13). The average elevation of the site is approximately 58 meters M.S.L. (from the 1:50,000 Port Royal quadrangle). Surface topographic features are minimal with the total amount of topographic relief on the sites being less than one meter. The ridge crest that the sites occupy appears to be the product of erosion of the Pleistocene terrace deposits by surface wash and the extension of the drainage network of Portabago Creek and its tributaries around the ridge. Active geomorphic processes include the continuation of erosion of the ridge and weathering of the underlying terrace sediments.

Rapid weathering of the sandy deposits at the sites has produced a sandy clay soil (CL) which appears to be somewhat homogeneous in horizontal extent over both sites on the ridge crest (Tables 8–11). Almost all samples taken at 22 locations on both sites were classified as sandy clay (CL) or clayey sand (SC). The soils at FP20 are slightly sandier than those at FP22 with an average of 55.7 percent and 51.4 percent sand, respectively. A trace of gravel was found on both sites. All Plasticity Indices (PI), Liquid Limits (LL) and Plastic Limits (PL) were low. The amount of sand versus fines (silt and clay) generally appears to increase with depth, which suggests that the sandy soils are not deeply weathered and that the clays found at depth will be alluvial, have sharp contacts, and possibly be laterally discontinuous. Field observations of the soils from these two sites reveal that they are generally dense, brown to gray, and moist (Tables 12 and 13).

Although no specific deep stratigraphic information exists for the sites, the unconsolidated sedimentary deposits beneath the site probably extend for more than 120 meters in depth (Baker 1979). These terrace deposits likely consist of interbedded fluvial (cross bedded) sands, silts, and gravels with some clay lenses. The amount of gravel and size of sand grains increases with depth while the occurrence of clay strata diminishes. The base of the terrace deposits is clearly defined as a sandy gravel overlying the dense massive clay of the Calvert Formation (Onuschak 1973; Mixon and Newell 1978).

Surface water drainage of the two sites is good to excellent. Overland flow is easily achieved by the existing natural drainage network on the land surface. The permeability of the soil is somewhat lower in the upper three meters, but increases rapidly below the weathered zone. The water table is probably greater than 10 to 30 meters below the surface throughout the year but may fluctuate significantly by season.

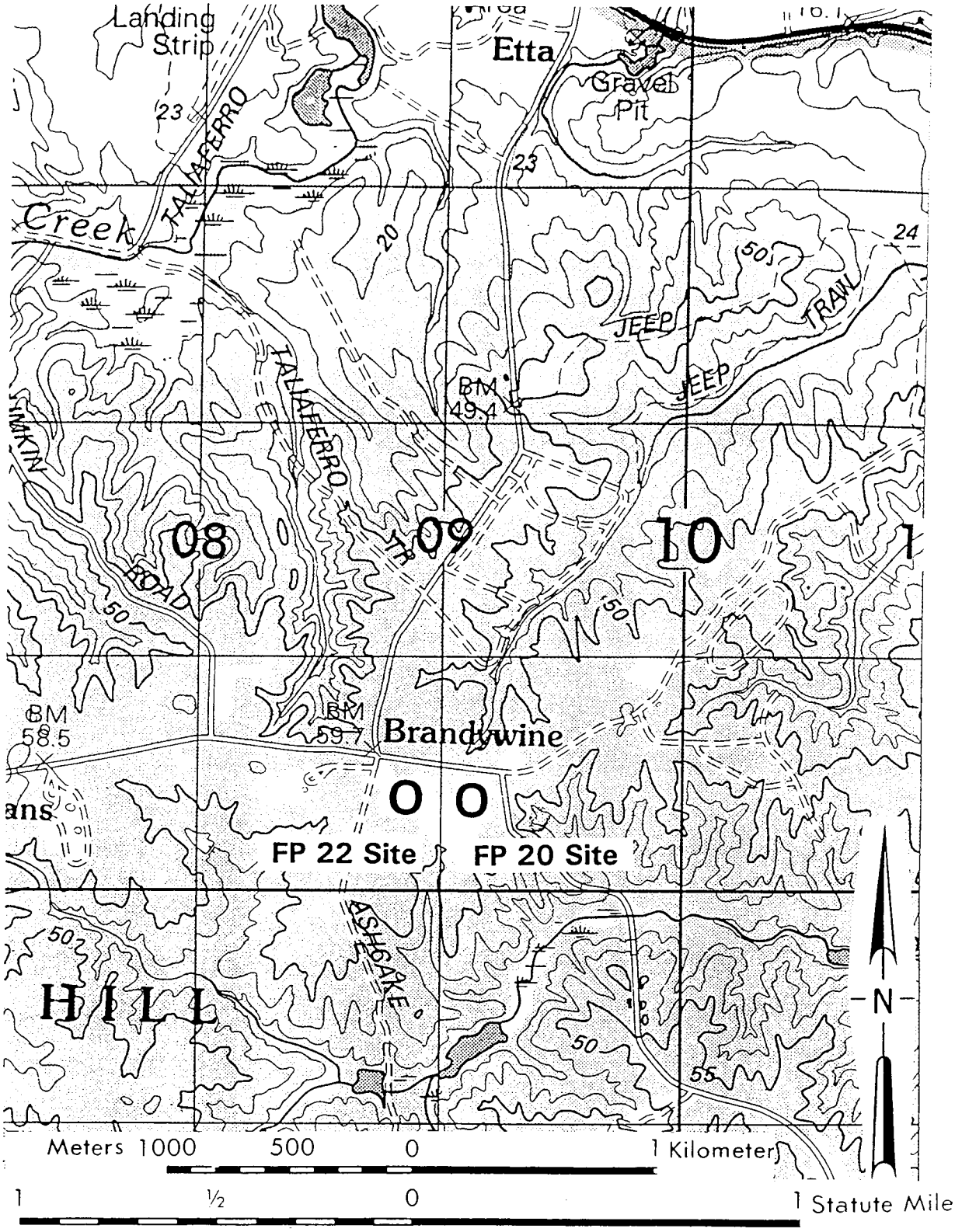

Figure 13. Topography of the Firing Points 20 and 22 sites, Fort A.P. Hill, Virginia (Port Royal, VA, 1:50,000 DMA quadrangle)

Table 8
Summary of Sieve Analysis, Firing Point 20, Fort A. P. Hill, VA

Location	Depth (m)	Classification	Color	% Gravel	% Sand	% Fines	PI*	LL**	PL***	Moisture Content
27.5E, 73N (Reg. 1-1)	0	Clayey sand, SC	Brown	0	60.5	39.5	8	24	16	15.8
	0.5	Sandy clay, CL	Brown	0	46	54	15	32	17	19.3
	1	Silty sand, SM	Brown	1.4	77.9	20.8	--	NP†	--	7.2
65E, 10.5N (Reg. 4-1)	0	Sandy clay, CL	Brown	0	49.4	50.6	15	24	15	13.1
	0.5	Clayey sand, SC	Brown	0	52.6	47.4	16	32	16	16
	1	Clayey sand w/ gravel, SC	Brown	6	60.1	33.9	17	32	15	13.1
27.5E, 73N	upper 10 cm	Silty clayey sand, SC	Gray	0	59.2	40.8	9	31	22	18
40E, 23N	upper 10 cm	Clayey sand, SC	Brown	0	55.7	44.3	11	29	18	16.4
52.5E, 85.5N	upper 10 cm	Sandy silty clay, CL	Brown	0	45.6	54.4	7	26	19	23
65E, 10.5N	upper 10 cm	Clayey sand, SC	Brown	0	51.5	48.5	12	31	19	14.7
77.5E, 60.5N	upper 10 cm	Clayey sand, SC	Brown	0	54.3	45.7	7	24	17	21.4

*Plasticity Index PI = LL - PL **Liquid Limit ***Plastic Limit †Non-Plasitc

Table 9
USDA Soil Classification, Firing Point 20, Fort A. P. Hill, VA

Location	Depth (m)	Texture	Munsell Color	Chroma & Hue
27.5E, 73N	upper 10 cm	Sandy loam	dark grayish brown	2.5Y 4/2
40E, 23N	upper 10 cm	Loam	light olive brown	2.5Y 5/4
52.5E, 85.5N	upper 10 cm	Sandy loam	olive brown	2.5Y 4/4
65E, 10.5N	upper 10 cm	Loam	olive brown	2.5Y 4/4
77.5E, 60.5N	upper 10 cm	Loam	olive brown	2.5Y 4/4

JPG 1-Ha Site

Jefferson Proving Ground is located within a humid/temperate climatic regime. The total annual precipitation averages 102 cm, of which 60 percent usually falls in April through September. The wettest month is usually May, averaging 12 cm, and the driest month October, averaging 6 cm. The average seasonal snowfall is 43 cm, with the majority usually falling in January (average 11 cm). In summer the average temperature is 22 degrees Celcius with sunshine about 70 percent of the time. An average temperature during the winter months is –0.6 degrees with about 40 percent of the days having sunshine. Generally, the coldest month is January (average –1.9 degrees Celcius) and the warmest month July (average 23 degrees Celcius).

The following soil and regional geologic information was taken from JPG Demonstration Site reports (PRC Environmental Management, Inc. 1994, 1996). JPG is located in the Muscatatuck Regional Slope physiographic unit of southeastern Indiana, where the development of modern surface features have been controlled by normal degradational processes such as weathering, stream erosion, entrenchment, and mass movement (Schneider 1966). This physiographic unit lies within the Glaciated Outer Bluegrass section of the interior Low Plateau Province (Fenneman 1938 and Ray 1974). Although a northern portion of the Muscatatuck Regional Slope was glaciated during the Wisconsin Age, the entire unit was covered by glacial ice in the early Pleistocene Epoch. Stream valleys are typically steep-sided because channels have developed through relatively thin, unconsolidated deposits and subsequently cut into the upper portions of underlying limestones and dolomites. Upland areas between drainages are typically broad and nearly flat to undulating. The upland flat JPG is located in functions as a local drainage divide between the Lower Ohio and Muscatatuck watersheds (both of which are in the Ohio River drainage basin). The 1-hectare site is located along the upper reaches of Big Creek

Table 10
Summary of Sieve Analysis, Firing Point 22, Fort A. P. Hill, VA

Location	Depth (m)	Classification	Color	% Gravel	% Sand	% Fines	PI*	LL**	PL***	Moisture Content
27.5E, 73N (Reg. 1-1)	0	Sandy clay, CL	Gray	0	37.9	62.1	16	41	25	26.3
	0.5	Sandy clay, CL	Brown	0.7	44.9	54.5	17	33	16	24.5
	1	Sandy clay, CL	Brown	1.8	47	51.2	23	39	16	21.8
65E, 10.5N (Reg. 4-1)	0	Clayey sand, SC	Brown	0	57	43	9	25	16	17.1
	0.5	Clayey silty sand, SM-SC	Brown	1.3	59.8	38.9	6	20	14	15
	1	Clayey sand, trace of gravel SC	Brown	3.6	58	38.4	9	22	13	12.5
27.5E, 73N	upper 10 cm	Sandy silty clay, CL	Brown	0	41.2	58.8	13	35	22	17.4
40E, 23N	upper 10 cm	Silty clayey sand, SC	Brown	0	56.3	43.7	10	31	21	13.1
52.5E, 85.5N	upper 10 cm	Sandy clay, CL	Brown	0	47	53	10	29	19	15.1
65E, 10.5N	upper 10 cm	Clayey sand, SC	Brown	0	58.5	41.5	9	28	19	17.2
77.5E, 60.5N	upper 10 cm	Clayey silty sand, SM	Gray	0	57.8	42.2	10	35	25	12.7

*Plasticity Index PI = LL - PL **Liquid Limit ***Plastic Limit

Table 11
USDA Soil Classification, Firing Point 22, Fort A. P. Hill, VA

Location	Depth (m)	Texture	Munsell Color	Chroma & Hue
27.5E, 73N	Upper 10 cm	sandy clay loam	Light olive brown	2.5Y 5/4
40E, 23N	Upper 10 cm	sandy loam	Olive brown	2.5Y 4/4
52.5E, 85.5N	Upper 10 cm	sandy clay loam	Light olive brown	2.5Y 5/4
65E, 10.5N	Upper 10 cm	sandy clay loam	Olive brown	2.5Y 4/4
77.5E, 60.5N	Upper 10 cm	sandy clay loam	Dark grayish brown	2.5Y 4/2

Table 12
Soil Sample Moisture Contents, Firing Point 20, Fort A. P. Hill, VA

Depth (m)	Location				
	0E, 60N	27.5E, 73N (Reg. 1-1)	65E, 10.5N (Reg. 4-1)	122E, 8N	123E, 97N
0	12.3	15.8	13.1	13.4	16.1
0.5	10.1	19.3	16	15.8	13.2
1	11.7	7.2	13.1	19.4	9.9

Table 13
Soil Sample Moisture Contents, Firing Point 22, Fort A. P. Hill, VA

Depth (m)	Location				
	2E, 60N	27.5E, 73N (Reg. 1-1)	65E, 10.5N (Reg. 4-1)	122E, 8N	123E, 97N
0	14.4	26.3	17.1	9.8	14.5
0.5	18.6	24.5	15	14.6	13.8
1	18.2	21.8	14	16.3	15

(also known as Big Camp Creek) and drains west into the creek.

Bedrock underlying JPG is Laurel Dolomite, a Silurian-aged dolomite approximately 14 meters thick. The Laurel Dolomite is described as gray, cherty, dolomitic limestone. The residuum of this dolomitic limestone is rich in chert nodules, which are abundant in the subsoils that formed on this bedrock. Below the Laurel Dolomite are 91 to 122 meters of interbedded shales and limestone of the Silurian and Ordovician Systems.

The soils in this area are mapped by the U.S. Department of Agricultue (USDA) Soil Conservation Service (SCS) as Avonburg and Rossmoyne silt loam soils. General characteristics of each soil are discussed below.

The Avonburg soils occur on uplands of glacial drift plains and have either gently sloping or nearly level topographic features. The soils were formed from a thin mantle of loess (wind transported silt) and underlying glacial drift. Avonburg soils have a dark grayish-brown color within the 25.4 cm (10 in.) epipedon. Avonburg subsoils are friable and mottled. The upper subsoil horizon generally consists of a yellowish-brown silt loam and light brownish-gray silty clay loam appearance. The middle subsoil horizon is generally mottled light brownish-gray fragipan (loamy, brittle, low porosity, low organic content, appears cemented). The lower subsoil horizon is generally mottled, brownish-gray in color, friable and consists of a silt loam texture. Drainage is poor, as Avonsburg soils have slow permeability.

The Rossmoyne silt loam forms on 2 to 6 percent slopes. It is deep, moderately well drained soil found on uplands. A 22.9 cm (9 in.) thick brown silt loam makes up the surface layer. The subsurface of the Rossmoyne soil extends to a depth of 71.1 cm (28 in.) and consists of a light brownish-yellow, friable silt loam in the upper horizon and a friable, mottled, yellowish-brown silt loam in the lower horizon. Below this horizon there is an 203 cm (80 in.) thick fragipan. It is a very firm mottled light gray silt loam and silty clay loam.

A summary of the soil properties determined from laboratory analysis of the soil samples collected at the 1-hectare site is provided in Table 14. The USCS classification of the soil at 10 cm depth is silt with clay and/or sand. The soil samples collected at 0.5 and 1 m depth are identified as sandy or silty clay. None of the soil samples contain gravel-size particles. All samples contain at least 40 percent fines (silt and clay size), with 12 of the 15 samples having greater than 75 percent fines. The soil moisture content generally ranges from 20 to 36 percent, the exceptions being the samples collected at (122E, 8N) (moisture content 13-18%) and (123E, 97N), 1 m depth, (moisture content 18.6%). Although the upper one meter of soil has a relatively high percentage of clay size particles, an x-ray diffraction analysis of soil samples collected at the nearby 40- and 80- acre sites (Llopis et al. 1998) indicates that the soil has only a small fraction of *mineralogical* clay material. The soil is very fine grained and has cohesion, particularly when wet. If the plasticity index and liquid limit given in Table 14 were plotted on the chart in Table 1, the points would lie close to the A Line, which is the boundary between clays and silts.

Table 14
Summary of Sieve Analysis, JPG 1-Hectare Site

Location	Depth (m)	Classification	Color	% Gravel	% Sand	% Fines	PI*	LL**	PL***	Moisture Content
27.5E, 73N (Reg. 1-1)	0.1	Sandy clayey silt, ML	Brown	0	12.9	87.1	10	34	24	26.6
	0.5	Silty clay, CL	Brown	0	10.5	89.5	10	31	21	24.4
	1	Sandy clay, CL	Brown	0	22.1	77.9	15	33	18	20.7
65E, 10.5N (Reg. 4-1)	0.1	Clayey silt, ML	Brown	0	5.7	94.3	10	36	26	30.7
	0.5	Silty clay, CL	Brown	0	6.1	93.9	15	40	25	30.7
	1	Silty clay, CL	Brown	0	11.6	88.4	12	35	23	29.0
122E, 8N	Surface	Sandy clayey silt, ML	Brown	0	41.2	58.8	13	35	22	17.4
	0.5	Sandy clay, CL	Brown	0	56.3	43.7	10	31	21	13.1
	1.0	Clay, CL	Brown	0	47	53	10	29	19	15.1
123E, 97N	Surface	Silty clay, CL	Brown	0	9.1	90.9	13	37	24	31.3
	0.5	Clay, CL	Brown	0	8.1	91.9	15	37	22	24.7
	1.0	Sandy clay, CL	Brown	0	19.4	80.6	10	28	18	18.6
40E, 23N	0.1	Clayey silt, ML	Brown	0	11	89	12	38	26	33.0
52.5E, 85.5N	0.1	Sandy clayey silt, ML	Brown	0	13.6	86.4	12	39	27	35.5
77.5E, 60.5N	0.1	Sandy silt, ML	Brown	0	16.4	83.6	10	38	28	33.6

*Plasticity Index PI = LL - PL **Liquid Limit ***Plastic Limit

3 Geophysical Test Principles and Field Procedures

This section details the site characterization plan, concepts of the geophysical methods used, and field procedures. The same general site layout and surveying (spatial and geophysical) procedures were followed at each of the sites. The number of flagged internal grid lines and density of a particular geophysical data set (primarily electrical resistivity soundings) varied among sites depending on local site conditions. Four geophysical methods were chosen to characterize the sites: electrical resistivity, electromagnetics, magnetics, and ground penetrating radar. These techniques are complimentary and provide (a) both detailed and larger scale subsurface stratigraphy, (b) soil resistivity and conductivity, (c) local magnetic total field strength, and (d) electromagnetic wave velocity of the soil. A comparison of the conductivity and magnetic data allows differentiation of metallic and non-metallic material, and ferrous and non-ferrous objects.

Geophysical Test Principles

Electrical resistivity survey

Electrical resistivity is a measure of how well the soil conducts an electrical current. Resistivity values can vary over several orders of magnitude depending on the type of earth material and on the degree of compaction. Major factors influencing the resistivity measurement are the amount of pore fluid present, the salinity of the pore fluid, and the presence of conductive minerals; an increase in any of these factors will cause the resistivity to decrease. A linear array of four metal rods or electrodes is generally used in an electrical resistivity survey. The array consists of two outer current electrodes and two inner potential electrodes (see following illustration). Current is introduced into the ground through one current electrode (positive electrode) and flows through the subsurface to the other current electrode (negative electrode). The subsurface material acts as a natural resistor and a potential difference is generated across the two potential electrodes. Knowing the amount of current injected into the ground, the electrode separation, and the measured potential difference, an apparent resistivity can be computed.

There are two types of resistivity surveys, horizontal profiling and vertical sounding. The profiling technique is used to identify lateral variations at a given depth of investigation, whereas the sounding method gives variations in resistivity with depth at a particular location. Resistivity sounding employing a Schlumberger

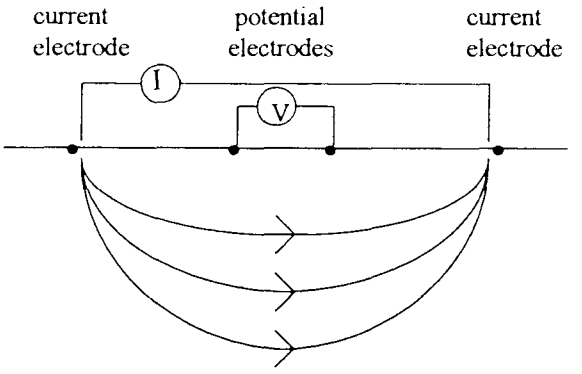

array was used in this study. When performing a sounding, the center of the electrode array remains fixed and measurements are taken at increasing current electrode spacings; the greater the current electrode spacing, the greater the depth of investigation. The sounding data represent the subsurface resistivity structure below the center point of the array. A general rule of thumb is that the depth of investigation is equal to 0.2–0.5 times the spacing between current electrodes, depending on the actual values of the material resistivities. The unit of electrical resistivity is the ohm-meter (Ω-m). Resistivity is the reciprocal of electrical conductivity, which is measured in an electromagnetic survey. To convert from resistivity, in ohm-meters, to conductivity, in millisiemen per meter, divide 1000 by the resistivity value. The apparent resistivity data are plotted versus electrode spacing on logarithmic paper. The number of subsurface layers present and the resistivity and thickness of each layer can be estimated from the shape of the resistivity sounding curve. A resistivity inversion computer program was used to aid in the interpretation of the data.

Electromagnetic survey

The electromagnetic (EM) induction method is commonly used to measure an apparent terrain conductivity. The conductivity of a material is dependent on the degree of water saturation, the types of ions in solution, porosity, the chemical constituents of the soil, and the physical nature of the soil. Due to these factors, conductivity values can range over several orders of magnitude.

The EM system consists of a transmitter and receiver coil separated by a fixed distance. An alternating current, commonly in the 1 to 20 kilohertz range, is passed through the transmitter coil, thus generating a primary time varying magnetic field. This primary field *induces* eddy currents in the subsurface conductive materials. (Where the common phrase EM induction is derived.) These eddy currents are the source of a secondary magnetic field which is detected by the receiver coil along with the primary field. Under a fairly wide range of conditions, the measured component that is ninety degrees out of phase (quadrature component) with the primary field is linearly related to the terrain conductivity (Keller and Frischknecht 1982, Dobrin 1976, Telford et al. 1973). Conductivity is measured in units of millisiemen per meter (mS/m).

There are two components of the induced magnetic field measured by the EM equipment. The first is the quadrature phase component, sometimes referred to as the out-of-phase or imaginary component, which gives the ground conductivity measurement. Disturbances in the subsurface caused by compaction, soil removal and fill activities, or buried objects may produce conductivity readings different from that of the background values, thus indicating anomalous areas. Electrical conductivity is a positive valued parameter. However, due to the design of the instrument used in this survey to collect conductivity data, it is possible to obtain a negative value when the instrument passes over a metallic object. Although a negative conductivity value is physically meaningless, it does aid in the detection of metallic material. The second component is the inphase or real component, which is the ratio of the induced secondary magnetic field to the primary magnetic field. The inphase component is primarily used for calibration purposes, however, it is also significantly sensitive to metallic objects and therefore very useful when looking for buried metal (Geonics Limited 1984). The inphase component is measured relative to an arbitrarily set level and assigned units of parts per thousand (ppt). Since it has an arbitrary reference level, the reading can be either a positive or negative value.

A Geonics EM31 terrain conductivity meter was used for this investigation. The EM31 has a transmitter-receiver coil separation of 12 ft (3.7 m) and an effective depth of investigation of approximately 20 ft (6.1 m) (Geonics Limited 1984). The EM31 meter reading is a weighted average of the earth's conductivity as a function of depth; half of the instrument's readings result from features shallower than about 9 ft (2.7 m), and the remaining half from below that depth (Bevan 1983). When the EM31 is carried at a height of approximately 3 ft (0.9 m), it is most sensitive to features at a depth of about 1 ft (0.3 m). Carrying the instrument about 3 ft (0.9 m) above the ground surface reduces the meter reading by 12 percent, however, the instrument has been calibrated to read correctly when carried at this height (Geonics Limited 1984). For this survey, the EM31 was carried at hip level, which is approximately 3 ft (0.9 m). The instrument can be operated in both a horizontal and vertical dipole orientation, each having different depths of investigation. The instrument is normally operated with the dipoles vertically oriented (coils oriented horizontally and co-planar) which gives the maximum depth of penetration.

Ground penetrating radar survey

Ground penetrating radar (GPR) is also an electromagnetic method, however it differs significantly from the induction EM methods described above and warrants a separate discussion. At the lower frequencies (kilohertz range) where EM induction instruments operate, conduction currents (currents which flow via electrons in a metallic matrix or ions in solution) dominate and energy diffuses into the ground. At the higher frequencies (megahertz range) which GPR utilizes, displacement currents (currents associated with charges which are constrained from moving any distance) dominate and EM energy propagates into the ground as a wave.

GPR is used to image the subsurface by transmitting an electromagnetic pulse into the earth and measuring the return signal. While in the earth, the EM signal undergoes refraction, reflection, scattering, and dispersion. The frequencies employed in GPR typically range from 10 to 1000 MHz. Contrast in the dielectric

permittivity at layer boundaries causes the EM wave to be reflected and refracted. The dielectric permittivity is the proportionality factor relating the displacement current to the energy. Since electromagnetic fields consist of both electric and magnetic fields, any properties of the geologic material which affect either of these fields will also affect the propagation of the EM wave in the subsurface. Generally, the electrical properties of the soil and rock have a greater influence on the EM wave propagation than do the magnetic properties. Soil conductivity is a major factor in determining if GPR can be used successfully at a site. High conductivity soils, such as those with a high clay and moisture content, can significantly attenuate the EM signal and frequently render GPR virtually useless.

A Sensors & Software, Inc. modified pulseEKKO IV system and a pulseEKKO 1000 system were used to collect the GPR data. The pulseEKKO IV is a low frequency antenna system (12.5–200 MHz) whereas the pulseEKKO 1000 is a high frequency antenna system (225–1200 MHz). The frequencies utilized in this investigation were 50, 100, 200, and 900 MHz. Both reflection profiling and velocity sounding GPR surveys were performed. In reflection mode, the transmitter and receiver antennas are kept a fixed distance apart and both antennas are simultaneously moved along the survey line. The time (in nanoseconds) required for the EM wave to travel through the subsurface and return to the receiver is recorded at each sample station. The received signal is plotted against two-way travel time at each sample station along the survey line. Figure 14 illustrates the reflection mode concept and the corresponding GPR response for the hypothetical anomaly shown. The common-midpoint (CMP) technique was used to perform the velocity sounding. The transmitter and receiver antennas were initially placed a given distance apart, and then moved outward from the center at small, equal increments. By plotting antenna separation versus time, the various EM wavefronts can be identified and an approximate radar wave velocity obtained.

DICON probe

The following information describing the DICON probe was extracted from Miller et al. (1992). The DICON (DIelectric/CONductivity) probe provides the capability to measure the conductivity and dielectric constant of the soil at a frequency of 60 MHz. Each DICON probe unit consists of two separate pieces of equipment, a probe assembly and a reflectometer. The probe head consists of two half-cylindrical-shaped brass plates attached to an insulating body of polytetrafluoroethylene (Teflon®), with a small gap between the plates. The brass plates on the probe head represent two capacitors; one internal to the probe with the Teflon as the dielectric and the other external with the soil as the dielectric. The plates behave as a simple capacitor with the soil in their immediate vicinity as the dielectric with virtually no electromagnetic radiation outside of the plates. The reflectometer houses the electronics of the DICON probe. A voltmeter placed on the top face of the reflectometer displays the real (R) and imaginary (I) components of the complex reflection coefficient.

After following a standard calibration procedure, soil conductivity and relative dielectric permittivity measurements are obtained. A one-inch diameter hole is augered in the soil and the probe is inserted into the hole to the desired depth and connected to the reflectometer. The real and imaginary components of the complex

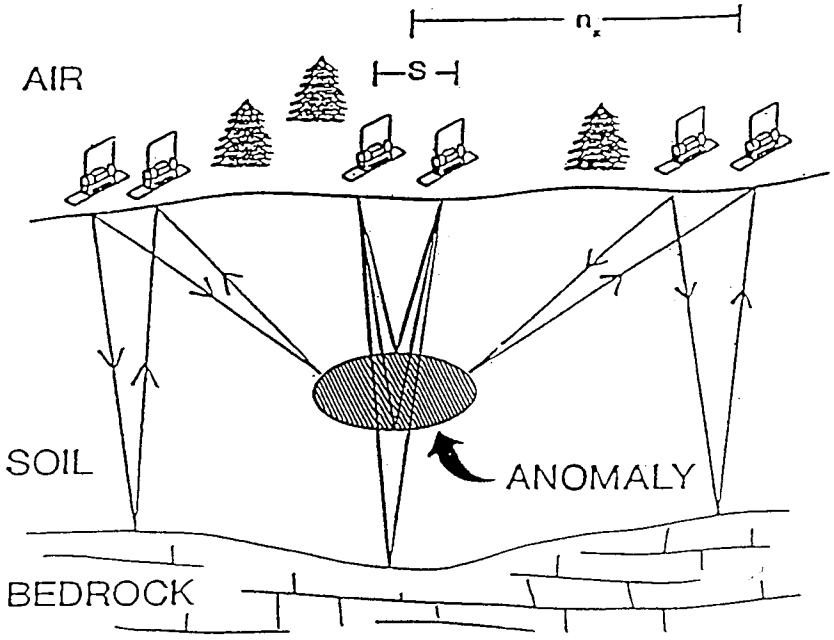

Schematic illustration of common-offset single-fold profiling.

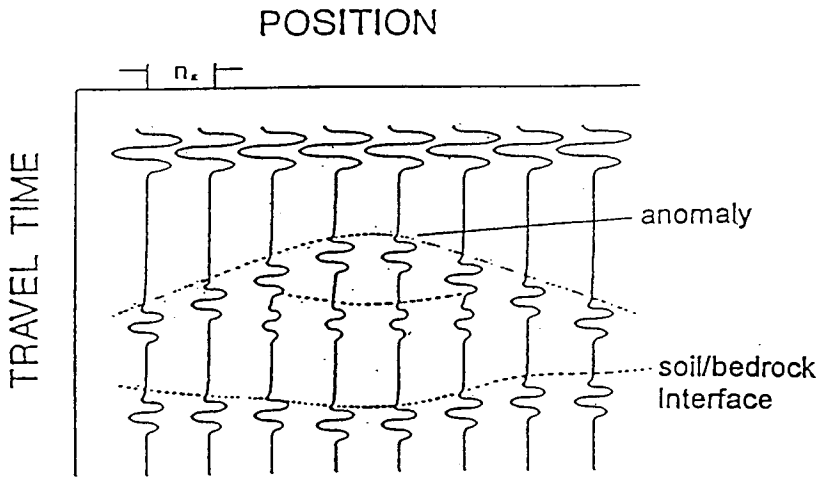

Format of a GPR reflection section with radar events shown for features depicted

Figure 14. Illustration of a reflection mode GPR survey and corresponding radar section for anomaly shown (adapted from Annan 1992)

reflection coefficient displayed on the voltmeter are then input to a program that calculates electrical conductivity and relative dielectric permittivity.

Magnetic survey

A magnetic survey measures changes in the earth's total magnetic field caused by variations in the magnetic mineral content of near surface rocks and soils or ferrous objects. These variations are generally local in extent. The magnetic response is attributed both to induction by the magnetizing field and to remanent magnetization. Remanent magnetization is permanent magnetization and depends on the thermal and magnetic history of the body; it is independent of the field in which it is measured (Breiner 1973). Induced magnetization is temporary magnetization that disappears if the material is removed from the inducing field. Generally, the induced magnetization is parallel with and proportional to the inducing field (Barrows and Rocchio 1990).

A GEM GST-19T proton precession magnetometer with an accuracy of 1 nanotesla (nT) was used to collect the magnetic survey data. This magnetometer is equipped with a sensor that contains a hydrogen-rich fluid as a source for the protons. The proton precession magnetometer is based on the principle that protons will precess freely in the presence of the earth's magnetic field. The hydrogen-rich fluid is subjected to an external magnetic field applied in a direction approximately perpendicular to the earth's field. The proton's moment will align in the direction of the resultant field between that of the external magnetic field and earth magnetic field. When the external field is removed, the magnetic moment of the proton will precess about the earth's field until it returns to its original alignment with the earth's magnetic field. The proton precesses at an angular frequency that is proportional to the magnetic field. Therefore, by measuring the frequency at which the protons precess the strength of the local magnetic field can be determined.

Any material or object having a magnetic susceptibility will contribute to the total magnetic field measured by the magnetometer. If an object is present such that its magnetization is great enough to perturb the ambient magnetic field, then it will appear as an anomaly on the magnetic data plot. The size, depth of burial, magnetic susceptibility, and remanent magnetization of the object determine the magnitude of the anomaly and thus affect the ability of the magnetometer to detect the object. For a given susceptibility and remanent magnetization, as the size of the object decreases and depth of burial increases, the magnitude of the anomaly decreases; eventually the anomaly will be undetectable.

Field Methods

The layout of the survey grid and data acquisition requirements were specified by DARPA. The perimeter of each grid was surveyed at 5 m intervals. The grids were oriented in a north-south direction relative to magnetic north. The initial dimensions of the grids at Fort Carson were 100 x 115 m but later modified to 125 x 115 m to accommodate changes in the site plan. The survey grids at Fort A. P. Hill and JPG measure 125 x 100 m. A plastic tent stake was placed at each 5 m

position along the grid perimeter and marked with a PVC flag. Additional PVC flags were placed at 2 m intervals along the southern and northern grid boundaries to aid survey navigation. North-south lines spaced 20 m apart and three to four east-west lines were also flagged at 2 m intervals. The southwest corner of each grid was designated as station (0E, 0N). (For reference to other project related reports, the 125 x 100 m grid area was subdivided into three sections: two side bars (0–15E, 0–100N), (115–125E, 0–100N) and a center square (15–115E, 0–100N)).

Schlumberger resistivity soundings were performed along selected survey lines, which included both north-south and east-west oriented lines. Six measurements per logarithmic decade were taken, with the electrode spacings approximately equally spaced on a logarithmic scale. The minimum current electrode spacing was 1.0 m and the maximum spacing was 120 m, allowing a maximum depth of investigation of about 15 m. The specified minimum data resolution for the EM31 was 2 m spaced survey lines and 1 m measurement intervals along survey lines; for the magnetometer, 1 m spaced survey lines and 1 m measurement intervals. The EM31 data were collected at 0.5 second (Fort Carson and Fort A. P. Hill) or 1 second (JPG) intervals along survey lines spaced 2 m apart. The magnetometer sensor was mounted on a backpack worn by the operator and positioned approximately 1.5 m above the ground surface. These data were collected at 0.5 second intervals but along 1 m spaced grid lines. A minimum of one data sample per meter along survey lines was recorded for each data set. Fiducial markers were placed in the data at 5 m intervals for position reference while collecting the data. A data logger connected to the EM31 was used to store the data during the surveys and at the conclusion of each survey, data were transferred to a field computer for later analysis. The magnetometer data were stored internally in the unit's control console and later transferred to a field computer.

Reflection GPR and CMP data were collected along both north-south and east-west oriented profile lines. Nominal antenna frequencies of 50, 100, 200, and 900 (Fort Carson and Fort A. P. Hill only) MHz were used. For the reflection GPR surveys, the transmitter and receiver antennas were kept at a constant spacing of 2.0, 1.0, 0.5, or 0.17 m, respectively, and oriented normal to the survey direction. The data were collected in high speed data acquisition mode at sampling intervals of 0.2 m (50, 100 MHz), 0.1 m (200 MHz), and 0.02 m (900 MHz). The data were recorded on a field computer for later processing. When performing the CMP surveys, the transmitter and receiver antennas were initially spaced at the respective antenna spacing used during the reflection survey, and then each antenna moved outward by a distance of 0.1 m (50, 100 MHz), 0.05 m (200 MHz), or 0.025 m (900 MHz). An average EM wave velocity of the medium was determined based on the CMP data.

DICON probe measurements were taken at nine stations within each grid and at three depths at each station. The readings were taken at depths of 0.1, 0.3, and 0.5 m. The location of a DICON probe measurement generally corresponded to the center of an electrical resistivity survey line or a position along a GPR profile.

4 Geophysical Results and Interpretation

Data Presentation

The data analyzed include electrical resistivity sounding data, electrical conductivity and inphase data, magnetic total field data, GPR profile data, and DICON probe measurements. The resistivity data are logarithmic plots of apparent resistivity versus electrode spacing with a corresponding interpreted resistivity versus depth profile; EM31 and magnetometer data are presented as contour plots; GPR data are shown as profiles with distance along survey line plotted against time and depth (both increasing downward); DICON probe data are in tabular form giving the measured conductivity and relative dielectric permittivity, and calculated EM wave velocity. The resistivity sounding data show general variations in soil resistivity with depth. Anomalies on the conductivity and magnetic contour plots are identified as areas that differ significantly from the average or background value, and can be identified by a concentration of contour lines. On the GPR profile plots, anomalous areas are indicated by an interruption in reflector continuity. Anomaly detection is dependent not only on the type and size of material and the depth of burial, but also on the contrast between the soil and buried material.

The GPR data are presented as travel time versus distance along survey line. The time axis, in nanoseconds, is located on the left side of the plot and depth, in meters, is on the right. The depth scale is based on a subsurface radar velocity determined by analysis of the CMP and DICON probe data. There are two aspects of the GPR field data plot that require some explanation. The first notable feature is the lack of coincidence between zero time and zero depth (for example, see Figure 22). This offset is due to the separation of the transmitter and receiver antenna. The first arrival at the receiver is the reflection from the direct wave traveling from the transmitter to the receiver, not the reflection from the ground surface. The time span between zero time and zero depth is the one-way travel time of the direct wave between the transmitter and the receiver. The second point of initial confusion is the depth scale, in particular at very shallow depths where the scale is obviously nonlinear. The depth is determined based on the velocity of the media. Because the transmitter and receiver antenna are separated by a finite distance and the transmitted pulse has a lobe-shaped radiation pattern, the ray of the transmitted pulse that arrives at the receiver does not strike the subsurface interface at normal incidence, but at an acute angle. The depth scale is corrected for non-normal

incidence of the transmitted ray path.

There are six common features that can often be identified in a GPR record: continuous reflector, discontinuous reflector, chaotic or disturbed reflection, no reflection, hyperbolic reflection, and multiple (Figure 15). A continuous reflector identifies a relatively smooth and uninterrupted boundary, whereas a discontinuous reflector represents a rough and intermittent boundary. A chaotic reflection is caused by a disturbance of the subsurface material, such as soil that has been removed and then backfilled, or rapid deposition. An area of no reflection on the radar record can represent a loss of signal strength caused by a highly conductive or magnetic material, system power limitations, or a homogeneous material that exhibits no variations in EM properties that would cause a reflection or scattering of energy. Hyperbolic reflection patterns are generated by the radar signal reflecting off a buried object (natural or man-made) as the antenna (which are located on the surface) pass over the object. A multiple is not a true reflection surface, but is generated by the transmitted pulse traversing an indirect path between the transmitter, a given reflection surface, and receiver (reflecting off multiple internal boundaries prior to reaching the receiver). Multiple reflections can travel various paths depending on the number of true subsurface reflectors, and the travel time of the multiple will always be greater than the reflection travel time of the true reflector (Simms et al. 1995). The reflection characteristics described above are used to qualitatively interpret the radar record and identify anomalous areas.

The magnetic data have a nominal background value of 53,600 nT at Fort Carson, 53,500 nT at Fort A. P. Hill, and 54,000 nT at the JPG 1-ha site. Some data sets were filtered to eliminate spikes caused by spurious noise.

The DICON probe data are used as index parameters to assess lateral and vertical variability of point in situ EM properties, for comparison with the EM31 conductivity data, and to aid in estimating velocities used in presenting the GPR data.

Fort Carson, Colorado

Seabee Site

Site description. The location of the Seabee site is shown in Figure 5. A topographic contour map of the site (Figure 16) shows that the elevation increases 5 m from the northeast corner to the southwest corner. The western half of the site has a slightly steeper gradient than the eastern portion. Few rocks are visible on the ground surface. The survey grid extends 125 m to the east and 115 m to the north, although this project is concerned only with the initial 100 m north. Figure 17 shows the location of the resistivity soundings, GPR profiles, and the DICON probe measurements.

Electrical resistivity results. Six Schlumberger resistivity soundings were performed at the Seabee site; four lines were oriented north-south and two east-west. Plots of the resistivity field data with the best-fit curve superimposed, and the

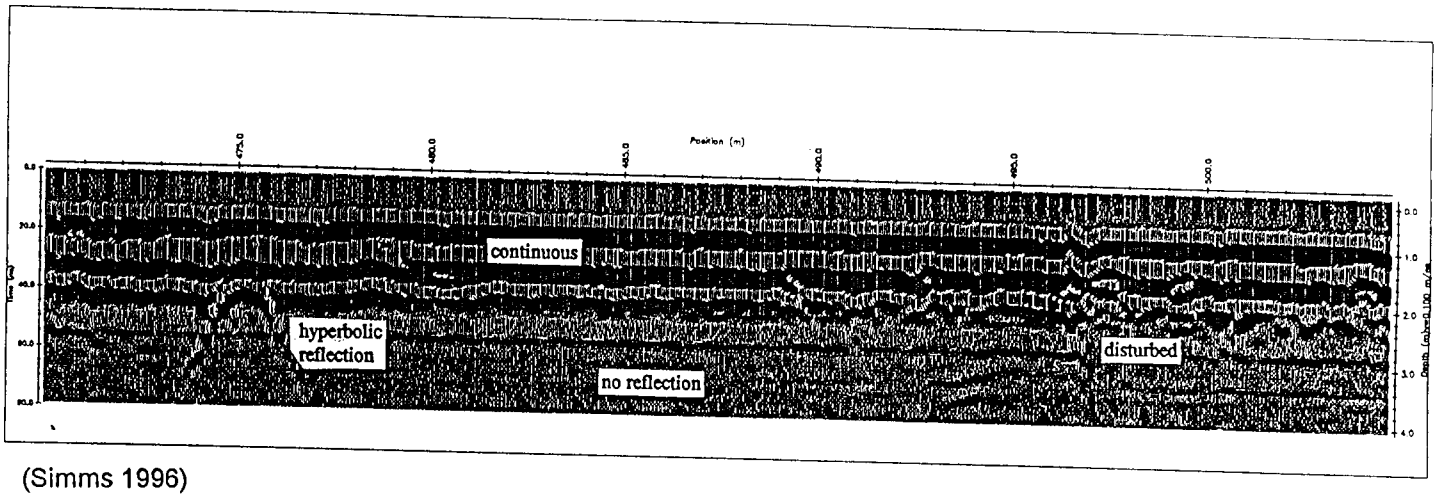

(Simms 1996)

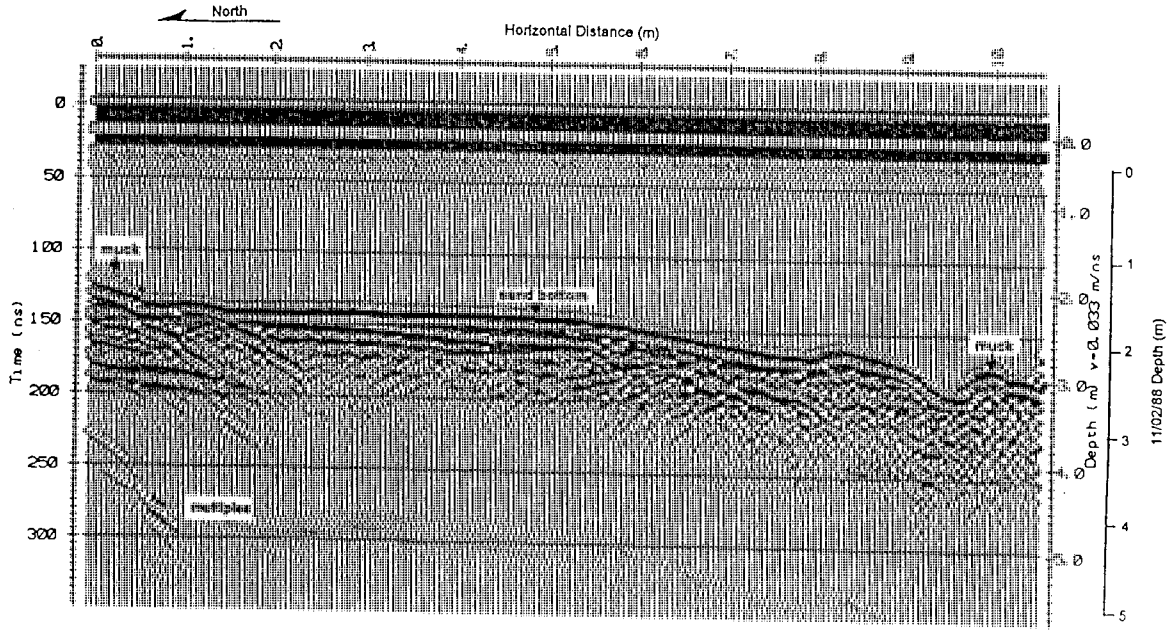

(Llopis and Sharp 1997)

Figure 15. Common features found on a GPR record

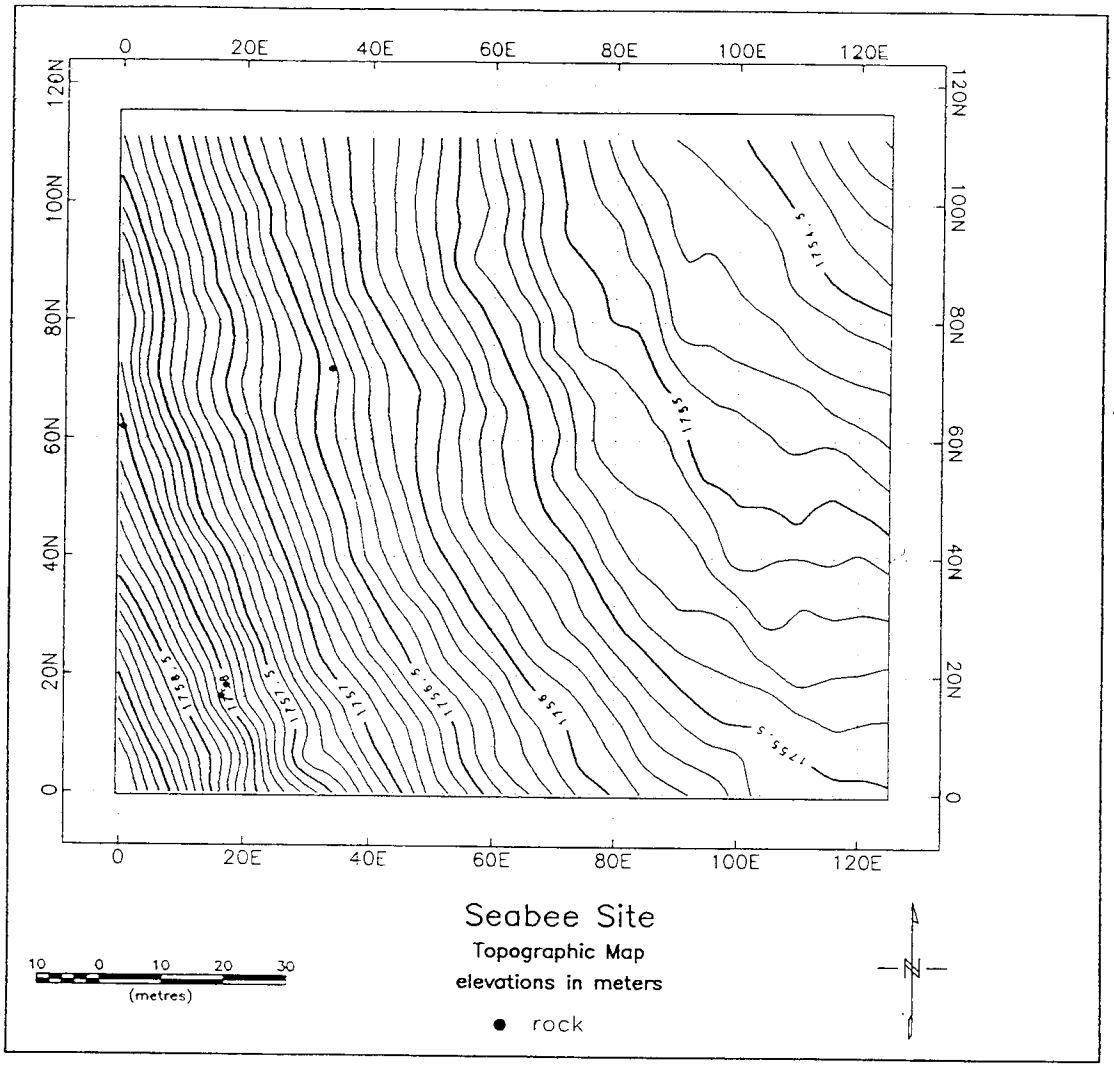

Figure 16. Topographic map, Seabee site, Fort Carson, CO

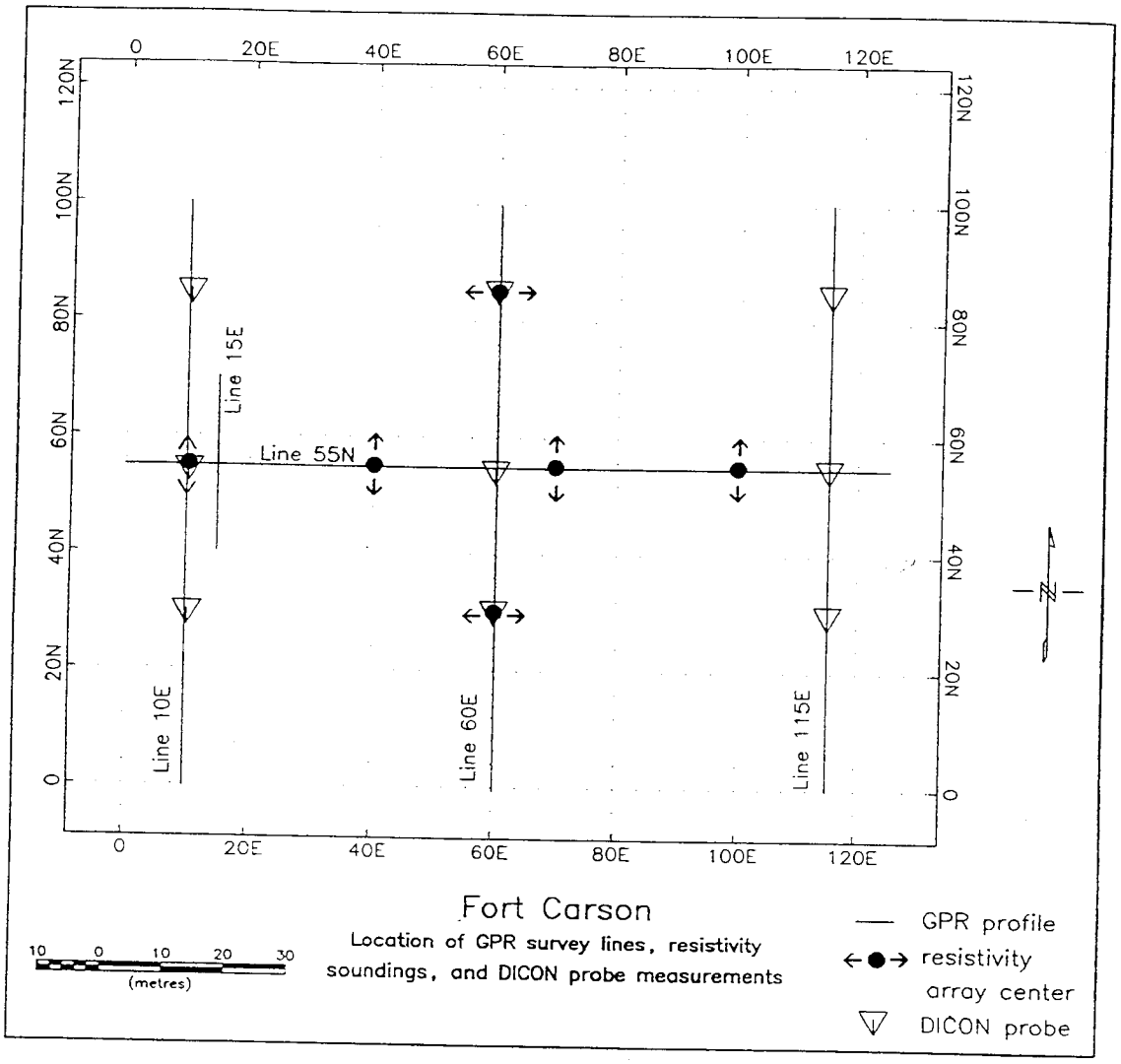

Figure 17. Location of resistivity soundings, GPR profiles, and DICON probe measurements at the Seabee and Turkey Creek sites, Fort Carson, CO

corresponding interpreted depth profile are provided in Appendix B. Figure 18 summarizes the interpreted resistivity–depth profiles. The interpreted layers do not exhibit a large variation in resistivity values. In general, the near-surface structure of the Seabee site can be characterized by four electrical layers: a thin (< 1 m) upper layer having a resistivity of 15 to 20 ohm-m; a more resistive (25–45 Ω-m) layer 1.4 to 3.6 m thick; a low resistivity (5–15 Ω-m) layer ranging from 1.8 to 3 m in thickness; and a slightly more resistive (10–15 Ω-m) underlying earth. The lower resistivity layers usually correspond to an increase in moisture and/or clay content. In terms of conductivity (inverse of resistivity), the magnitude of these values (20–200 mS/m) is comparable to the conductivity readings obtained using the DICON probe (Table 15). However, between the two measurement techniques there is no correlation of depth for which the conductivity values correspond. This discrepancy is attributed to the volume of material each measurement technique "sees". A resistivity sounding measurement is influenced by the hemisphere of soil bounded by the current electrodes, whereas the DICON probe measurement is only influenced by the material in the immediate vicinity of the probe. The DICON probe is sensitive to minor variations in soil moisture content.

EM31 results. The results of the EM31 inphase and conductivity surveys are presented in Figures 19 and 20, respectively. The inphase data (Figure 19) indicate an area of relatively low inphase values in the central portion of the site. The values decrease further towards the southeast part of the site. The inphase values have a fairly wide range and vary between approximately -5.25 and -3.00 ppt. The plot of the conductivity data (Figure 20) shows the same general trend as shown in the inphase plot; relatively high conductivity values surrounding a lobe-like pattern with lower conductivity values that extend from the center of the site towards the southeast corner. The general range of the conductivity data is 40 to 85 mS/m. These conductivity values are comparable to the resistivity sounding and DICON probe measurements. One relatively small anomalous feature is located at approximately (113E, 77N).

Magnetometer results. The results of the magnetometer survey are shown in Figure 21. The majority of the magnetometer values occur in a very narrow range between approximately 53,630 and 53,650 nT. The magnetometer results show numerous random to stripe-shaped anomalies[1], and one substantial, localized anomaly characterized by coupled high-low values located at approximately (5E, 8N). No general data trends are noted.

EM and magnetometer interpretation. The distribution and wide range of values displayed by the EM31 plots are indicative of varying soil and/or rock types in the upper 3 to 4 m. The low conductivity lobe that extends from the middle to the

1 The patchy to stripe-shaped anomalies oriented preferentially along the survey line direction result from (1) the difficulty in contouring nearly random, small variations in magnetic field strength (≅ 10 nT over the majority of the site) and (2) the data density is greater along the survey line than between survey lines.

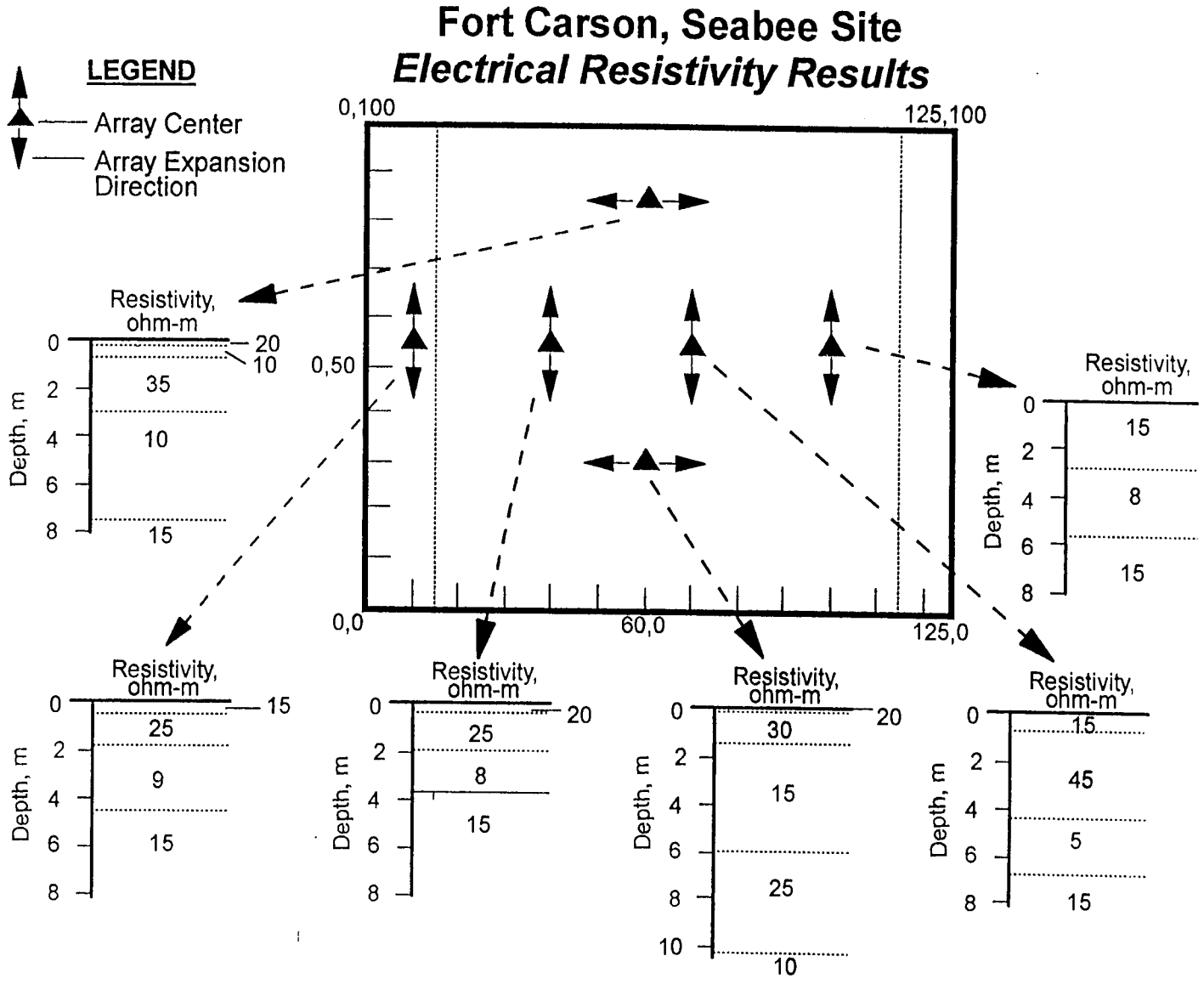

Figure 18. Model results of resistivity soundings, Seabee site, Fort Carson, CO

Table 15
DICON Probe Data, Seabee Site, Fort Carson, CO

Location	Depth (m)	Relative Dielectric Permittivity	Conductivity (mS/m)	Wave Speed (m/ns)
10E, 30N	0.1	24	75	0.061
	0.3	38	151	0.049
	0.5	36	136	0.050
10E, 55N	0.1	20	67	0.067
	0.3	31	122	0.054
	0.5	35	135	0.051
10E,85N	0.1	14	41	0.080
	0.3	32	135	0.053
	0.5	34	135	0.051
60E, 30N	0.1	22	66	0.064
	0.3	29	91	0.056
	0.5	28	80	0.057
60E, 55N	0.1	24	84	0.061
	0.3	26	82	0.059
	0.5	38	136	0.049
60E, 85N	0.1	23	79	0.063
	0.3	28	103	0.057
	0.5	41	164	0.047
115E, 30N	0.1	32	100	0.053
	0.3	38	131	0.049
	0.5	36	118	0.050
115E, 55N	0.1	37	111	0.049
	0.3	30	94	0.055
	0.5	40	141	0.047
115E, 85N	0.1	39	152	0.048
	0.3	32	110	0.053
	0.5	46	192	0.044

southeastern corner of the site may be caused by a decrease in the clay content of the soil. The variability in soil conductivity is not assumed to be attributable to changes in the magnetic mineral content of the soil since the magnetometer values exhibit little variation throughout the site. The anomaly detected by the EM31 at location (113E, 77N) is likely caused by a non-ferrous metallic object since it was not detected by the magnetometer. The numerous elongated, low-valued, magnetic anomalies occurring predominantly between lines 38E and 70E are judged to be spurious values and not caused by ferrous objects. However, the magnetic anomaly at approximately (5E, 8N) is considered to be caused by a buried ferrous object, likely too deep or too small to significantly affect the lower resolution inphase and conductivity EM31 measurements.

GPR results. Five grid lines were either partially or totally profiled using GPR at the Seabee site. Locations of the survey lines are shown in Figure 17. Lines 10, 15, 60, and 115 were profiled in the north-south direction, whereas line 55 was surveyed

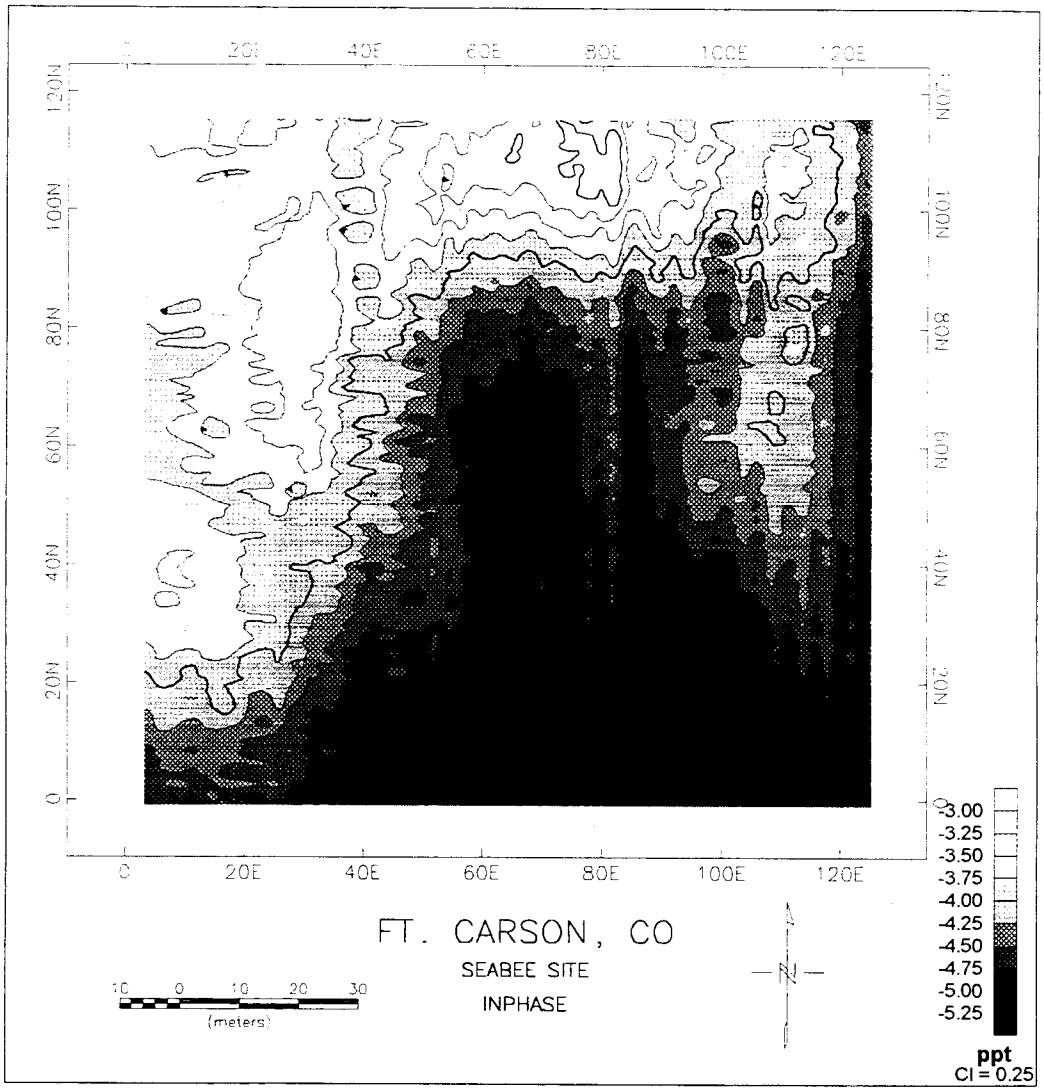

Figure 19. Results of inphase survey, Seabee site, Fort Carson, CO

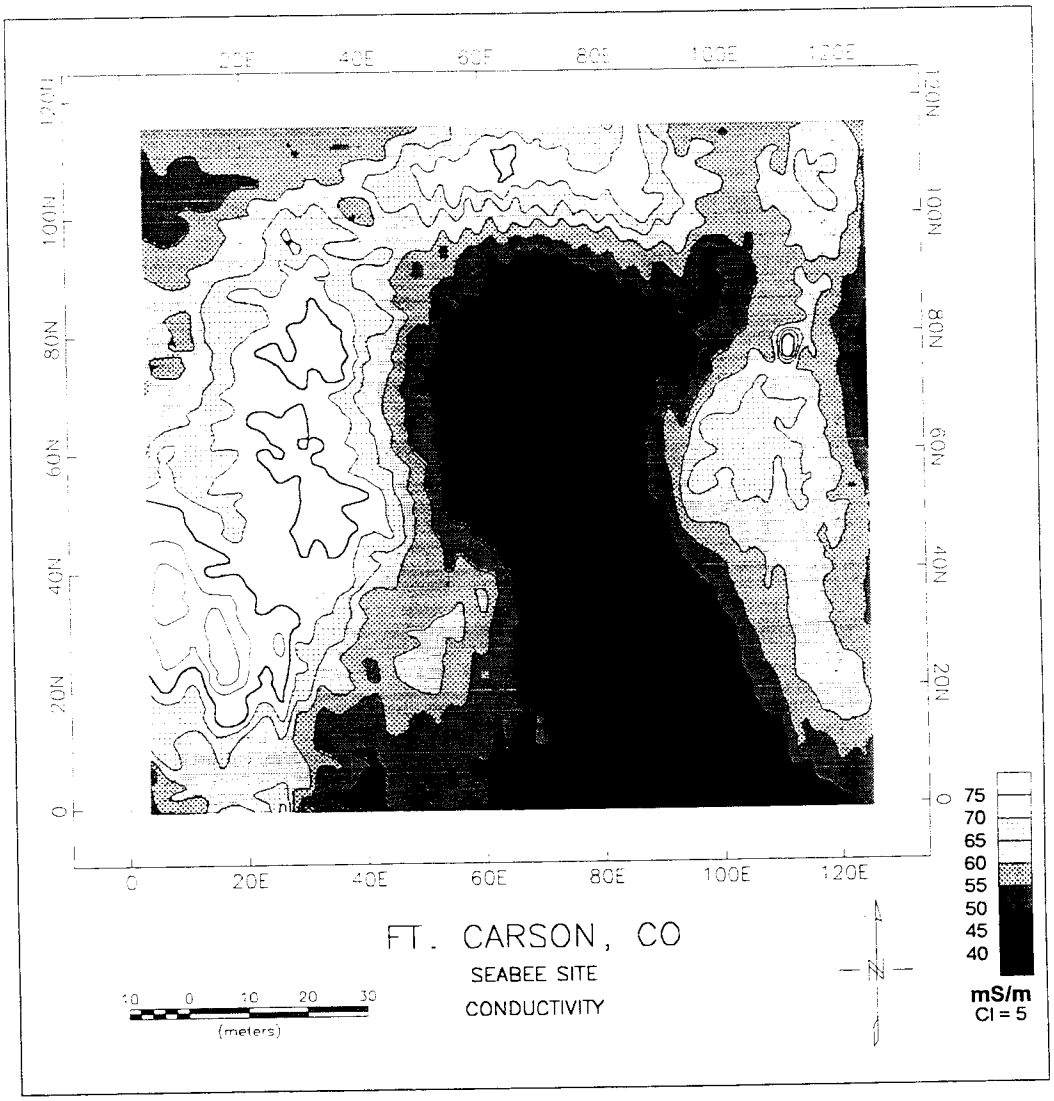

Figure 20. Results of conductivity survey, Seabee site, Fort Carson, CO

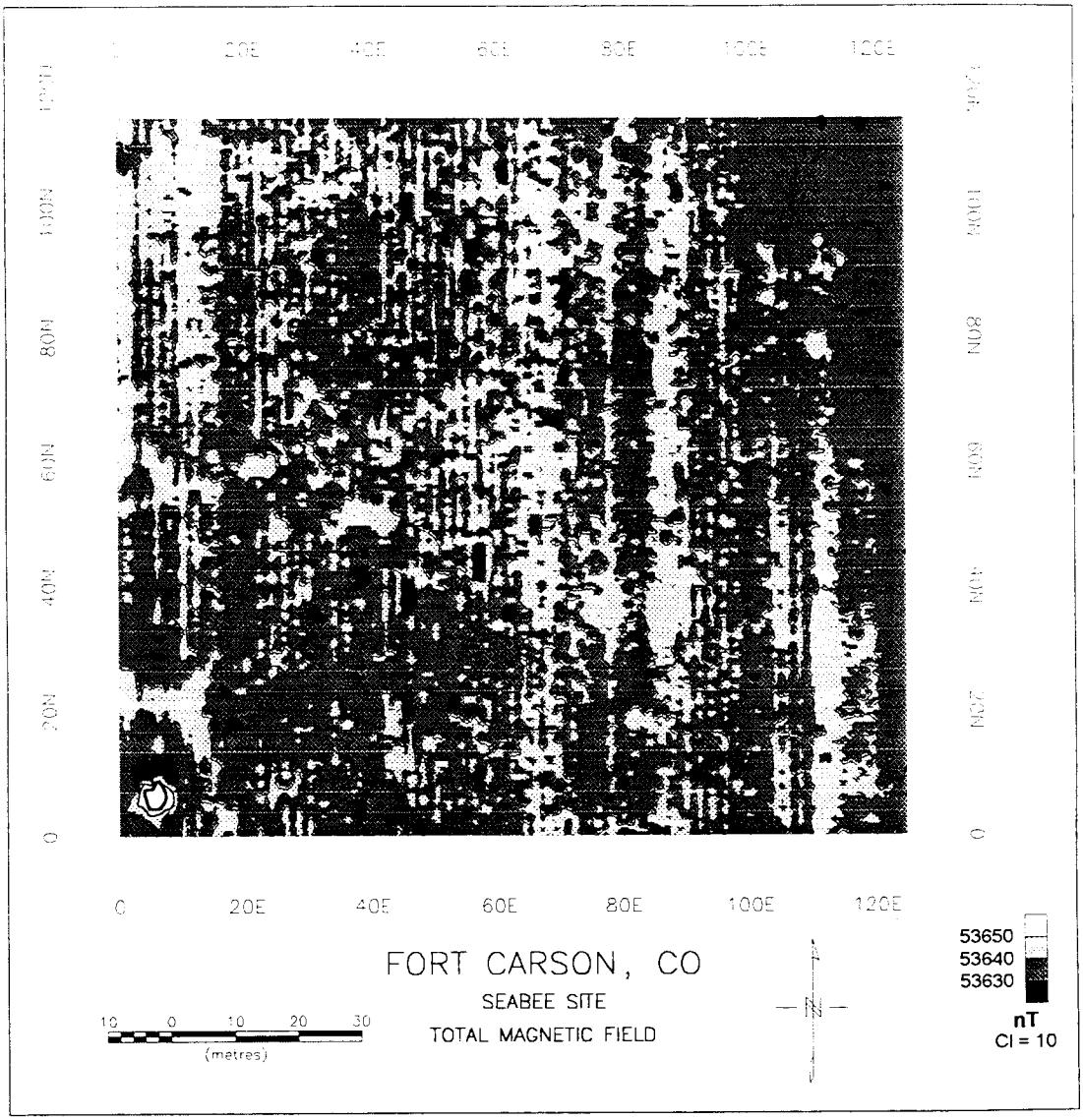

Figure 21. Results of magnetometer survey, Seabee site, Fort Carson, CO

east-west. The 50, 200, and 900 MHz antennas were used along lines 60E, 115E, and 55N; 50 and 200 MHz along line 10E; and 900 MHz along line 15E. The 900 MHz antenna was only run along a 30 m section of the line. A total of twelve GPR profile lines were collected at this site and are compiled in Appendix C. The high soil conductivities at this site were not conducive for GPR and signal penetration did not exceed 1.6 m with the 50 MHz antenna. A review of the conductivity values obtained for the upper half meter of soil using the DICON probe (Table 15) indicate a minimum conductivity value of 41 mS/m, with values often exceeding 75 mS/m. The EM31 data also indicate conductivity values between 40 and 85 mS/m. The practicality of performing higher frequency (> 80 MHz) GPR surveys is questionable when the near-surface soil conductivity exceeds 35 mS/m because of the reduction in signal penetration and resolution. Representative GPR profiles obtained at this site are presented in Figure 22. These data were collected along line 60E using the 50, 200, and 900 MHz antenna (Figure 22a, b, and c, respectively). Although the quality of the data is poor, the decrease in depth of investigation and increase in resolution as antenna frequency increases is observed. The 50 MHz data identify a continuous reflector at a depth of 1.6 m with a broad anomaly beneath station 33 meters north. (In subsequent references to GPR station locations, only the station number will be given, meters north is inferred). Two reflectors are mapped with the 200 MHz antenna, one at a depth of 0.4 m and the other at 1.2 m. The 900 MHz antenna has a much shallower depth of investigation, less than 20 cm at this site; a discontinuous reflector is seen at about 8 cm depth. Some similarity in subsurface structure within the upper 2 m is observed between the GPR and electrical resistivity data. Compare the layer depths obtained using GPR (0.08, 0.4, 1.2, and 1.6 m) with those from the resistivity soundings in Figure 18. GPR gives a more detailed picture of the shallow subsurface than electrical resistivity, however, resistivity soundings are helpful in providing a broader view of both the shallower and deeper layer structure.

Turkey Creek site

Site description. Figure 7 shows the location of the Turkey Creek site. The topographic map (Figure 23) shows that this site is approximately 200 m higher in elevation than the Seabee site. Elevation at the site increases about 5 m from the southeast to the northwest. Numerous rocks are located in the eastern half of the grid. The location of the resistivity soundings, GPR profiles, and DICON probe measurements are shown in Figure 17.

Electrical resistivity results. Six resistivity soundings were conducted at Turkey Creek and the sounding data with interpreted depth profiles are provided in Appendix E. The resistivity–depth sections (Figure 24) indicate that the near-surface soil can reasonably be described using three electrical layers: a thin (< 1 m) upper layer having a resistivity of 20 to 25 ohm-m, and a 1.5 to 4 m thick high resistivity layer (> 290 Ω-m) underlain by a moderately resistive earth (50 to 65 Ω-m). The site appears to be more complex beneath the western half, where a low resistivity layer (~30 Ω-m) is present below the high resistivity layer. Resistivity values are higher at the Turkey Creek site than the Seabee site, with the major distinction being the presence of the high resistivity layer at about 1 m depth. A comparison of the near-surface resistivity values (conductivities of 40–50 mS/m) with the DICON probe conductivity data (Table 16) shows that only the

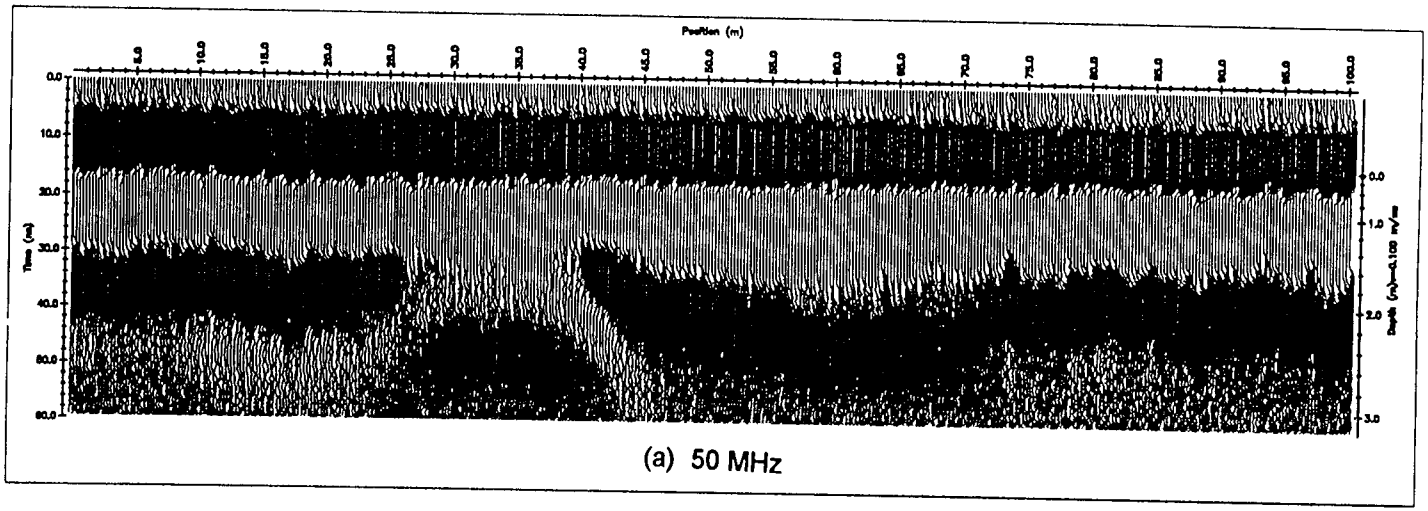

Figure 22. GPR profiles (north-south), line 60E, Seabee site, Fort Carson, CO.
a) 50 MHz, b) 200 MHz, c) 900 MHz

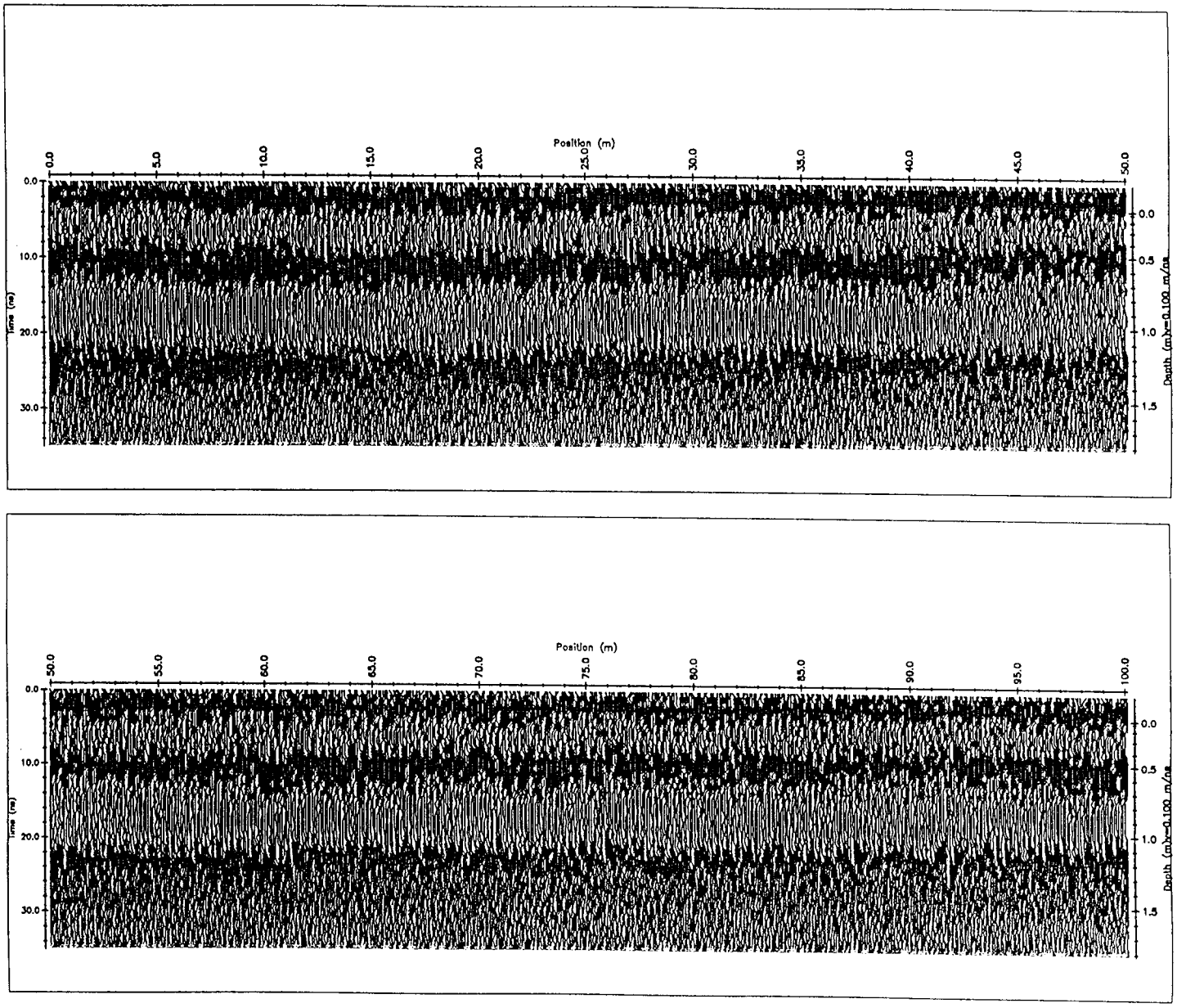

Figure 22. Continued. (b) 200 MHz

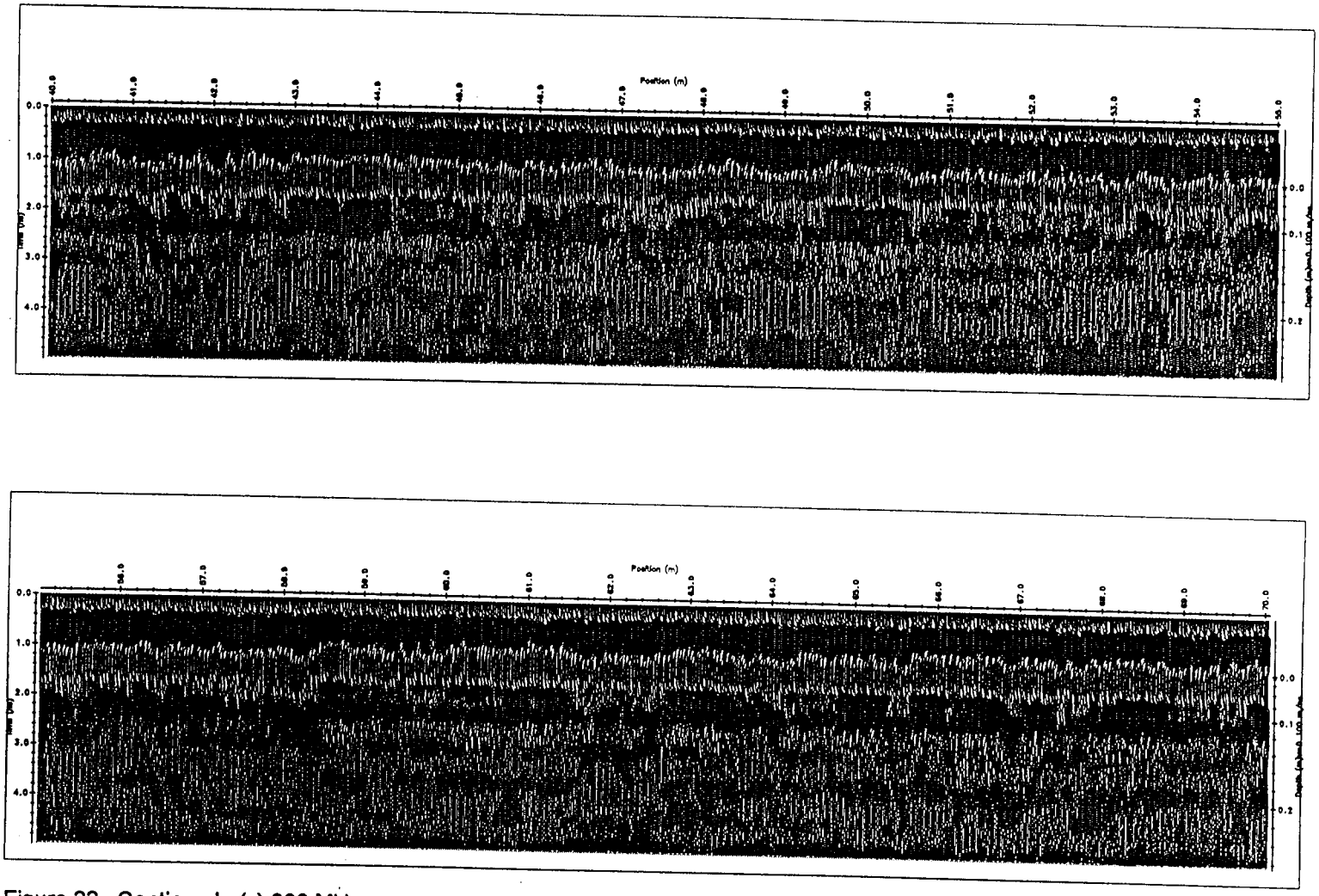

Figure 22. Continued. (c) 900 MHz

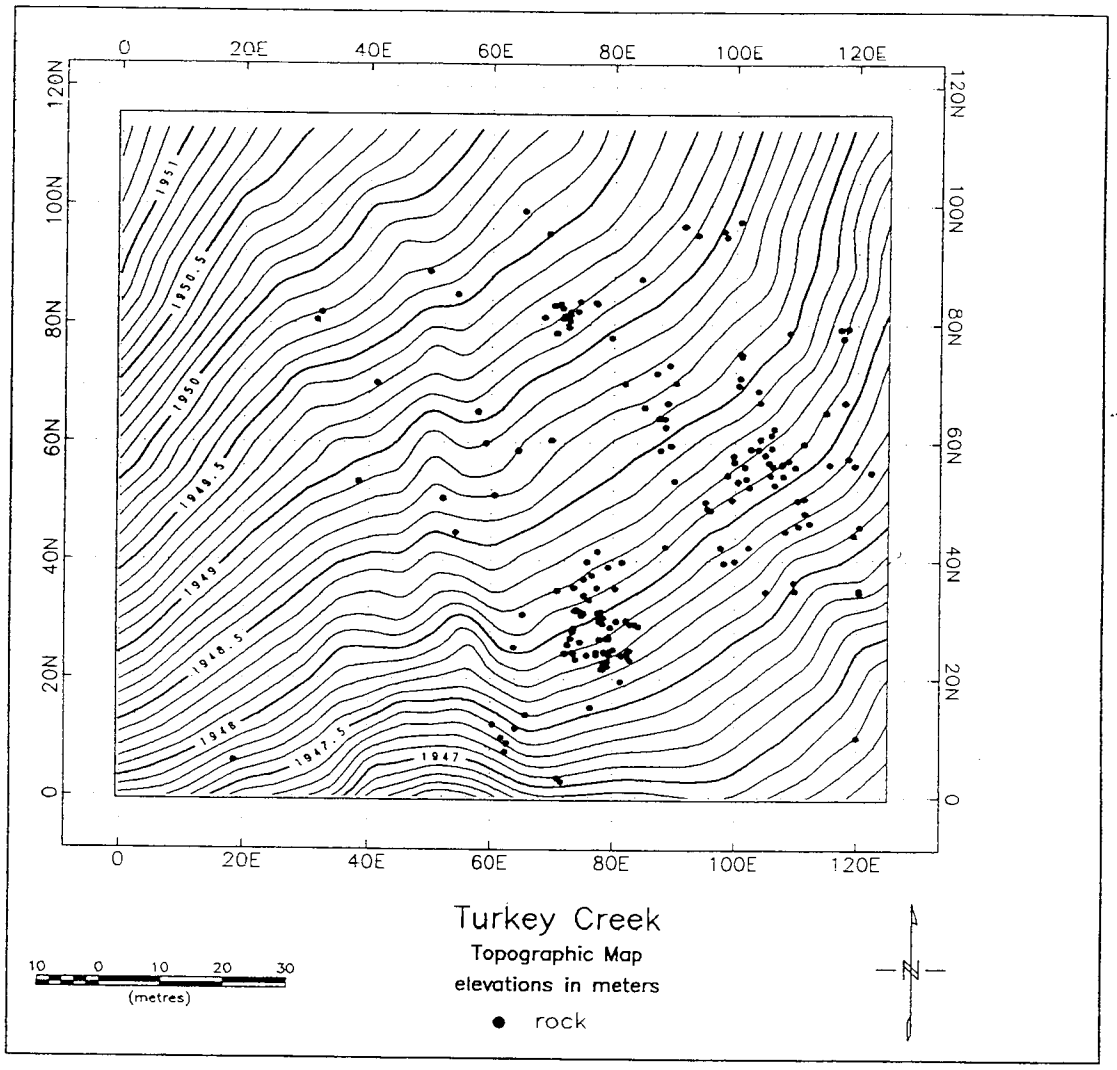

Figure 23. Topographic map, Turkey Creek site, Fort Carson, CO

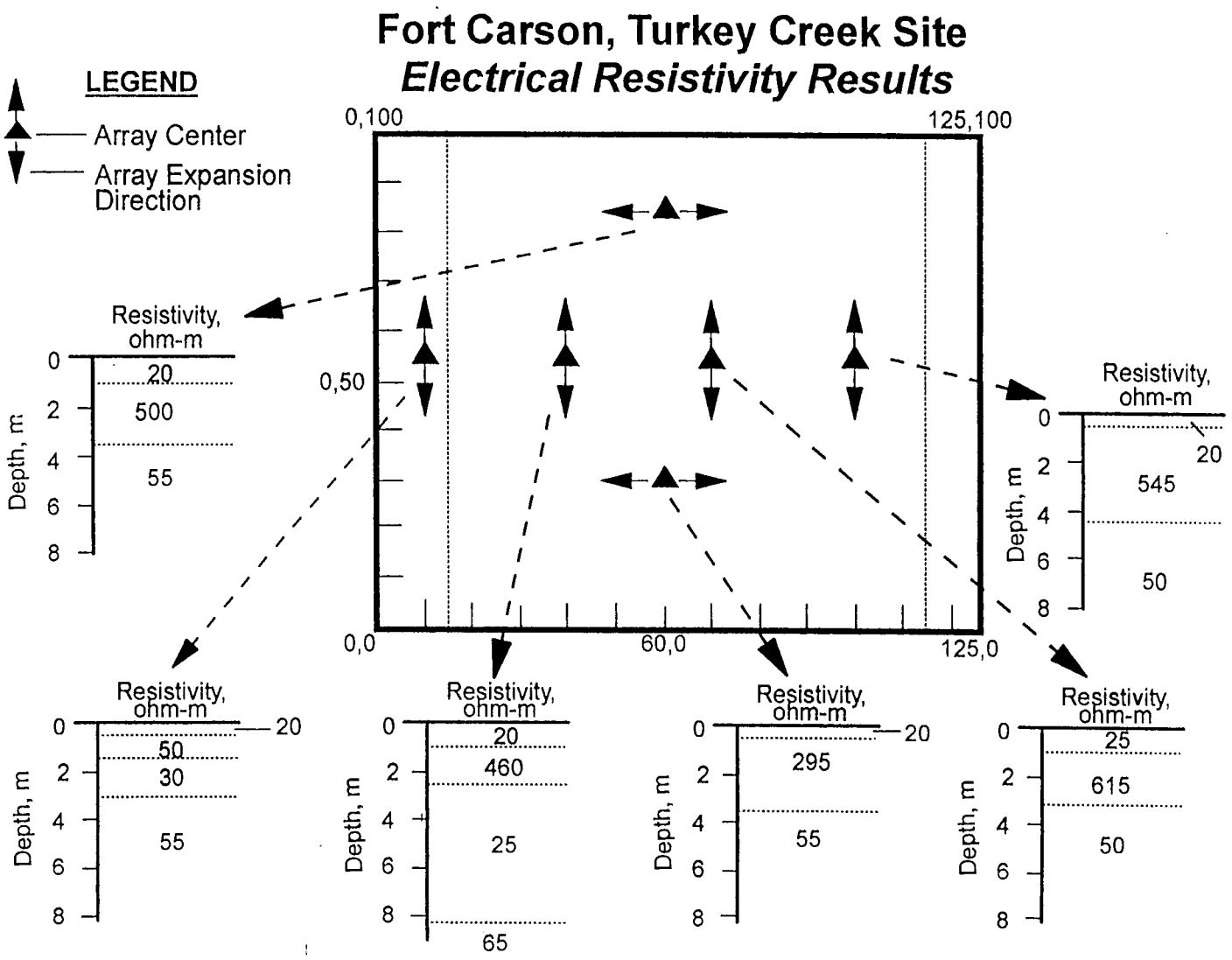

Figure 24. Model results of resistivity soundings, Turkey Creek site, Fort Carson, CO

Table 16
DICON Probe Data, Turkey Creek, Fort Carson, CO

Location	Depth (m)	Relative Dielectric Permittivity	Conductivity (mS/m)	Wave Speed (m/ns)
10E, 30N	0.1	12	12	0.087
	0.3	26	98	0.059
	0.5	28	98	0.057
10E, 55N	0.1	13	36	0.083
	0.3	23	78	0.063
	0.5	26	86	0.059
10E,85N	0.1	13	35	0.083
	0.3	33	113	0.052
	0.5	35	125	0.051
60E, 30N	0.1	12	30	0.087
	0.3	27	95	0.058
	0.5	31	109	0.054
60E, 55N	0.1	11	23	0.090
	0.3	28	89	0.057
	0.5	25	71	0.060
60E, 85N	0.1	15	39	0.077
	0.3	28	95	0.057
	0.5	38	145	0.049
115E, 30N	0.1	15	41	0.077
	0.3	34	130	0.051
	0.5	31	117	0.054
115E, 55N	0.1	17	51	0.073
	0.3	18	52	0.071
	0.5	20	61	0.071
115E, 85N	0.1	10	21	0.095
	0.3	27	76	0.058
	0.5	10	18	0.095

measurements taken at 10 cm depth are in agreement; the deeper probe measurements were greatly affected by a slight decrease in moisture content.

EM31 results. The results of the EM31 inphase and conductivity surveys are presented in Figures 25 and 26, respectively. These data indicate a gradual decrease in values towards the east and northeast. The EM31 plots show background inphase and conductivity values of approximately 3.5 to 4.5 ppt and 10 to 35 mS/m, respectively. Two small anomalies are shown at approximately (73E, 64N) and (117E, 98N) in the inphase plot. In contrast, the conductivity plot does not detect the anomaly located at (117E, 98N) and shows little variation at (73E, 64N). The range of EM31 conductivity values is in general agreement with the resistivity sounding models.

Magnetometer results. The results of the magnetometer survey are shown in Figure 27. The majority of the magnetometer values occur in a relatively narrow

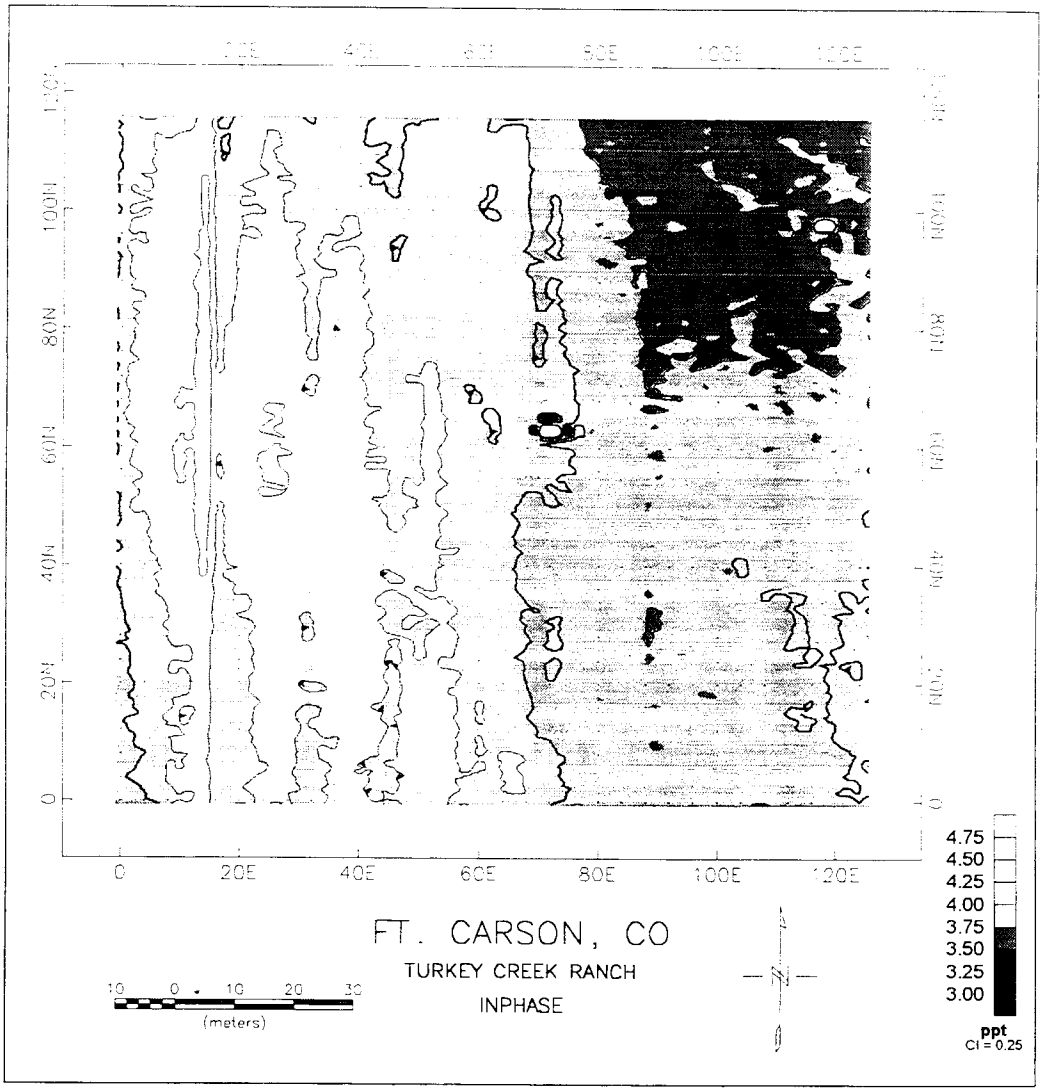

Figure 25. Results of inphase survey, Turkey Creek site, Fort Carson, CO

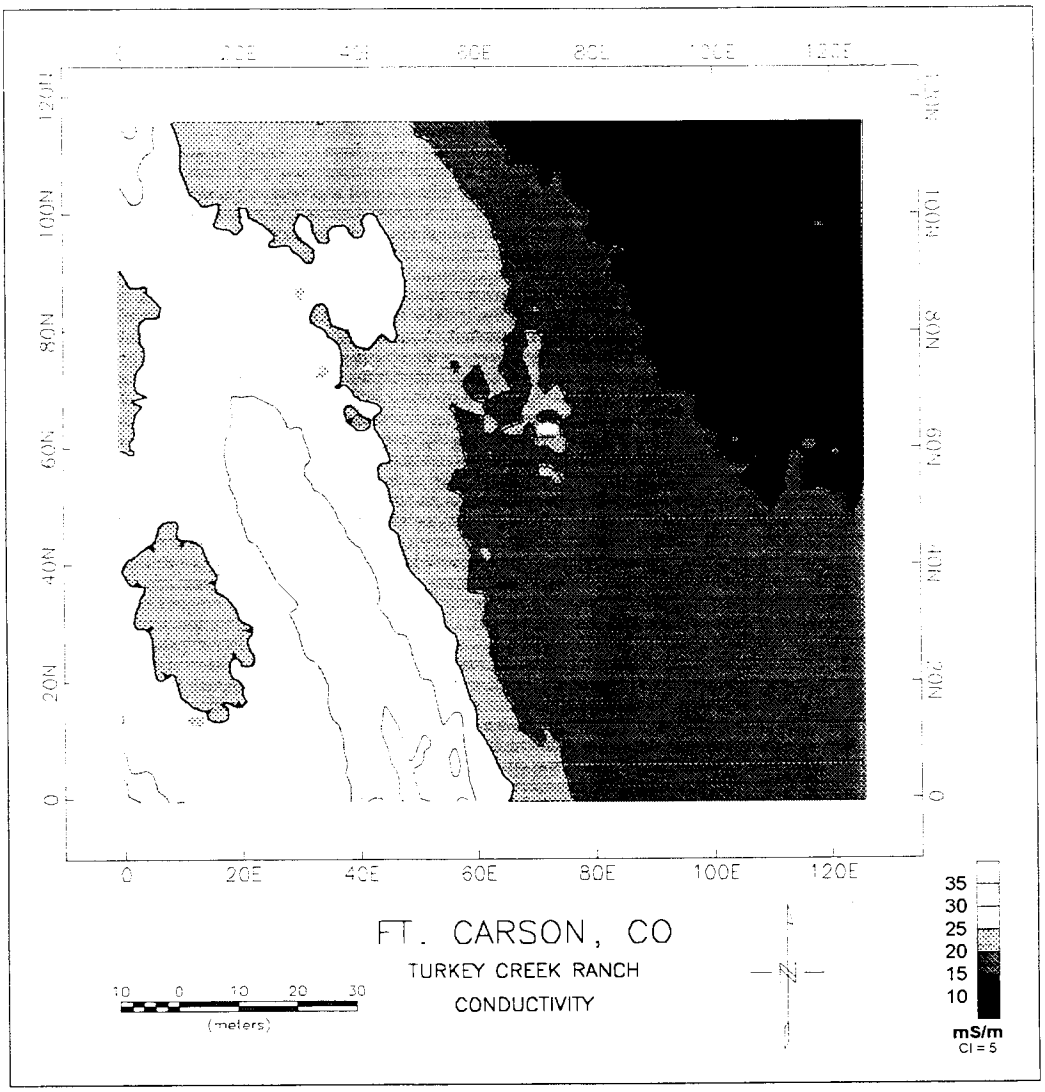

Figure 26. Results of conductivity survey, Turkey Creek site, Fort Carson, CO

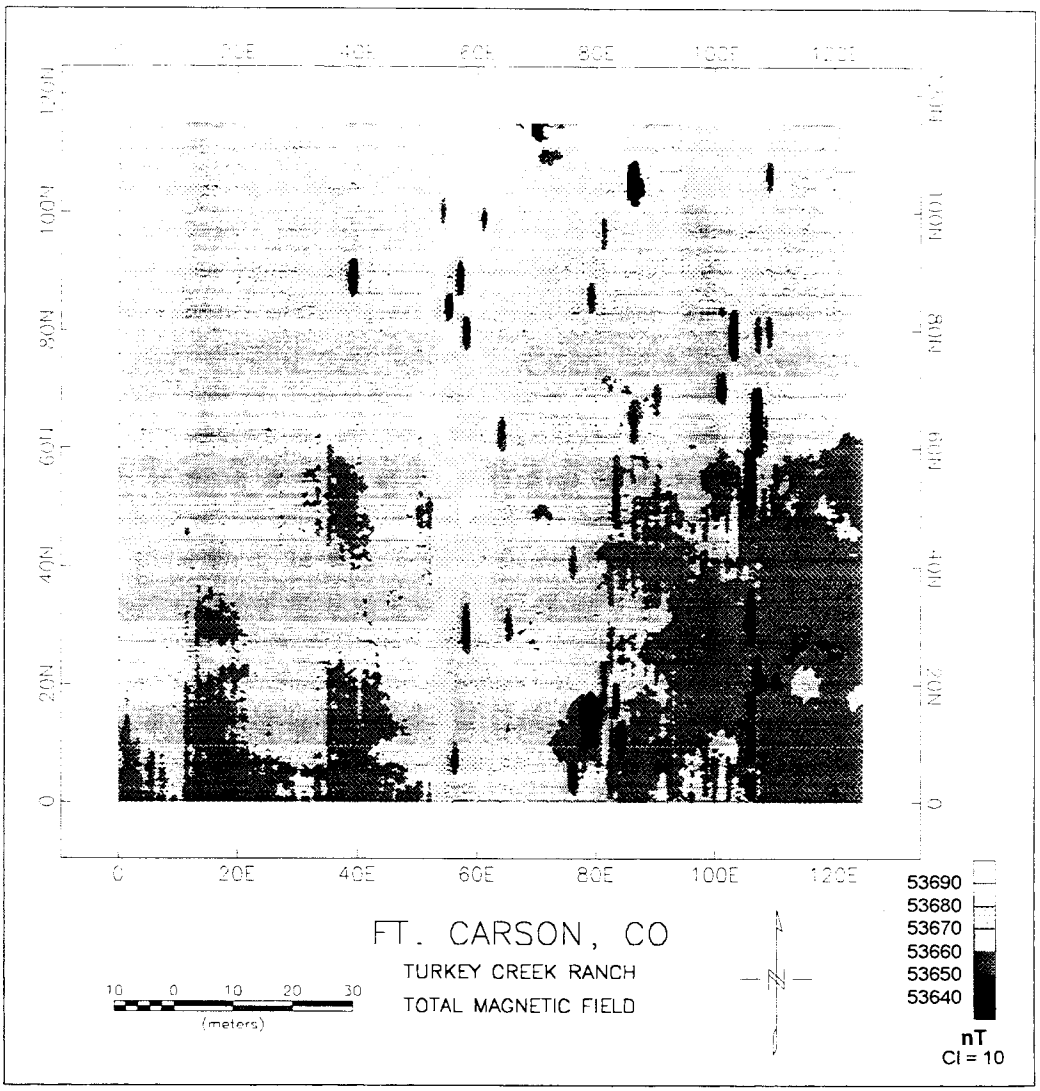

Figure 27. Results of magnetometer survey, Turkey Creek site, Fort Carson, CO

band which range between 53,650 and 53,680 nT. The magnetometer results show numerous low-valued anomalies. No general trends in the data are noted.

EM and magnetometer interpretation. The distribution and range of values displayed by the EM31 plots are indicative of varying soil and/or rock type in the upper 3 to 4 m. The decrease in conductivity values to the east-northeast may be caused by a decrease in the clay content of the soil. The trend in the EM values do not appear to reflect the general topography of the site. For instance, the elevation gradient trends basically in a northwest-southeast orientation while the EM gradient has a northeast-southwest trend. The variability in the soil conductivity is not assumed to be attributable to changes in the magnetic mineral content of the soil since the magnetometer values are fairly constant across the site. The anomalies detected with the EM31 at locations (73E, 64N) and (117E, 98N) are presumed to be caused by small non-ferrous metallic objects since they were not detected with the magnetometer. The numerous elongated, low-valued, magnetic anomalies occurring predominantly between lines 58E and 107E are judged to be spurious values and not caused by ferrous objects.

GPR results. The locations of the GPR profile lines are shown in Figure 17. Four lines (10E, 60E, 115E, 55N) were surveyed using three antenna frequencies (50, 200, 900 MHz). Appendix F contains the radar records for each line surveyed. The DICON probe results (Table 16) indicate that the near-surface (< 10 cm) soil is much less conductive than the soil below. The depth of investigation is comparable to that obtained at the Seabee site. Radar records collected along line 60E are plotted in Figure 28. A prominent reflector at a depth of 1 m is evident in the 50 MHz data. This same reflector is detected with the 200 MHz antenna, along with a shallower layer at 0.3 m depth. It is questionable if the reflection at 35 ns is a soil layer, or if it is a multiple involving these two reflectors. Several hyperbolic reflections are easily seen in the 900 MHz record; rocks are a likely source of these reflections since large rocks are scattered on the surface and in the subsurface (observed in nearby stream channel walls). The continuity of the reflector at 6 cm depth is interrupted by some hyperbolic reflections (e.g. stations 57.8 and 59). The reflectors at 0.3 and 1 m depth mapped using GPR correlate with the 0.4/0.5 and 1 m layers modeled from the electrical resistivity data (Figure 24).

Fort A. P. Hill, Virginia

Firing Point 20

Site description. The location of Firing Point 20 is shown in Figure 13. There is little variation in topography (less than 1 m) at the site (Figure 29), however numerous holes and tire ruts are present. The signature of these surface features generally masks any shallow subsurface features in the GPR records. Figure 30 shows the locations of the electrical resistivity soundings, GPR profiles, and DICON probe measurements. Fewer electrical resistivity soundings were performed at Fort A. P. Hill (three rather than six) because it was deemed that three soundings would adequately characterize the resistivity background.

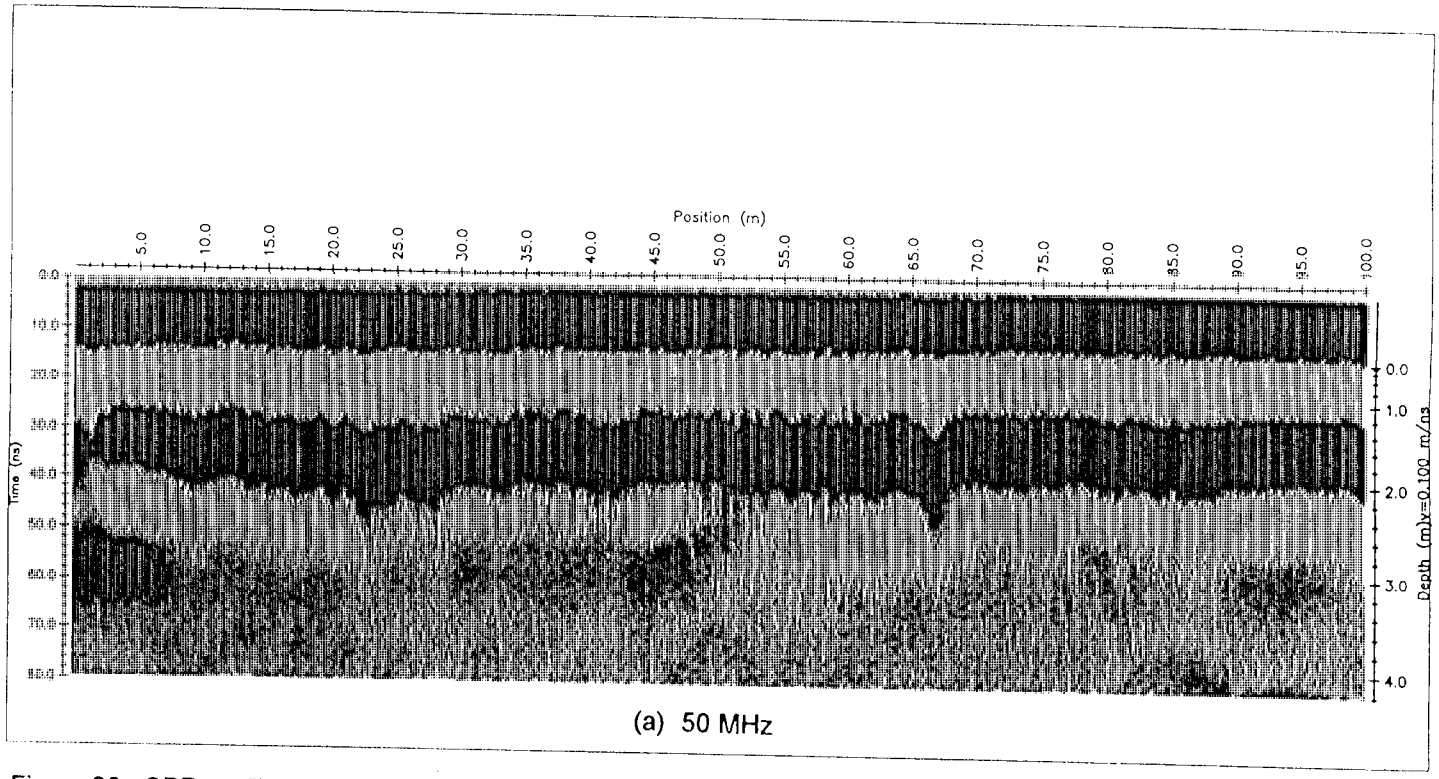

Figure 28. GPR profiles (north-south), line 60E, Turkey Creek site, Fort Carson, CO
a) 50 MHz, b) 200 MHz, c) 900 MHz

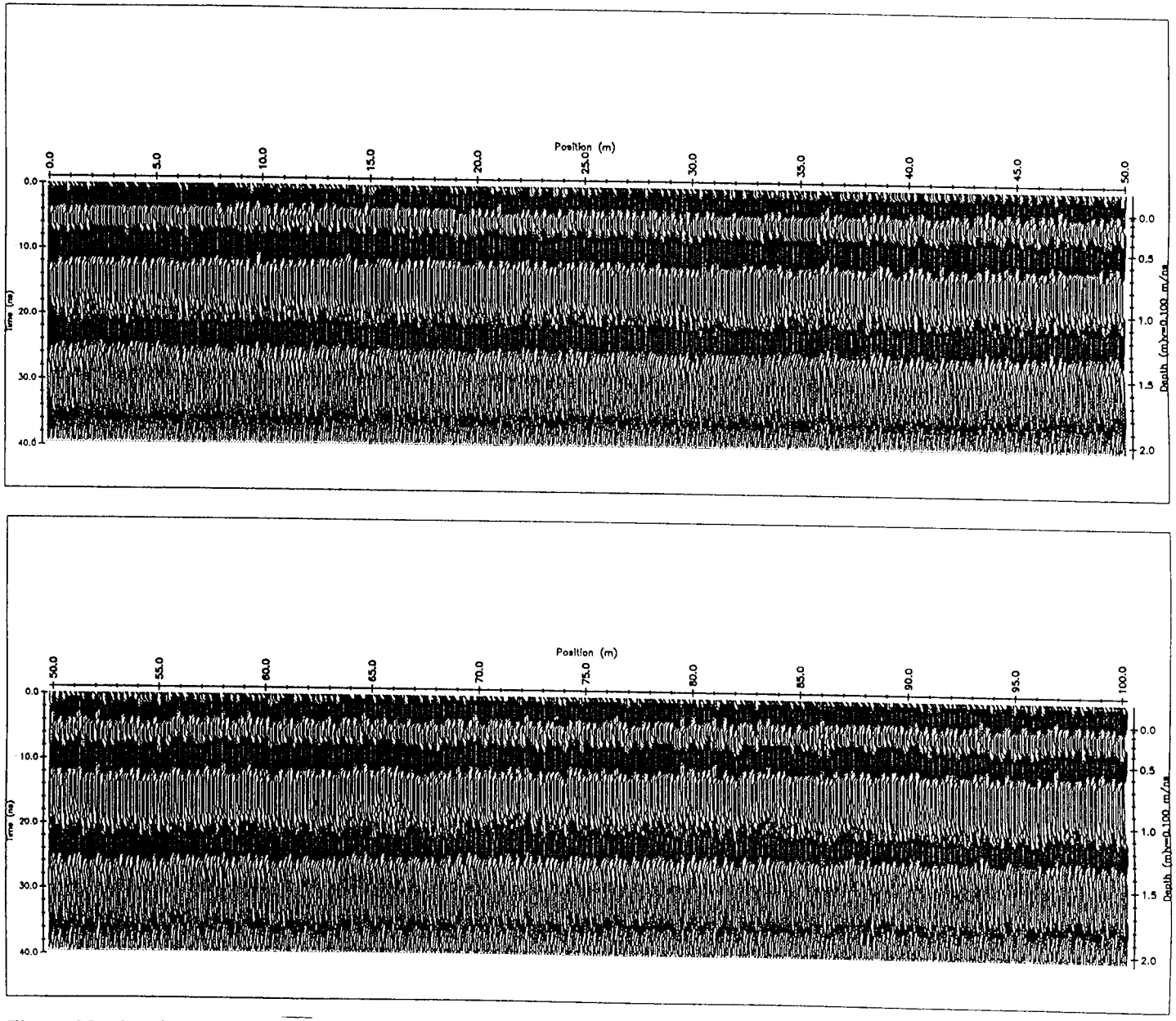

Figure 28. Continued. (b) 200 MHz

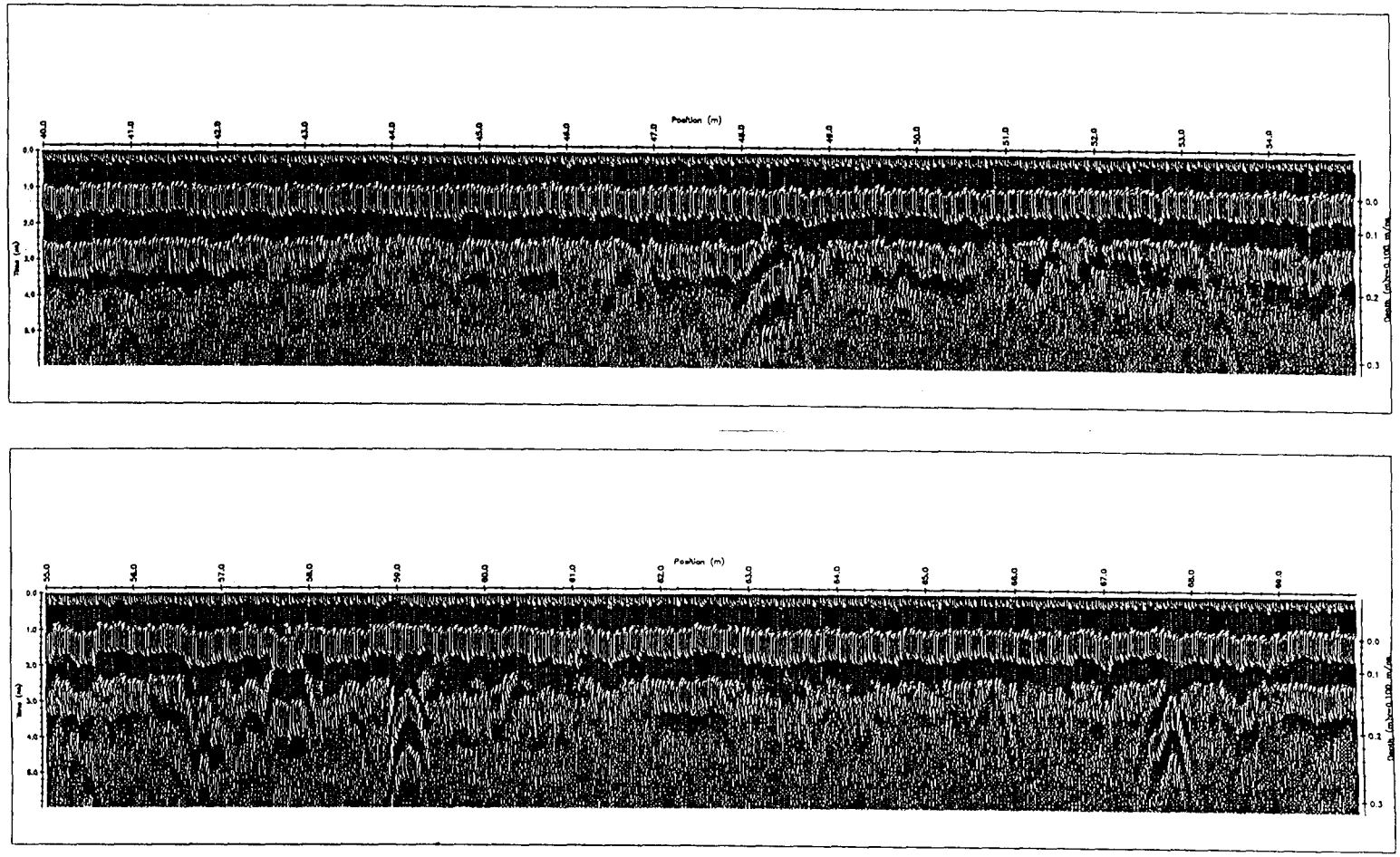

Figure 28. Continued. (c) 900 MHz

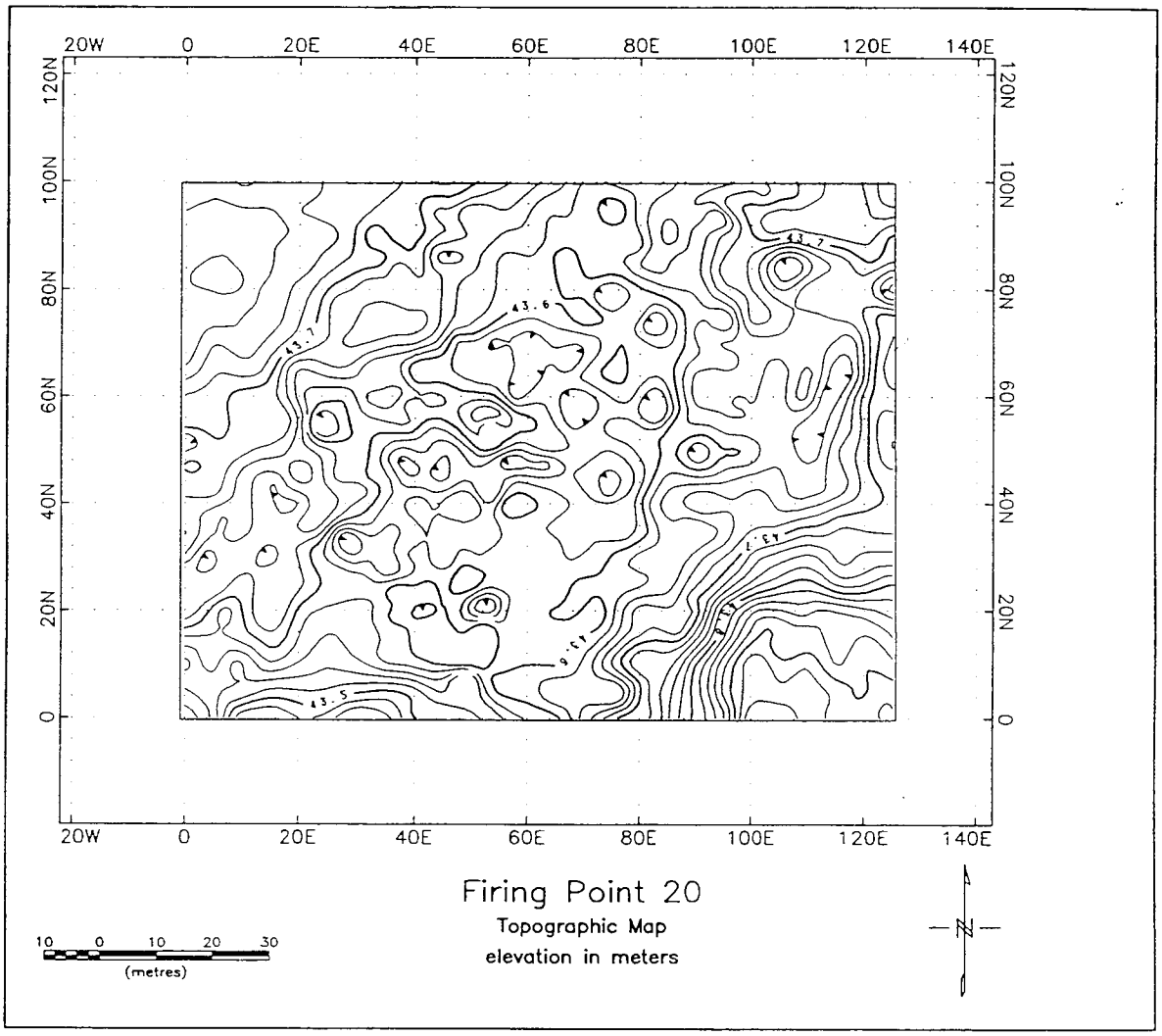

Figure 29. Topographic map, Firing Point 20, Fort A. P. Hill, VA

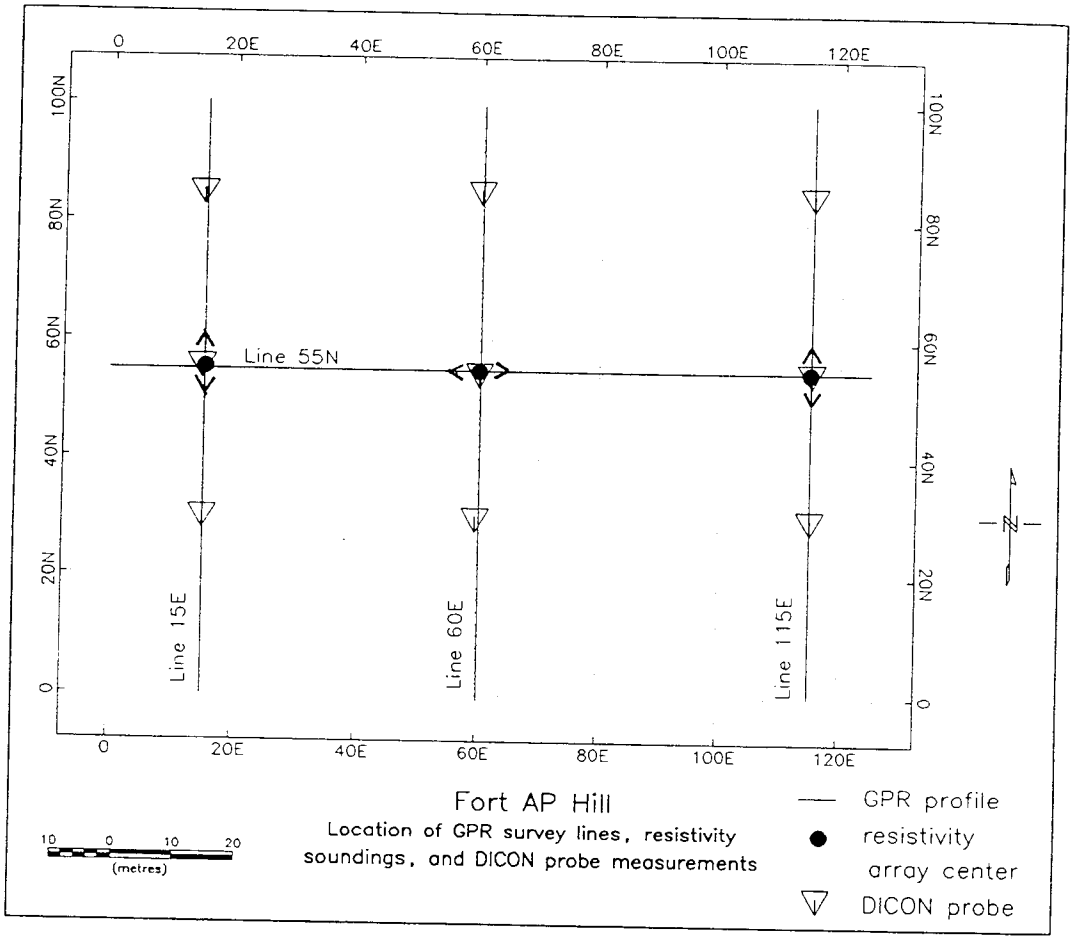

Figure 30. Location of resistivity soundings, GPR profiles, and DICON probe measurements, Firing Points 20 and 22, Fort A. P. Hill, VA

Electrical resistivity results. The location and orientation of the three resistivity soundings performed at Firing Point 20 are shown in Figure 30. Plots of the sounding data and best-fit layer models are provided in Appendix H. A three layer earth was used to model the resistivity sounding data collected near the eastern end of the site, whereas four layers were better suited for the central and western portions of the site (Figure 31). The four electrical layers include a thin, high resistivity layer near the surface (thickness 20–30 cm, > 850 Ω-m); a lower resistivity (300–600 Ω-m) layer 1.4 to 2 m thick; and a 5 to 15 m thick high resistivity (> 1000 Ω-m) layer underlain by a much lower resistivity (90 Ω-m) soil. The three-layer model lacks the high resistivity surface layer. These resistivity values are considerably higher than those at Fort Carson.

EM31 results. The results of the EM31 inphase and conductivity surveys are presented in Figures 32 and 33, respectively. The inphase and conductivity data show very little variability across the site and no general trends are obvious. The background inphase values range between -1.5 and -2.0 ppt, whereas the conductivity values lie within a range of 2 and 4 mS/m. Evident in both plots are two very prominent linear and nearly parallel anomalies oriented roughly in a northeast-southwest direction. The southern anomaly stretches between approximately (20E, 65N) and (125E, 100N), whereas the northern anomaly extends between (0E, 80N) and (80E, 100N). The two anomalies are spaced approximately 15 to 20 m apart. Two other less distinct, linear and parallel features with a northeast-southwest orientation can also be discerned. The western anomaly extends from (80E, 0N) to (115E, 85N) and the eastern anomaly lies between (95E, 0N) and (120E, 85N). These two anomalies are spaced approximately 10 m apart. The EM31 inphase and conductivity surveys also indicate numerous small anomalies, both in magnitude and spatial extent, scattered across the site. The locations of most of the small anomalies shown in the inphase plot also coincide with those found in the conductivity survey plot. The EM31 inphase and conductivity results indicate a large anomalous area in the northwestern corner of the site and an anomalous area in the southwestern corner. The low background conductivity values obtained using the EM31 agree well with the high resistivity layers modeled from the electrical sounding data. However, the shallow DICON probe measurements were influenced by the higher moisture content of the near-surface soil (upper 0.5 m), resulting in higher conductivity values (Table 17).

Magnetometer results. The results of the magnetometer survey are shown in Figure 34. Background magnetic values range between approximately 53,490 and 53,500 nT. No significant trends in the data are evident. The two linear anomalies detected by the EM31 between locations (80E, 0N) and (115E, 85N), and (95E, 0N) and (120E, 85N) are also detected by the magnetometer. The linear anomaly detected with the EM31 between (20E, 65N) and (125E, 100N) can barely be discerned in the plot of the magnetometer results, whereas the linear anomaly to the north, (0E, 80N)–(80E, 100N), is not detected. The magnetometer results also show numerous anomalies characterized by coupled high-low values such as occur at (8E, 55N), (10E, 40N), and (38E, 5N). Most of these small anomalies coincide with the location of the small anomalies detected with the EM31.

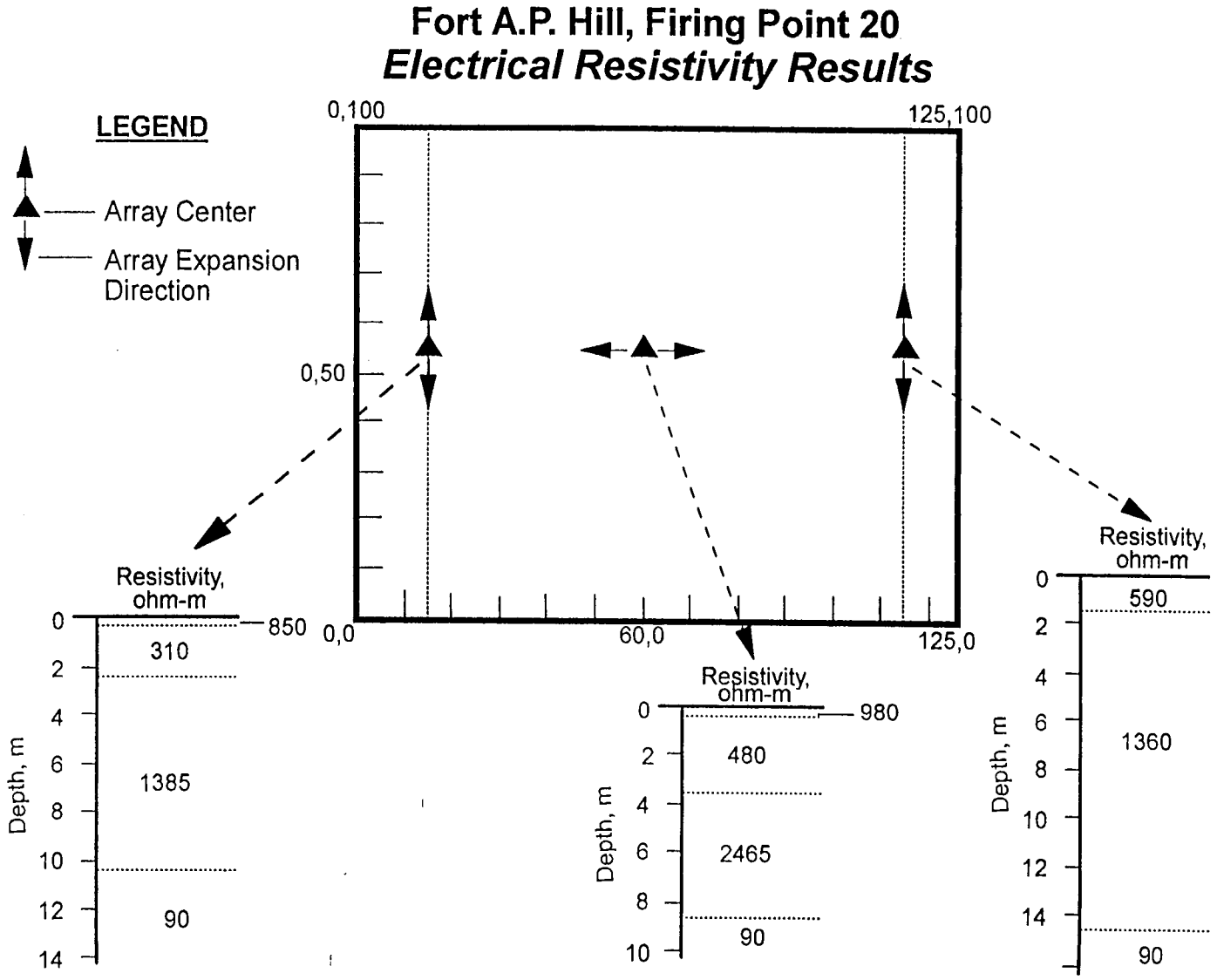

Figure 31. Model results of resistivity soundings, Firing Point 20, Fort A. P. Hill, VA

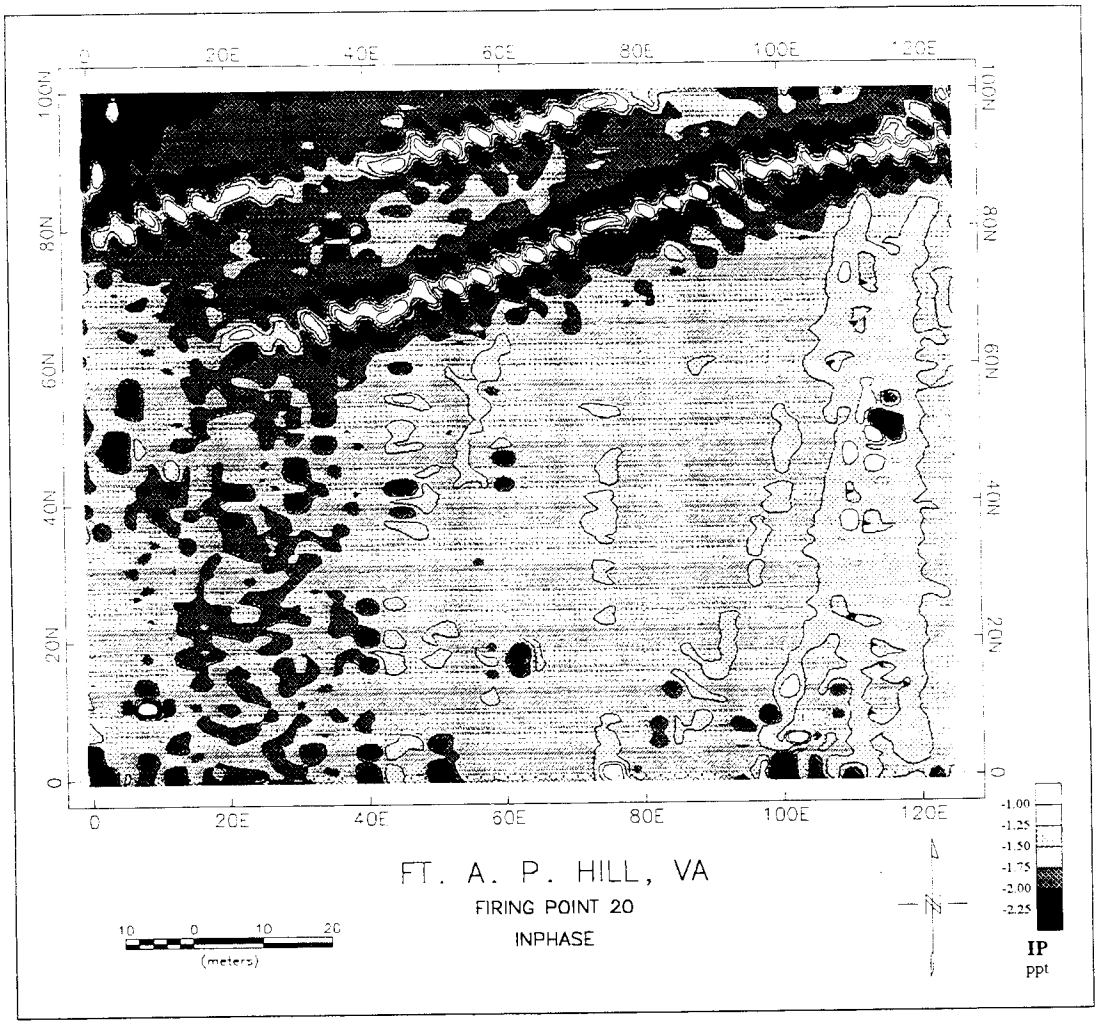

Figure 32. Results of inphase survey, Firing Point 20, Fort A. P. Hill, VA

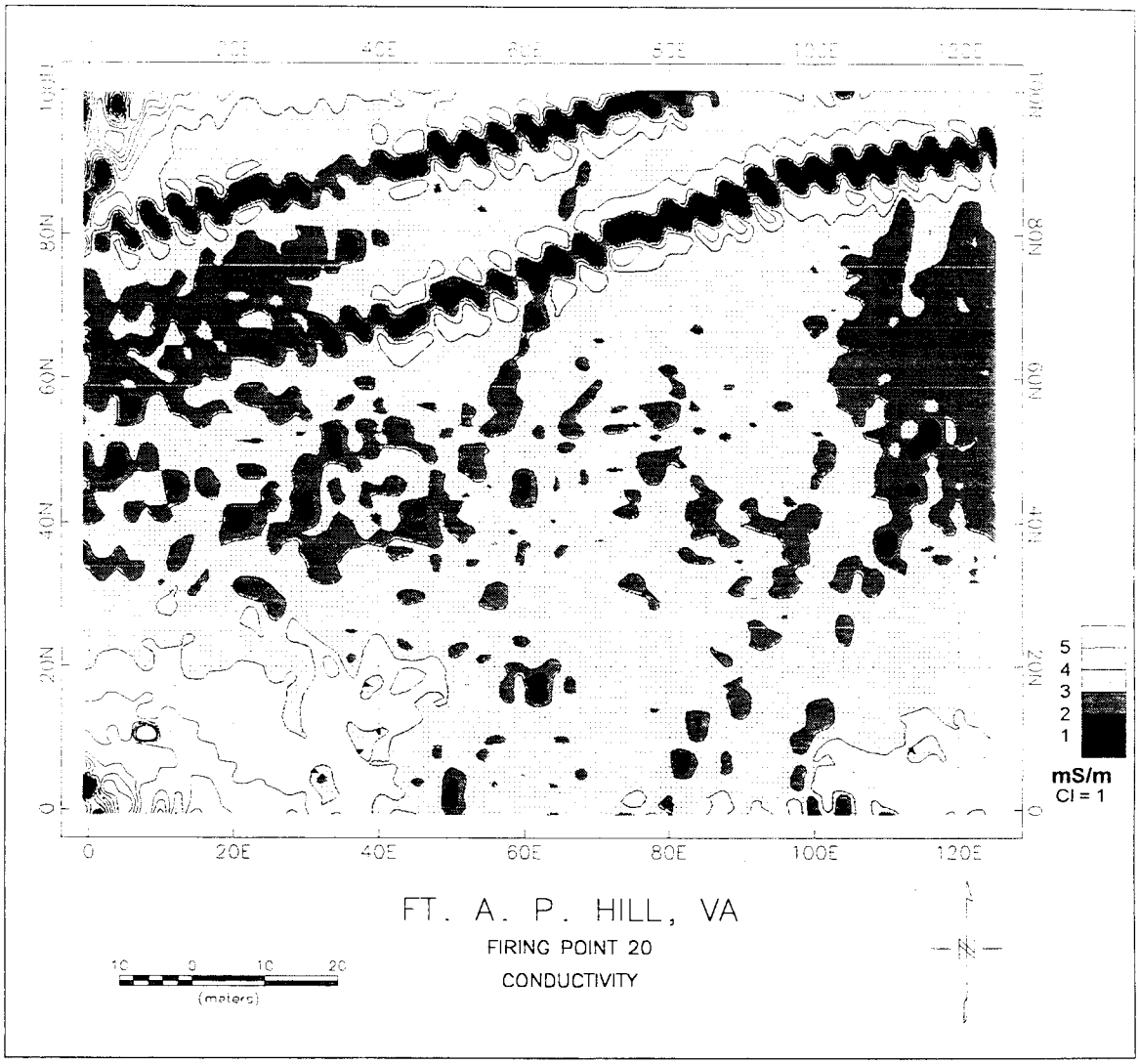

Figure 33. Results of conductivity survey, Firing Point 20, Fort A. P. Hill, VA

Table 17
DICON Probe Data, Firing Point 20, Fort A. P. Hill, VA

Location	Depth (m)	Relative Dielectric Permittivity	Conductivity (mS/m)	Wave Speed (m/ns)
15E, 30N	0.1	25	34	0.060
	0.3	23	41	0.063
	0.5	23	29	0.063
15E, 55N	0.1	18	15	0.071
	0.3	29	43	0.056
	0.5	34	53	0.041
20E,85N	0.1	16	12	0.075
	0.3	31	41	0.054
	0.5	30	42	0.055
60E, 30N	0.1	24	9	0.061
	0.3	27	20	0.058
	0.5	36	45	0.050
60E, 55N	0.1	28	18	0.057
	0.3	25	14	0.060
	0.5	30	29	0.055
60E, 85N	0.1	23	13	0.063
	0.3	33	24	0.052
	0.5	35	44	0.051
115E, 30N	0.1	20	18	0.067
	0.3	34	52	0.051
	0.5	28	34	0.057
115E, 60N	0.1	21	11	0.065
	0.3	28	28	0.057
	0.5	24	27	0.061
115E, 85N	0.1	22	17	0.064
	0.5	26	31	0.059
	0.3	28	37	0.057

EM and magnetometer interpretation. Three linear anomalies detected between (20E, 65N)–(125E, 100N), (80E, 0N)–(115E, 85N), and (95E, 0N)–(120E, 85N) are coincident to the EM31 and magnetometer survey plots. No visible surface features were noted that would account for these anomalies. Some partially buried copper cables were found along the western portion of the site. The linear anomalies are probably a result of trenching activities. Soil disturbance, associated with trenching activities, can cause the anomalies seen in the plots of the EM31 data. It is also possible that the linear anomalies may be caused by buried cables and/or by other buried ferrous and non-ferrous metallic objects. The linear anomaly which extends between (0E, 80N) and (80E, 100N) is not detected with the magnetometer and is probably caused by soil disturbance generated by trenching or by buried non-ferrous object(s). The anomalous EM31 and magnetometer values seen in the northwestern and southwestern corners of the site are probably caused by a buried ferrous object. The small scattered anomalies detected with the EM31 are probably caused by small, shallow (less than 2 m in depth), non-ferrous metallic

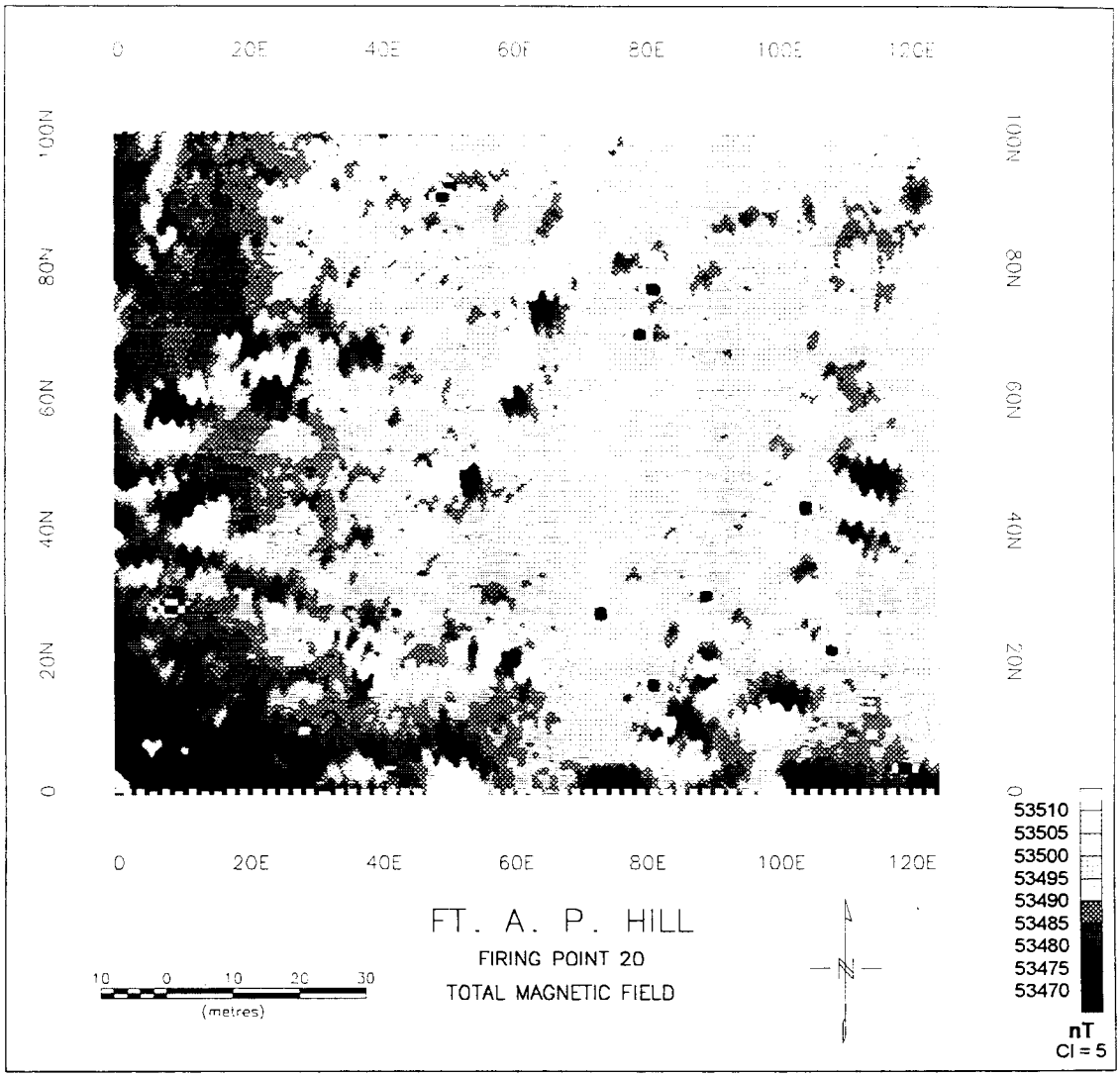

Figure 34. Results of magnetometer survey, Firing Point 20, Fort A. P. Hill, VA

objects. The small coincident EM31 and magnetometer anomalies are caused by small, shallow ferrous objects. The EM and magnetic properties were very consistent across the site and no significant trends were noted. This site appears to have had considerable human activity as shown by the numerous ferrous and non-ferrous buried objects detected.

GPR results. A lower soil conductivity at Fort A. P. Hill allowed a greater depth of investigation than at Fort Carson. Refer to Appendix I to view all of the GPR data collected at Firing Point 20. The GPR profiles obtained using the 50, 100, and 900 MHz antenna along line 60E (trending north-south) are plotted in Figure 35 ((a) 50 MHz, (b) 100 MHz, (c) 900 MHz). Numerous sharp, hyperbolic reflections are observed in the records. Some of these anomalies are caused by surface features, whereas others are a result of subsurface features. Strong reflections to a depth of 4 m were received with the 50 MHz antenna. An anomaly is detected at station 18 (depth 2 m) and station 33 (depth 2.6 m). The offsets in the record at stations 61 and 90 are caused by cable pulls incurred while surveying. The 100 MHz record provides more detail in the upper 2.5 m, identifying soil layers at depths of 1 m and 2 m. The anomalies at stations 45, 54, 88 and 94 were caused by an uneven ground surface (e.g. hole, tire rut, etc.); the signatures of these anomalies are seen in the ground surface reflection. The other hyperbolic reflections (stations 19, 34, 48, and 65) represent subsurface features and the anomalies at stations 19 and 34 are the same as those seen in the 50 MHz data. The 900 MHz data were affected by the irregular ground surface and lack of good contact between the antenna and the surface soil because of the stiff grass cover. No coherent reflector is seen in this data but the other 900 MHz profiles suggest a reflector at about 15 cm depth. The two shallow soil layers interpreted from the resistivity sounding data at 20–30 cm and 2.3 m depth appear to correlate with those identified in the GPR data at 15 cm and 2 m depth.

Firing Point 22

Site description. Firing Point 22 is located approximately 300 m west of Firing Point 20 (Figure 13) and has an increase in average site elevation of 0.5 m (Figure 36). This site has more holes and tire ruts than FP 20, especially in the central portion of the site. The resistivity soundings, GPR profiles, and DICON probe readings were collected at the same locations as Firing Point 20 (Figure 30).

Electrical resistivity results. The resistivity soundings conducted at Firing Point 22 had the same center coordinates and orientations as those at Firing Point 20. The field data and sounding curves are compiled in Appendix K. The resistivity layer structure of this site is similar to that of Firing Point 20, which is expected considering the close proximity of the two sites. A four layer earth also achieved the best data fit, however a major difference is a surface layer having a lower, rather than higher, resistivity than the layer below (Figure 37).

EM31 results. The results of the EM31 inphase and conductivity surveys are presented in Figures 38 and 39, respectively. The EM31 data fall in a fairly narrow band and no prevalent data trends across the site are noted. The background inphase values range between -1 and -1.5 ppt, whereas the conductivity values lie within a range of 2 and 4 mS/m. Five prominent localized anomalies are noted in

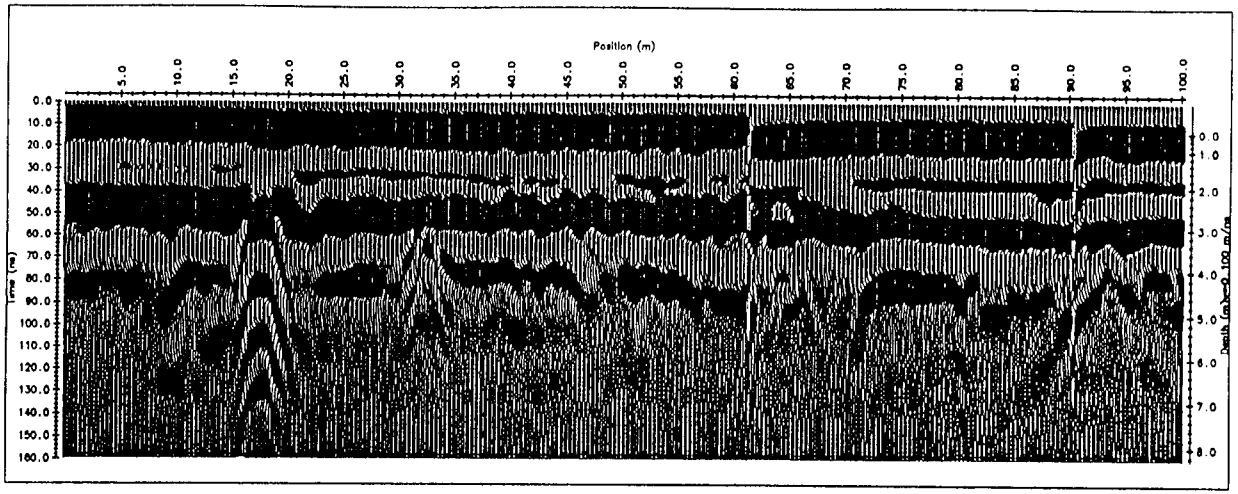

(a) 50 MHz

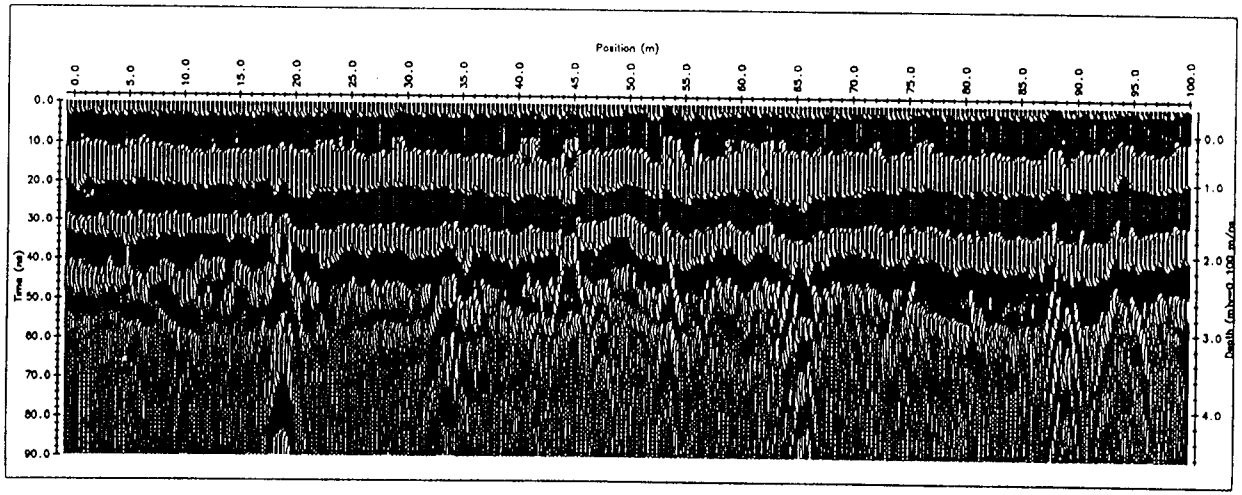

(b) 100 MHz

Figure 35. GPR profiles (north-south), line 60E, Firing Point 20, Fort A. P. Hill, VA.
a) 50 MHz, b) 100 MHz, c) 900 MHz

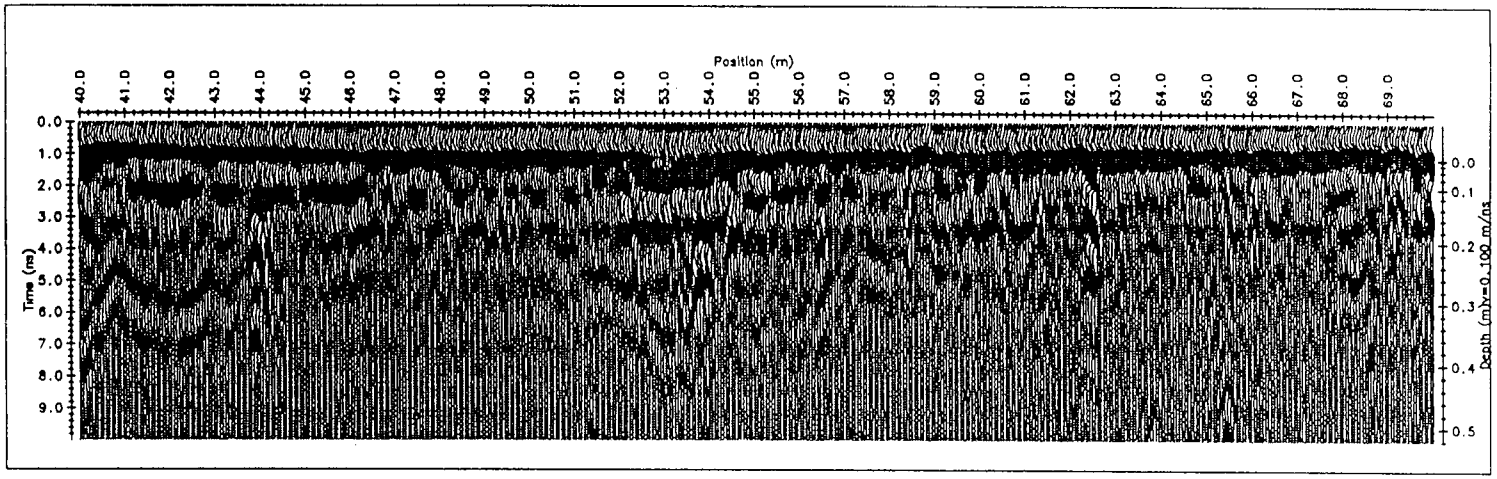

Figure 35. Continued. (c) 900 MHz

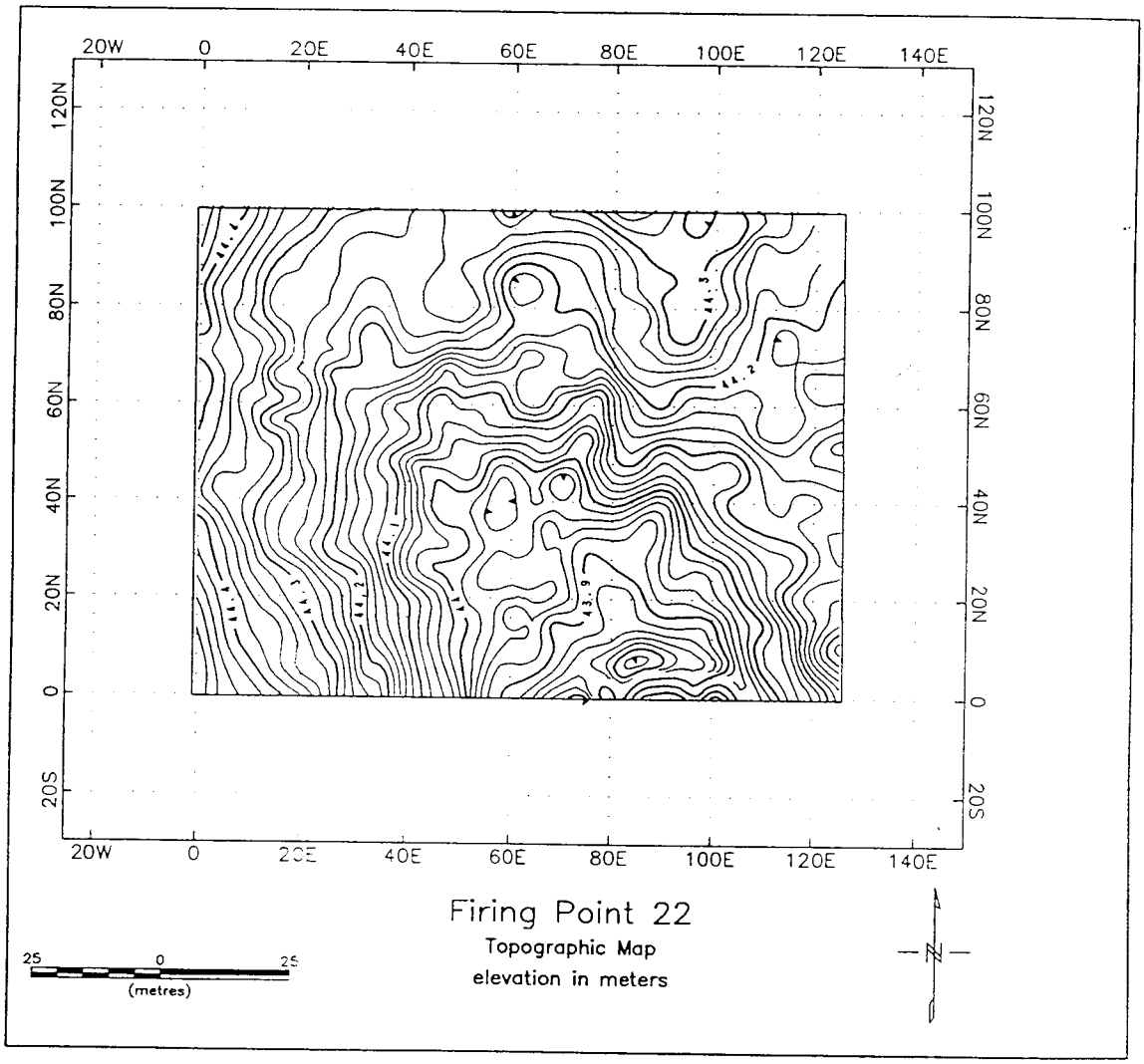

Figure 36. Topographic map, Firing Point 22, Fort A. P. Hill, VA

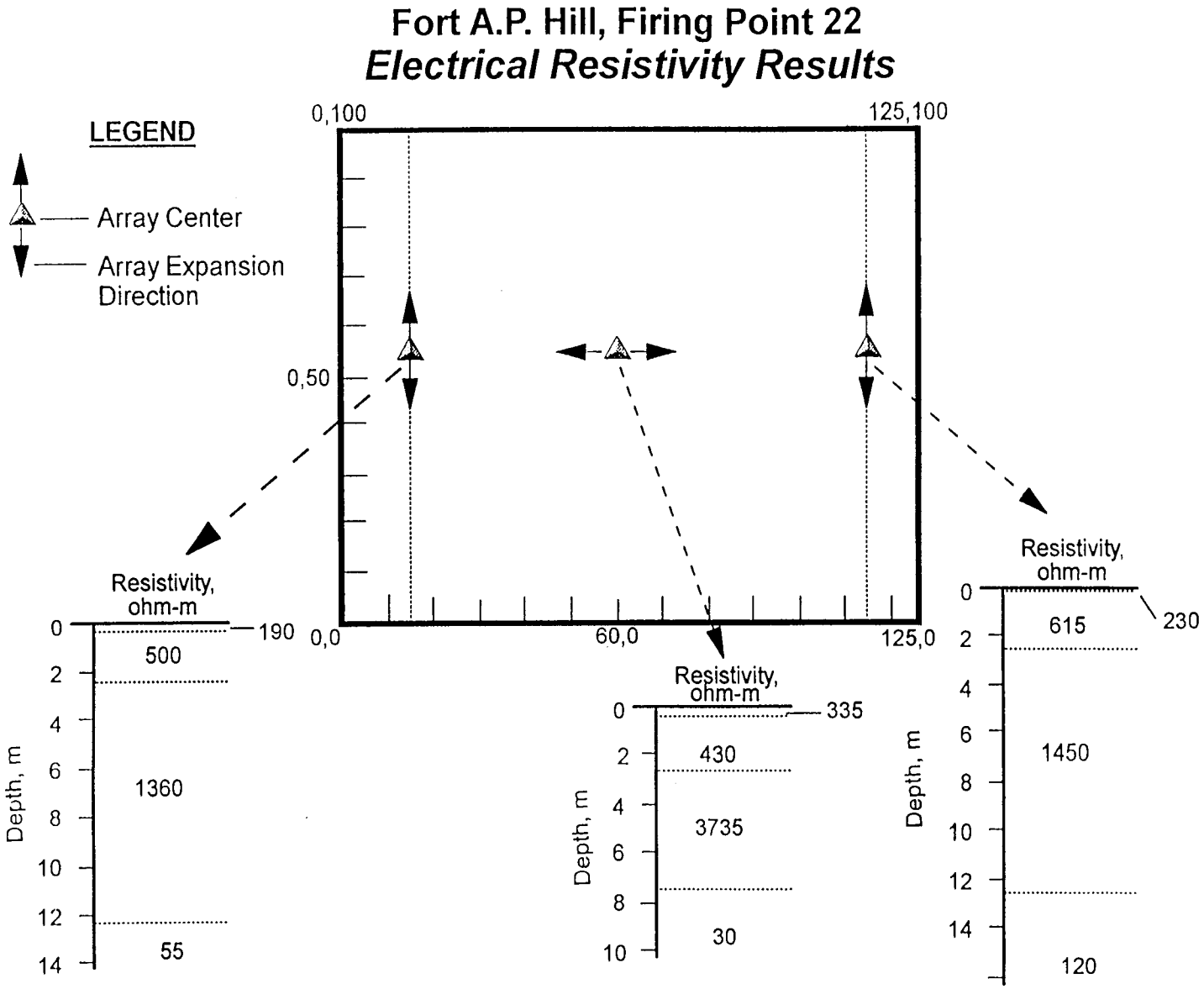

Figure 37. Model results of resistivity soundings, Firing Point 22, Fort A. P. Hill, VA

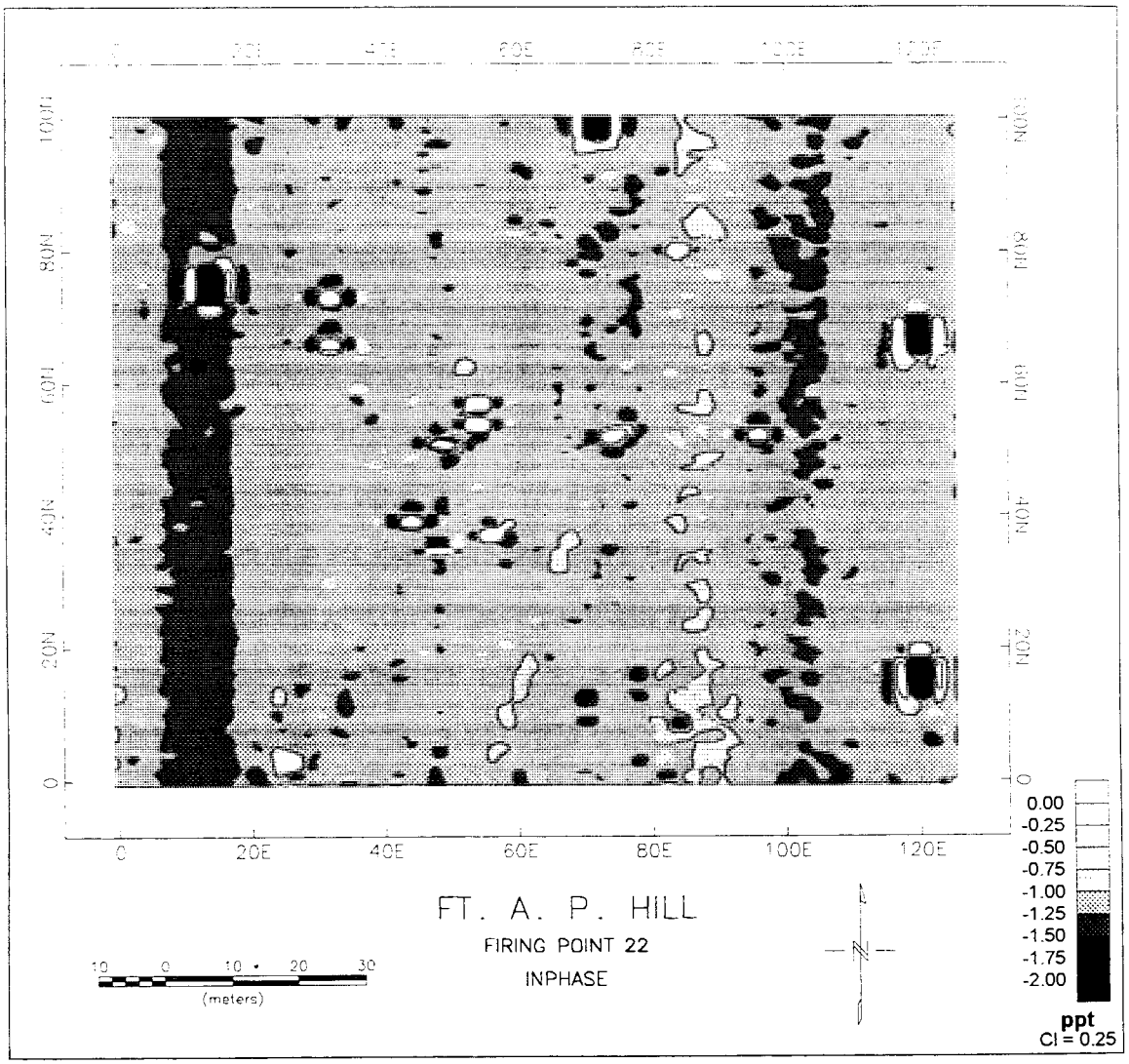

Figure 38. Results of inphase survey, Firing Point 22, Fort A. P. Hill, VA

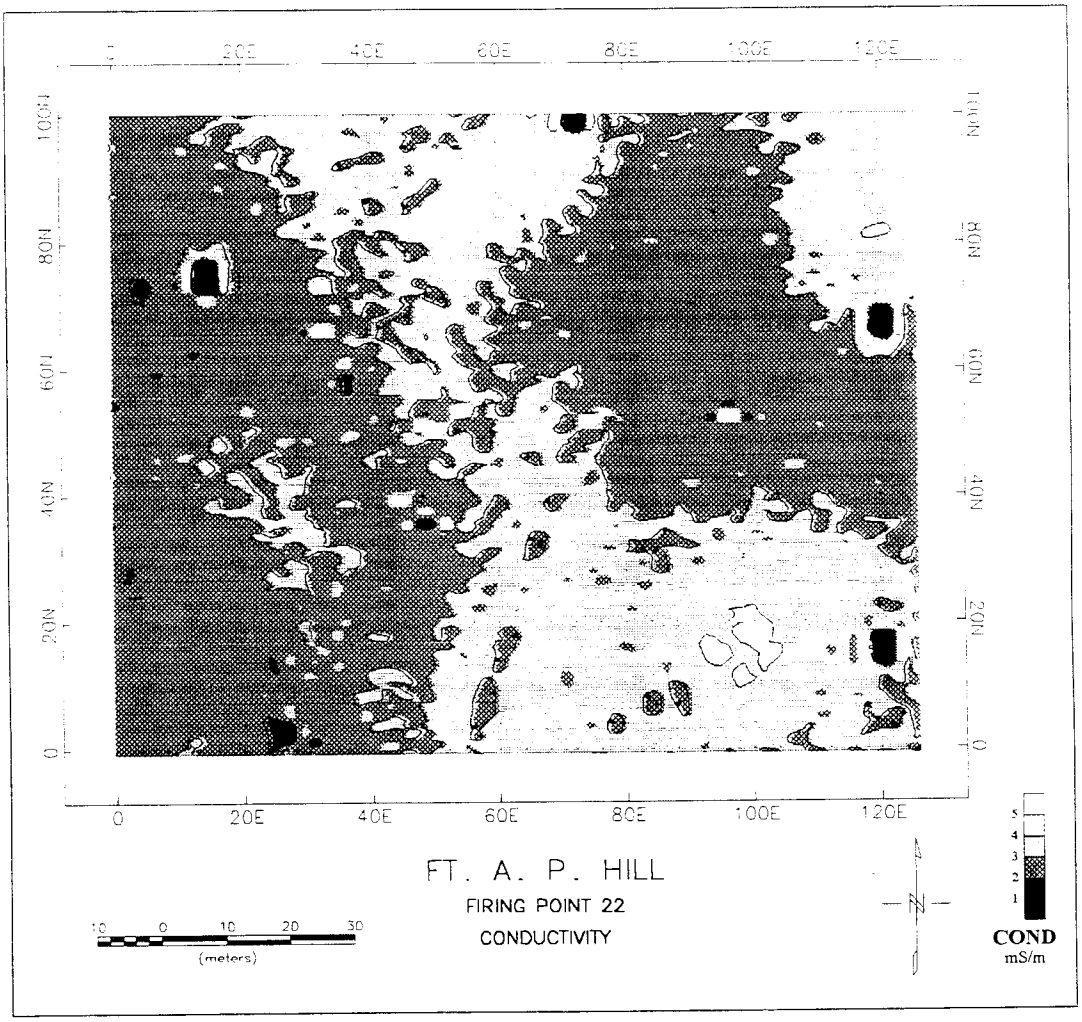

Figure 39. Results of conductivity survey, Firing Point 22, Fort A. P. Hill, VA

both of the EM31 plots at the following approximate locations: (15E, 75N), (25E, 5N), (72E, 100N), (120E, 15N), and (120E, 66N). Several other smaller anomalies coincident to the inphase and conductivity plots are also evident. There is a suggestion of a lineation between (55E, 0N) and (85E, 80N). As was the case at Firing Point 20, the high resistivities modeled for the upper two meters of soil based on the electrical resistivity data correlate well with the low conductivity values obtained using the EM31. Also, the higher conductivities measured using the DICON probe (Table 18) indicate a higher moisture content of the near-surface soil.

Table 18
DICON Probe Data, Firing Point 22, A. P. Hill, VA

Location	Depth (m)	Relative Dielectric Permittivity	Conductivity (mS/m)	Wave Speed (m/ns)
15E, 30N	0.1	14	15	0.080
	0.3	24	22	0.061
	0.5	15	13	0.077
15E, 55N	0.1	20	18	0.067
	0.3	17	9	0.073
	0.5	24	22	0.061
15E,85N	0.1	24	18	0.061
	0.3	26	16	0.059
	0.5	26	9	0.059
60E, 30N	0.1	22	16	0.064
	0.3	20	10	0.067
	0.5	24	18	0.061
60E, 55N	0.1	22	18	0.064
	0.3	24	14	0.061
	0.5	29	23	0.056
60E, 85N	0.1	25	19	0.060
	0.3	25	31	0.060
	0.5	23	30	0.063
115E, 30N	0.1	16	15	0.075
	0.3	21	16	0.065
	0.5	22	15	0.064
115E, 55N	0.1	22	16	0.064
	0.3	22	12	0.064
	0.5	30	46	0.055
115E, 85N	0.5	28	27	0.057
	0.1	19	22	0.069
	0.3	28	43	0.057

Magnetometer results. The results of the magnetometer survey are shown in Figure 40. No significant trends in the data are evident. The majority of the magnetometer values occur in a narrow band between 53,490 and 53,510 nT. The magnetometer results also show numerous anomalies characterized by coupled high-low values and many of these anomalies correspond to the EM31 anomalies. The five prominent anomalies detected with the EM31 are also detected with the magnetometer. As is the case in the EM data plots, there is a series of anomalies that define a line with end points located at approximately (55E, 0N) and (85E, 80N). A north-south linear feature located along line 33E is caused by a "stitch" in the data where two data sets, collected between two consecutive days, are joined together.

EM and magnetometer interpretation. One slightly detectable linear anomaly was detected with the EM31 and magnetometer. It is possible that this anomaly is the result of a backfilled trench in which a number of ferrous objects are buried. No visible surface features were noted which would account for this anomaly. The small, scattered anomalies detected with the EM31 are probably caused by small (less than 1 m diameter), shallow (less than 2 m in depth), non-ferrous metallic objects. The coincident EM31 and magnetometer anomalies are caused by shallow ferrous objects. The EM and magnetic properties were very consistent across the site and no significant trends were noted. This site also appears to have had considerable human activity as denoted by the numerous ferrous and non-ferrous buried objects detected.

GPR results. Appendix L contains a plot of the GPR records for Firing Point 22. The north-south profile along line 60E typifies the radar data collected at this site (Figure 41). The data identify continuous subsurface layers at depths of 0.1, 0.6, and 1.3 m, and deeper, discontinuous reflections below 3 m. This set of GPR profiles provides an excellent example of the improved resolution achieved at higher frequencies. For example, note the detail in Figure 41 at stations 10–15, 35–45, and 60 progressing from the 50 MHz to the 200 MHz records. Between stations 10–15 and 35–45 there is a cluster of objects between 0.5 and 1 m depth.

Jefferson Proving Ground, Indiana

Site description. The 1-hectare (ha) UXO backgrounds characterization test site on JPG is located north of the northeast boundary of the 40-acre site (Figure 42). For geophysical survey purposes, the southwest corner of the site was designated a local grid coordinate of (0E, 0N). Listed below are the corresponding latitude, longitude and UTM (NAD83) coordinates of the test site corners. The topographic map of the site (Figure 43) reveals a relatively flat (< 2% slope) surface (Figure 44). There is a 2.5 m change in elevation sloping from the southeast to the northwest corner, with a

Local Grid Coordinates	Latitude	Longitude	UTM (NAD83) (meters)
(0E, 0N)	38°55'32.209834"	85°22'00.280268"	641578.49963, 4309789.98145
(0E, 100N)	38°55'35.443670"	85°22'00.590840"	641569.23497, 4309889.53878
(125E, 0N)	38°55'32.521070"	85°21'55.108020"	641702.87797, 4309801.80845
(125E, 100N)	38°55'35.753606"	85°21'55.421461"	641693.54338, 4309901.32436

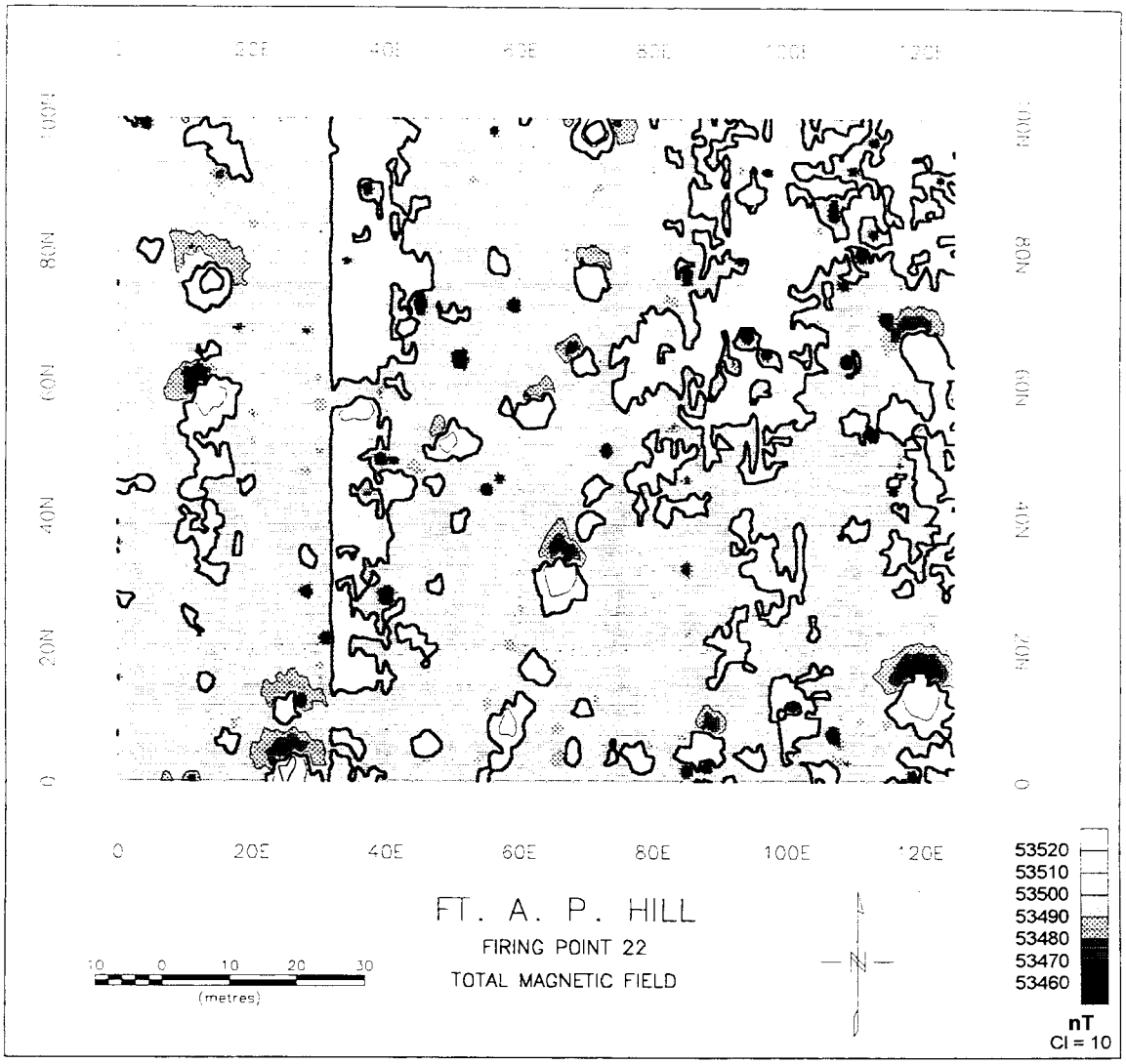

Figure 40. Results of magnetometer survey, Firing Point 22, Fort A. P. Hill, VA

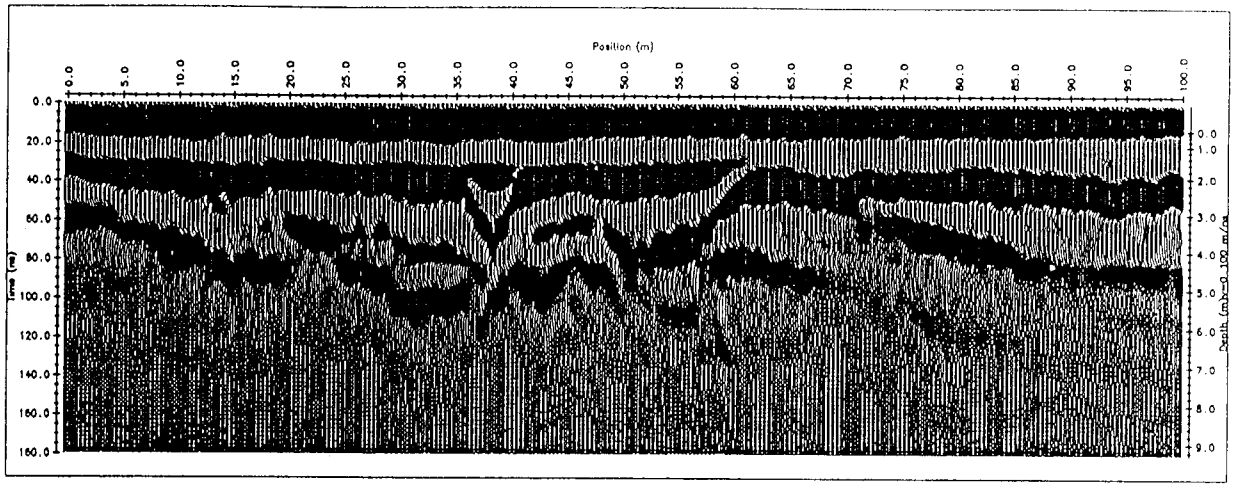

(a) 50 MHz

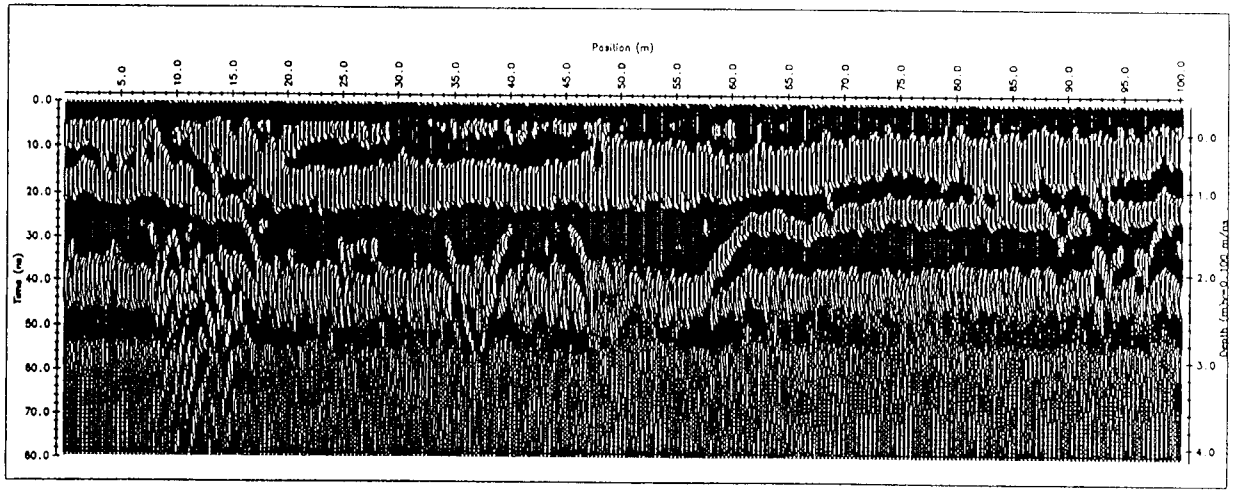

(b) 100 MHz

Figure 41. GPR profiles (north-south), line 60E, Firing Point 22, Fort A. P. Hill, VA.
a) 50 MHz, b) 100 MHz, c) 200 MHz, d) 900 MHz.

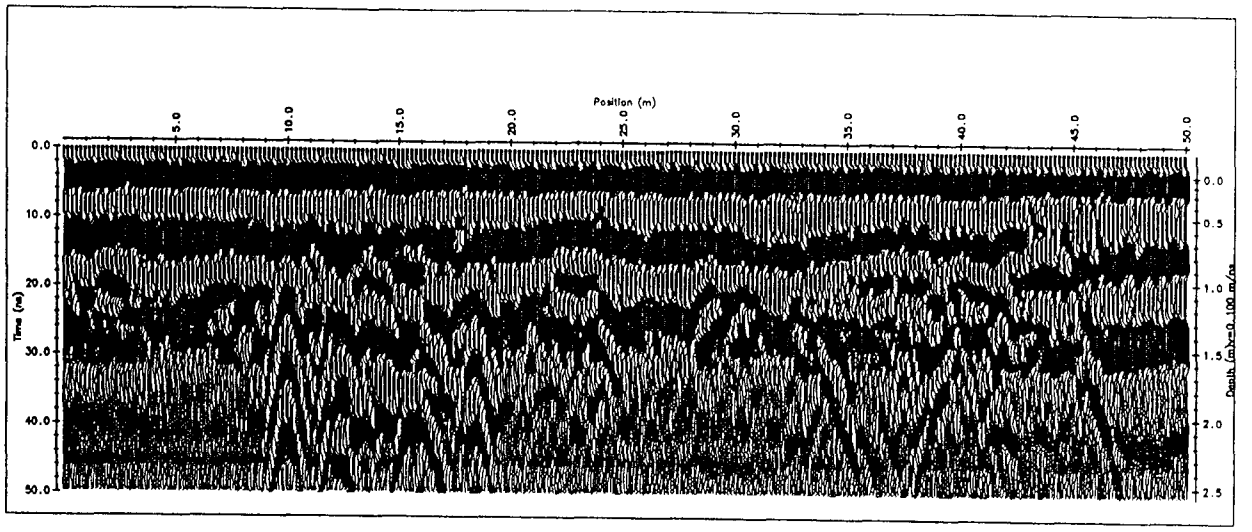

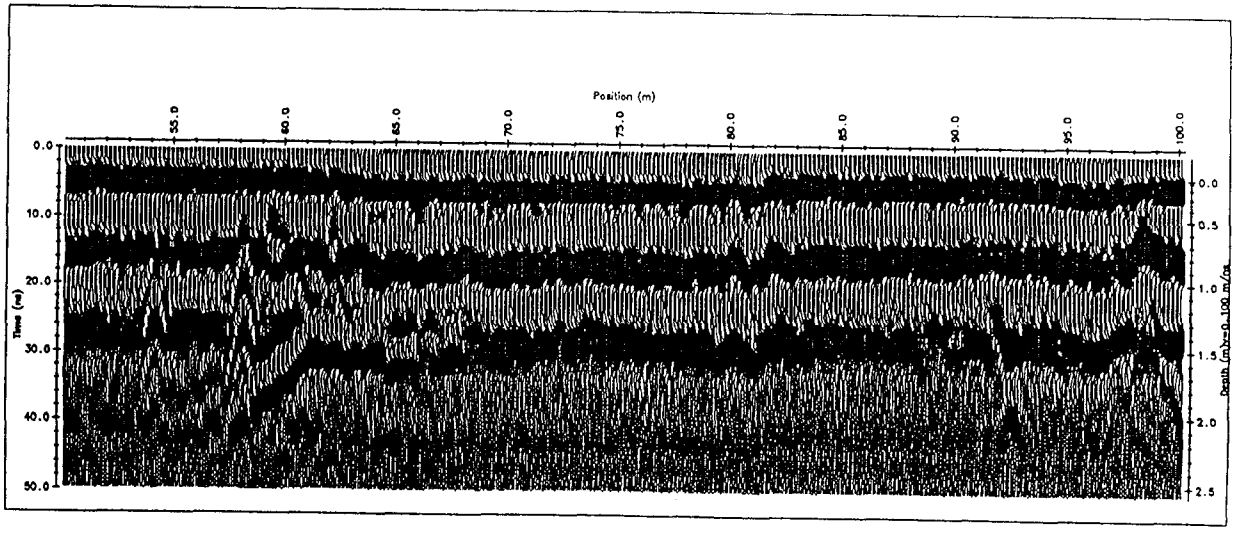

Figure 41. Continued. (c) 200 MHz

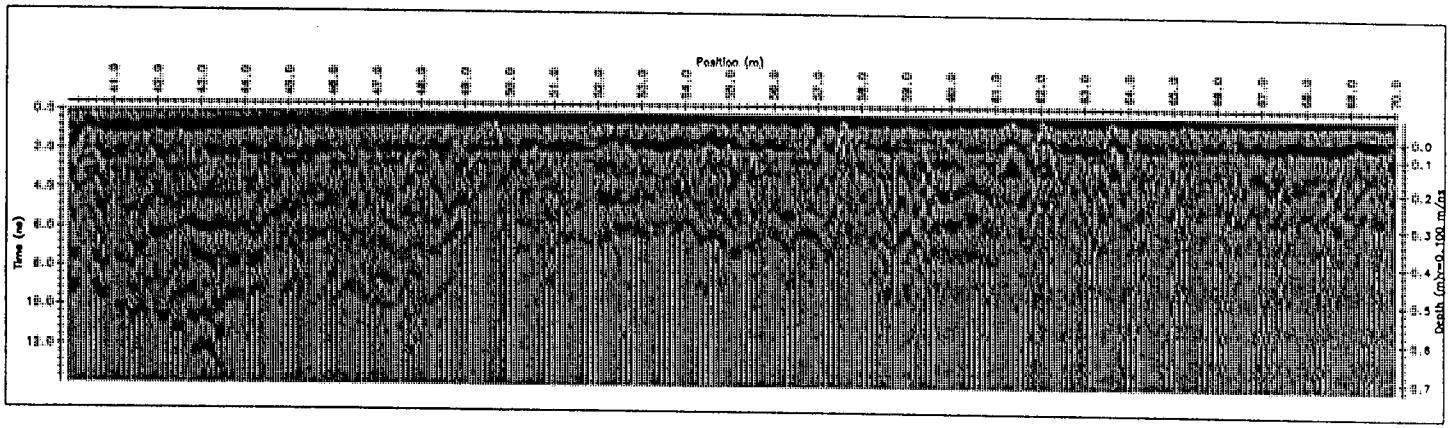

Figure 41. Continued. (d) 900 MHz

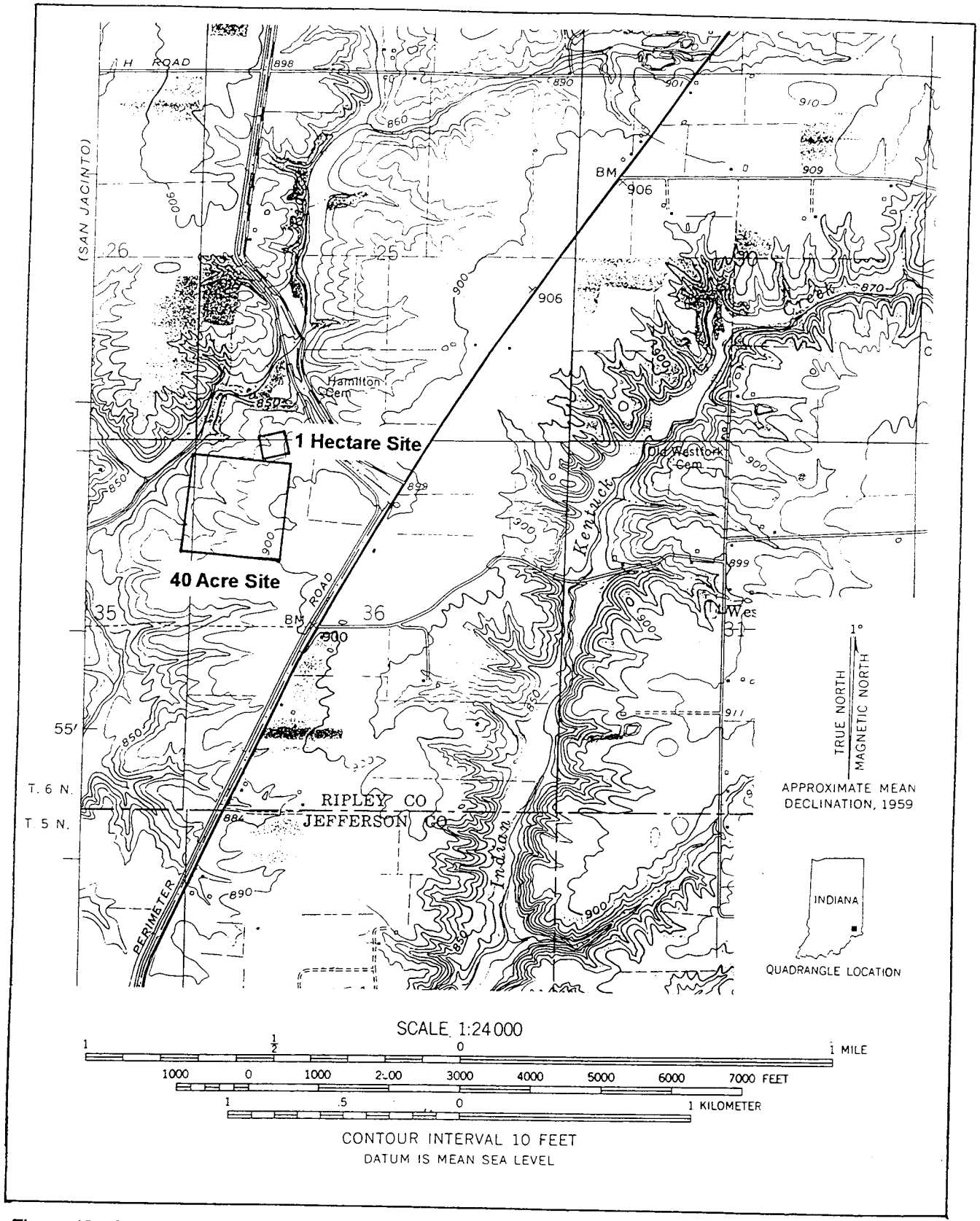

Figure 42. General location of 1 hectare site on Jefferson Proving Ground, Indiana (portion of U.S.G.S. Rexville, IN 7.5 minute quadrangle, 1959)

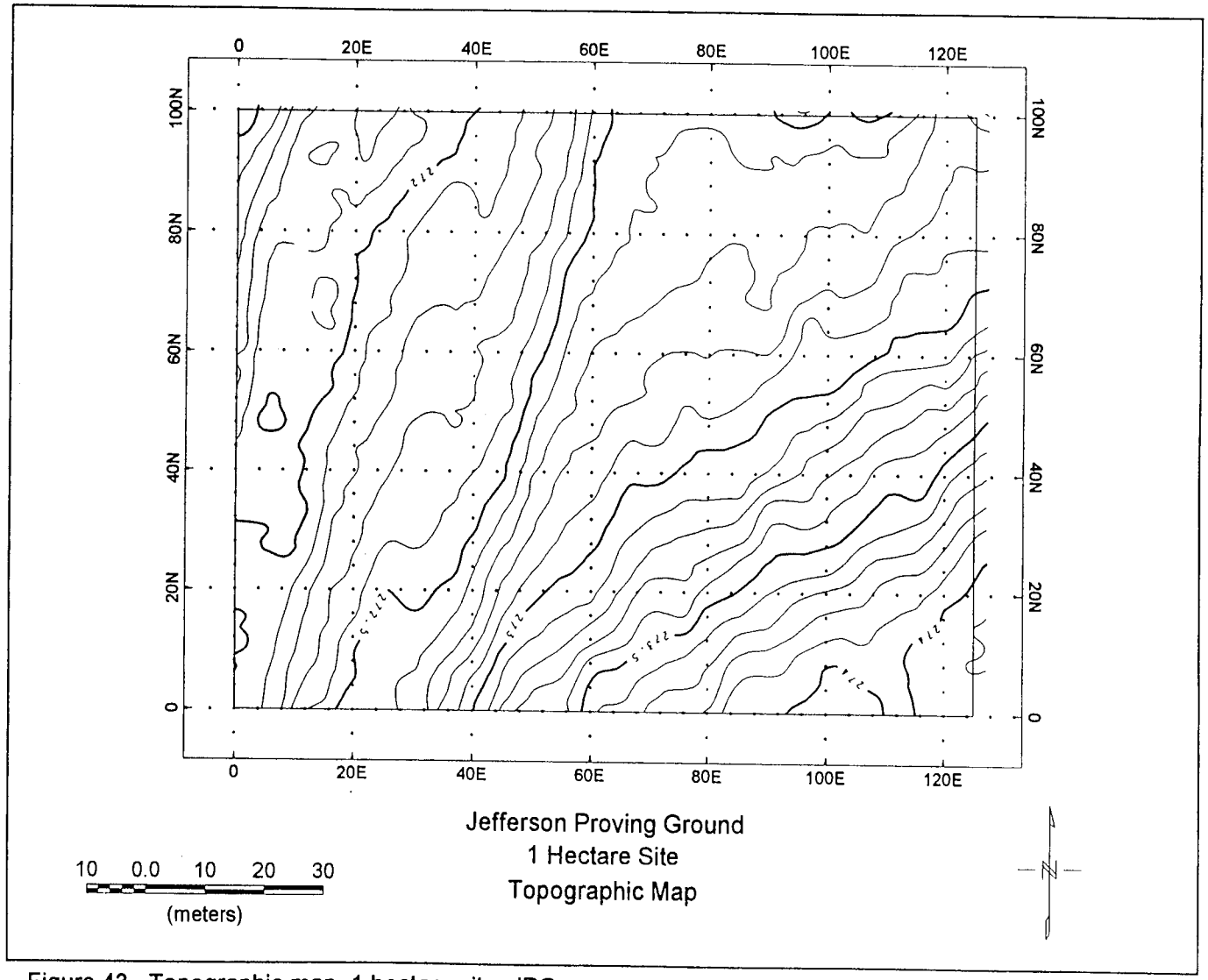

Figure 43. Topographic map, 1 hectare site, JPG

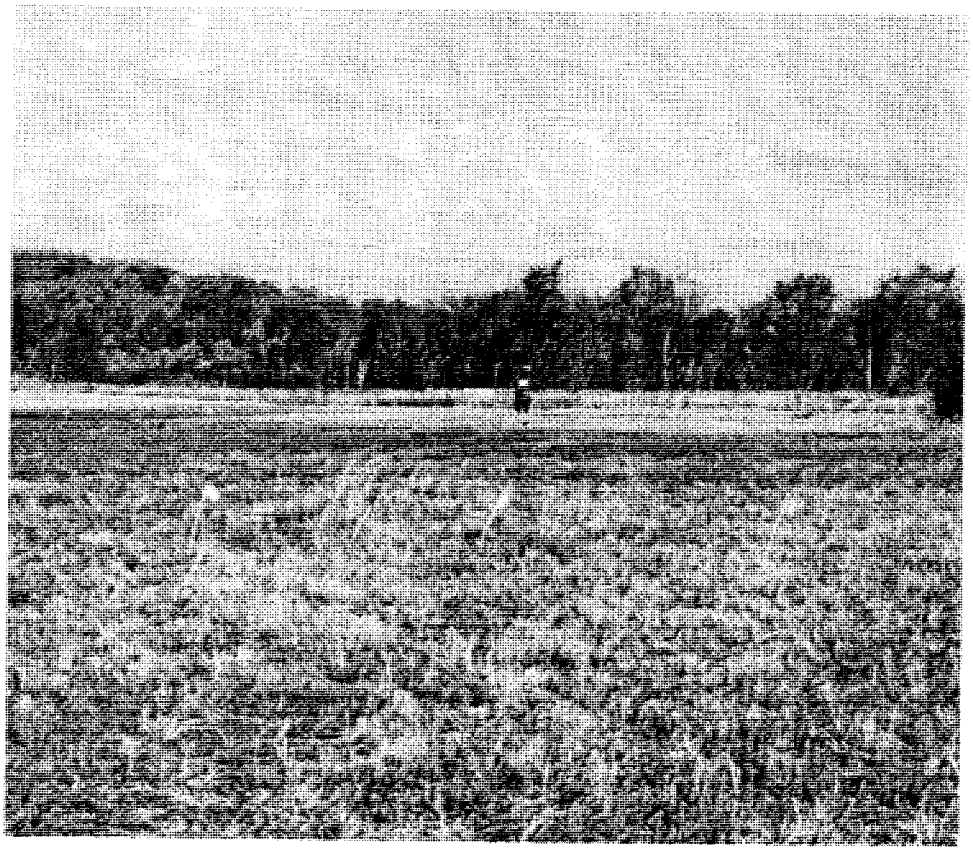

Figure 44. Photograph of JPG 1-ha site

general elevation of about 273 m. Numerous holes and ruts are present on the ground surface. Figure 45 shows where the electrical resistivity, GPR, and DICON probe data were acquired.

Electrical resistivity results. Six electrical resistivity soundings were performed. The center of each sounding and direction of expansion is depicted in Figure 46. Plots of the field data (Appendix N) suggest a (near surface) three layer earth structure having a high-low-high resistivity pattern. Results of the inverse modeling procedure are shown in Figure 46 with graphical and tabulated results provided in Appendix N. A three or four layer model best fits the data. When a fourth layer is present, it has an intermediate resistivity value between the initial high-low. The upper, high resistivity layer ranges in thickness from 0.2 to 0.8 meters with resistivity varying between 460 and 880 ohm-m. The middle layer exhibits little variation in both resistivity, 50-70 ohm-m, and thickness, 4.2-5.2 m. The lower-most resistivity interface detected extends to a depth of 4.7-5.5 m and is highly resistive, with a resistivity value exceeding 1000 ohm-m. The three interpreted layers are associated with a shallow silt underlain by a thicker clay, which resides on limestone bedrock. The 50-70 ohm-m resistivity is generally high for a mineralogical clay, unless the clay is dry. Recall that analysis of the upper one meter of soil revealed only a small fraction of clay minerals. However, while augering holes for the DICON probe pockets of predominantly clay soil were encountered, so it is likely that the percentage of clay minerals does increase below a depth of one meter. The estimated depth to bedrock determined from the resistivity soundings (4.7-5.5 m) is comparable to the 1.1-7.2 m depth of refusal encountered during soil sampling at the 40 acre site (PRC Environmental Management, Inc. 1996). The shallow depths of refusal are likely caused by cobbles or limestone "floaters", and the greater depths of refusal could be localized zones of enhanced weathering of the limestone surface.

EM31 results. The conductivity data show a general increase in conductivity from north to south (Figure 47). Average background values range from 15 to 20 mS/m. The northwest corner and northeast portion of the grid exhibit slightly lower values (11-15 mS/m). Conductivity values greater than 18 mS/m are found within the southern half of the survey grid, with values increasing toward the southwest and southeast corners. The most conductive area exists between (104-118E, 0-10N) where values exceed 24 mS/m.

Little variation is seen in the inphase data (Figure 48), with typical background values ranging from 0.4 to 0.8 ppt. Several small (lateral dimension), shallow and weak (intensity) isolated anomalies are located at (10E, 39N), (14E, 1N), (14E, 31N), (14E, 47N), (16E, 12N), (20E, 31N), and (78E, 14N).

Magnetometer results. A nonlinear filter was applied to the data to remove spikes caused by spurious noise. The magnetic data have a nominal background value of 54000 nT with an average variation of ±6 nT (Figure 49). The data show no apparent trends. Two moderate anomaly highs are located at (74E, 40N) and (102E, 32N), with a small anomaly low at (69E, 1N). No correlation is observed between the magnetic and conductivity anomalies.

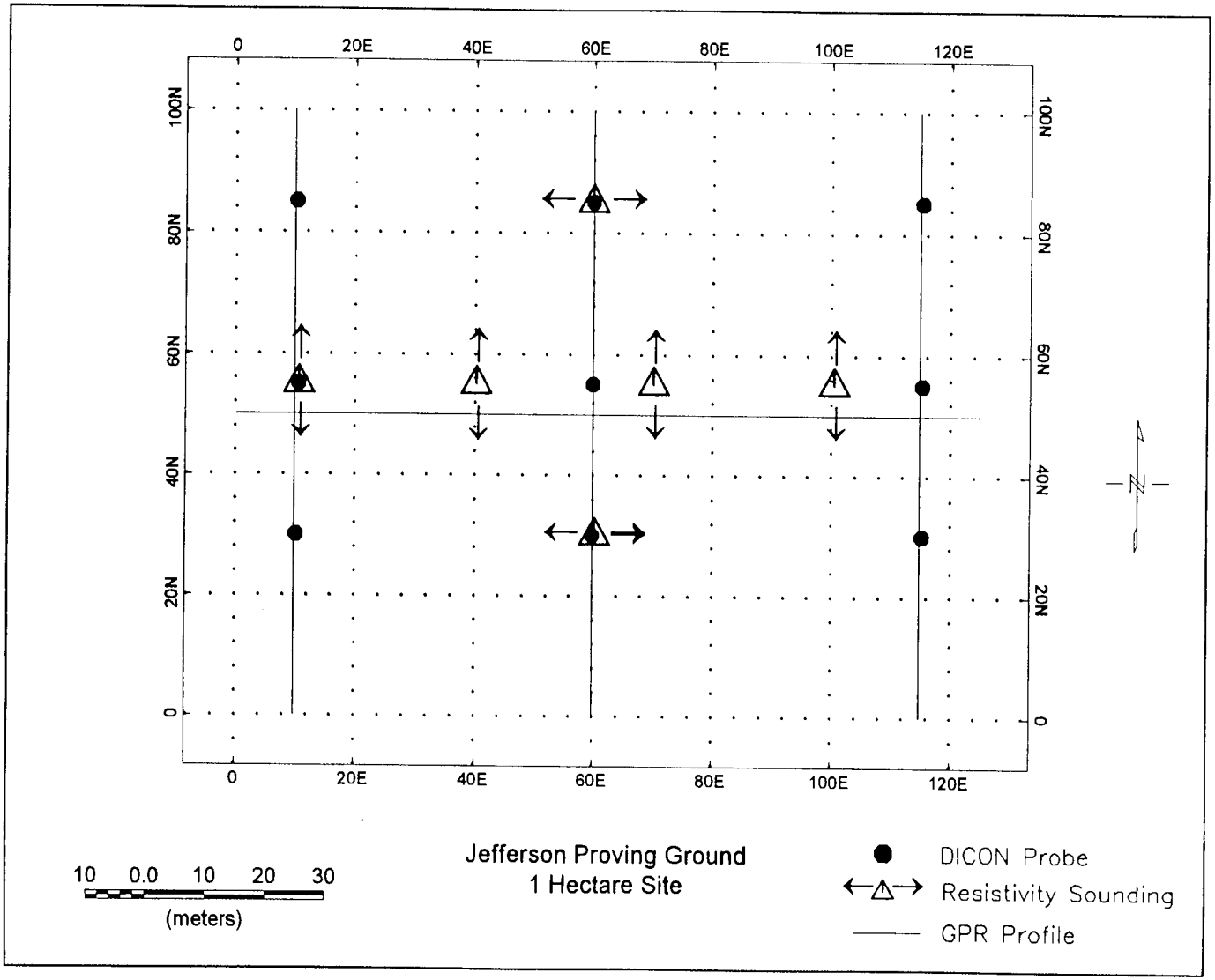

Figure 45. Location of resistivity soundings, GPR profiles, and DICON probe measurements, JPG 1-ha site

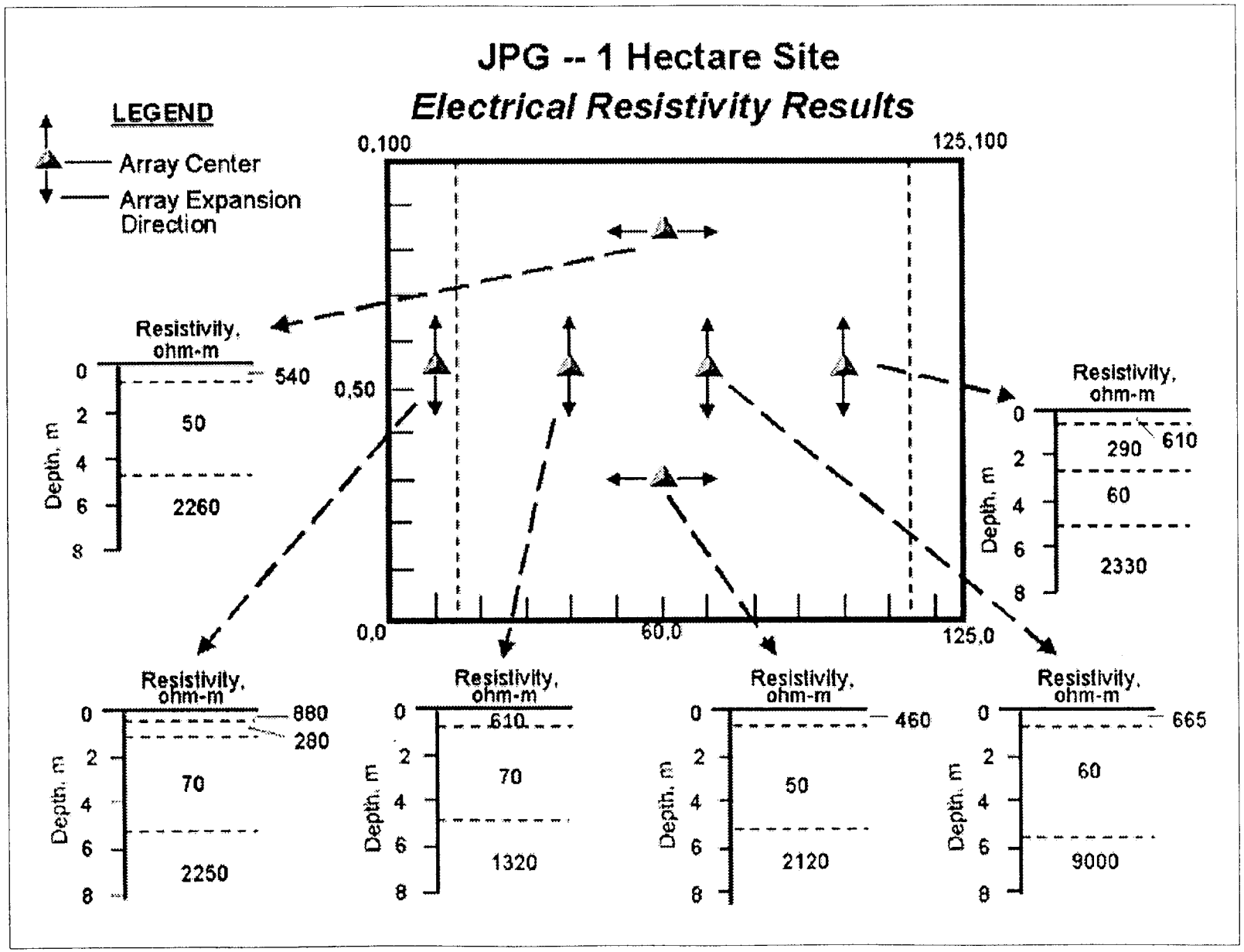

Figure 46. Resistivity model results, JPG 1-ha site

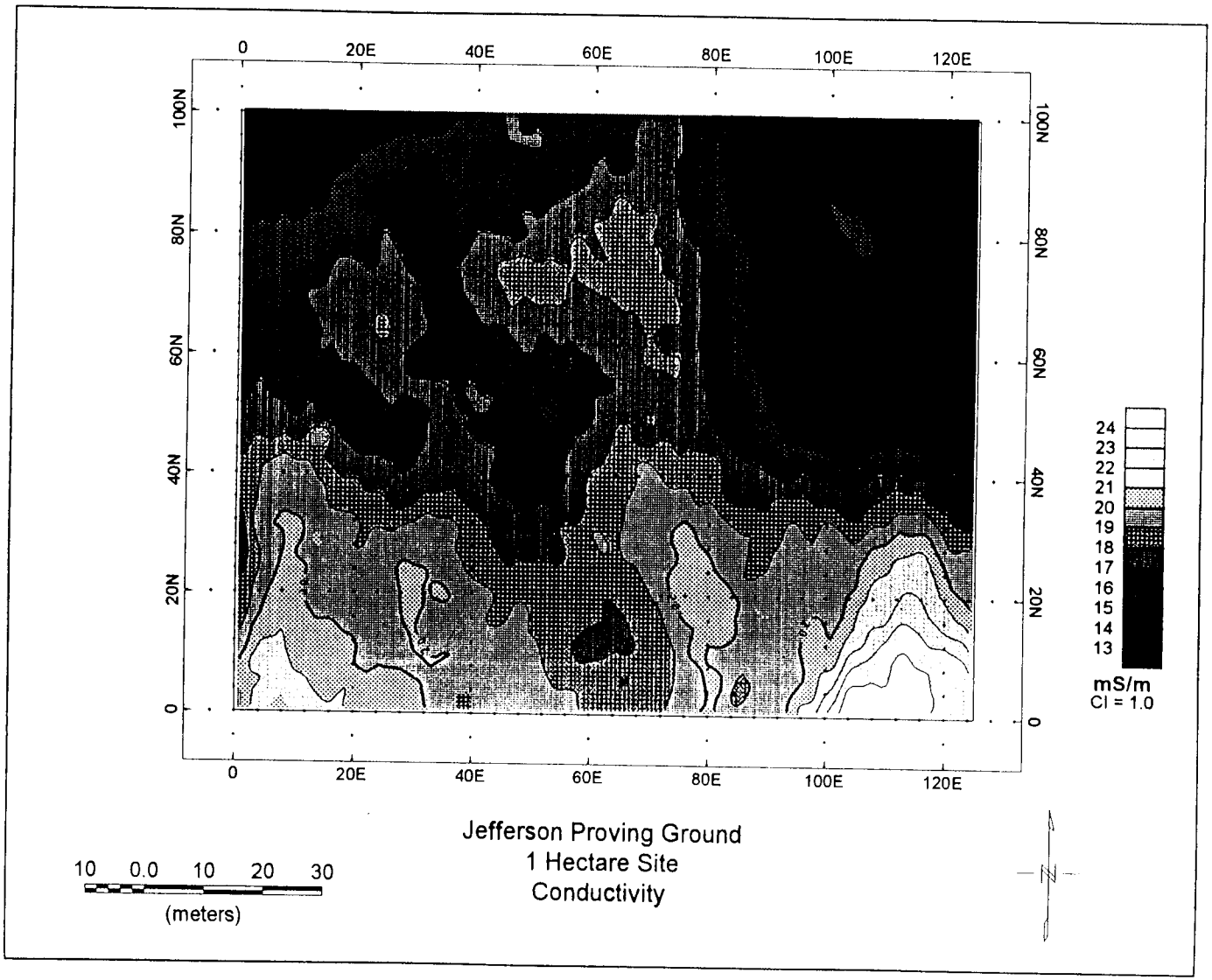

Figure 47. Results of conductivity survey, JPG 1-ha site

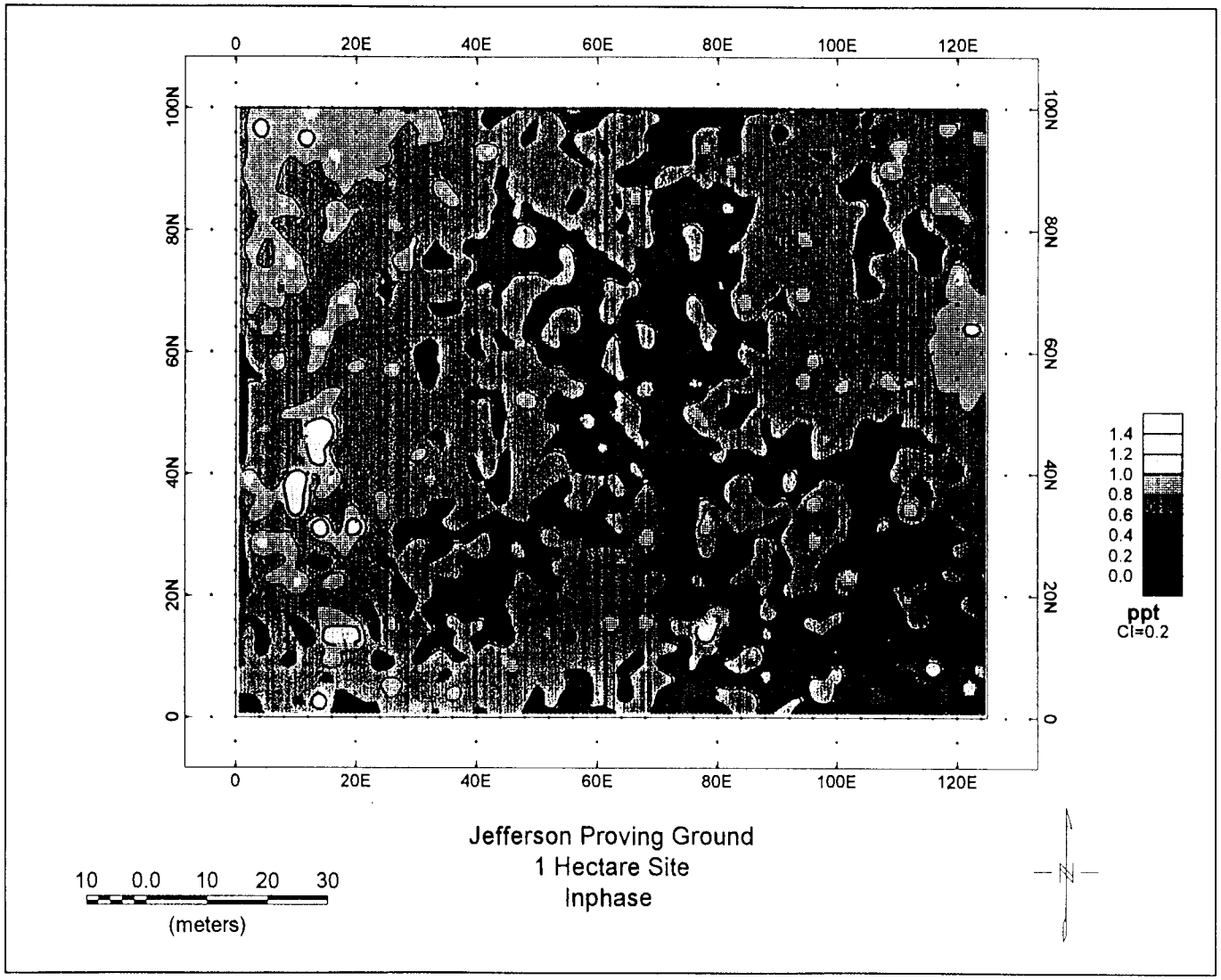

Figure 48. Results of inphase survey, JPG 1-ha site

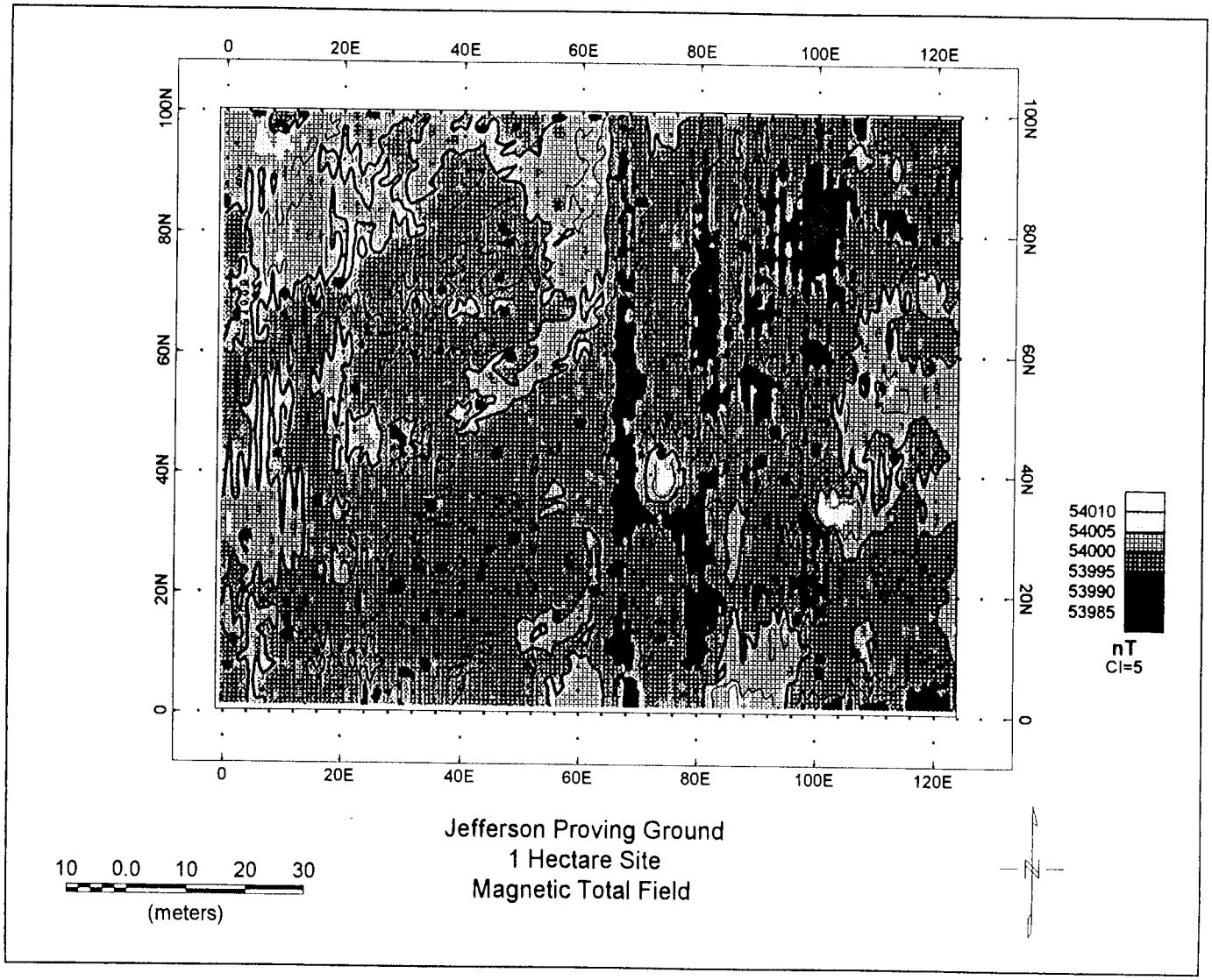

Figure 49. Results of magnetic survey, JPG 1-ha site

GPR results. Figure 45 shows the location of the GPR profiles. The profile data collected using the 50, 100, and 200 MHz antennas are given in Appendix O. A velocity of 0.07 m/ns, determined using both the CMP and DICON probe measurements, was used for estimating depth of investigation. The DICON probe data are tabulated in Table 19.

An investigation depth of about 3.5 m was obtained with the 50 MHz antenna. Figure 50a shows a typical profile collected at this site using the 50 MHz antenna. At this frequency, two prominent reflectors are resolved that extend across the site along each line profiled. These layers, at depths of 0.5-0.7 m and 1.6-2 m, are continuous and relatively flat. A third layer having a discontinuous and intermittent reflection boundary is detected at a depth of approximately 3.2 m. A broad, hyperbolic reflection is evident in the east-west profile data acquired along line 50N at position 88 (Figure 50a). This reflection has a calculated wave velocity of about 0.3 m/ns, that of an EM wave in air, indicating the reflection is caused by an object located on or above the ground surface.

Table 19
DICON Probe Data, JPG 1-Ha Site

Location	Depth (m)	Relative Dielectric Permittivity	Conductivity (mS/m)	Wave Speed (m/ns)
10E, 30N	0.1	23.3	15.4	0.062
	0.3	23.9	27.7	0.061
	0.5	25	28.9	0.060
10E, 55N	0.1	17.5	8.8	0.072
	0.3	19.1	18.5	0.069
	0.5	28	40.6	0.057
10E,85N	0.1	13.9	6.4	0.081
	0.3	14.6	7.6	0.079
	0.5	24.6	29.6	0.061
60E, 30N	0.1	21.7	11.4	0.064
	0.3	22.7	14.2	0.063
	0.5	24.7	24.5	0.060
60E, 55N	0.1	19	9.6	0.069
	0.3	19.9	15.1	0.067
	0.5	22.3	23.2	0.064
60E, 85N	0.1	19.9	9.7	0.067
	0.3	20.1	16	0.067
	0.5	27	34.3	0.058
115E, 30N	0.1	21	15.4	0.066
	0.3	27.7	34.9	0.057
	0.5	28	40.6	0.057
115E, 55N	0.1	25.4	16.2	0.060
	0.3	22.6	25.4	0.063
	0.5	26.7	29.2	0.058
115E, 85N	0.5	21.6	12.9	0.065
	0.1	23.1	16.1	0.062
	0.3	25.2	21.8	0.060

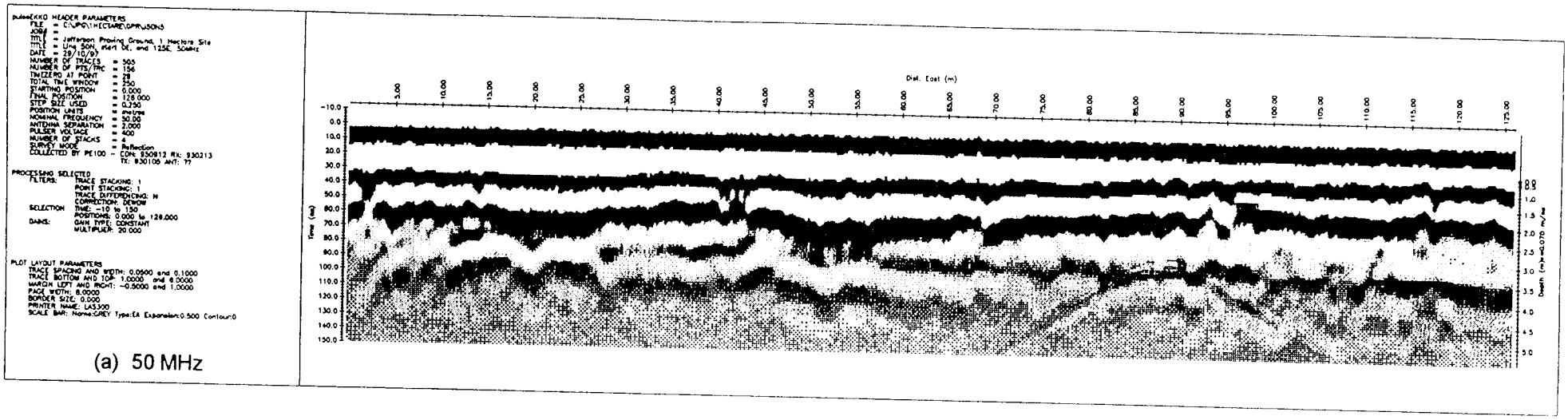

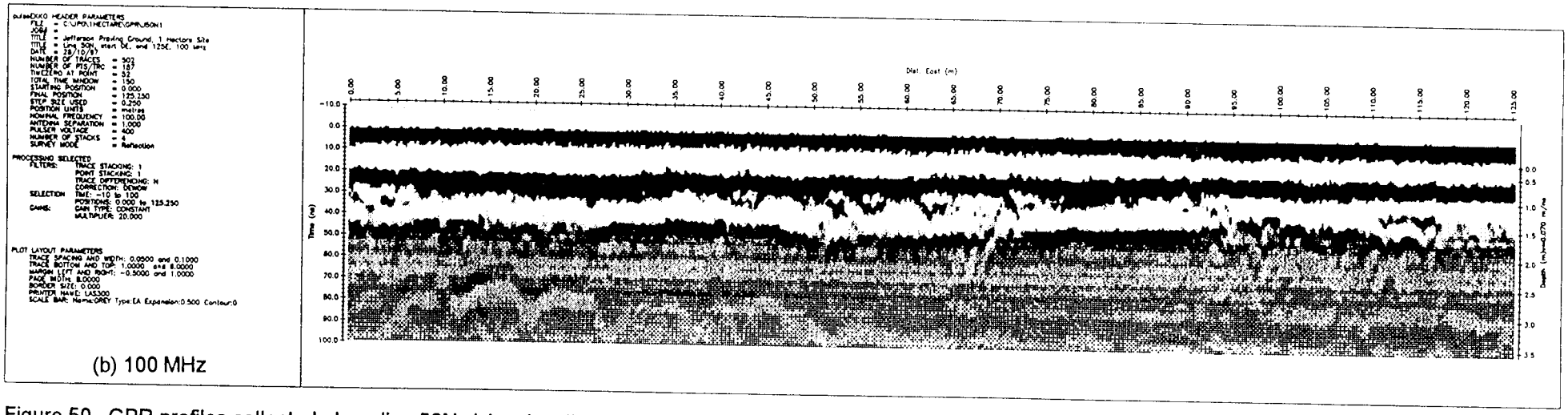

Figure 50. GPR profiles collected along line 50N, 1-ha site, JPG. (a) 50 MHz, (b) 100 MHz.

The 100 MHz profiles also image the two prominent reflectors identified in the 50 MHz data. The lower reflector (depth 1.5-2 m) is at the investigation depth limit for this frequency. The 100 MHz antenna detects a rough, discontinuous and intermittent reflector located between the other two layers at a depth of 0.9-1.2 m. A series of small, hyperbolic reflections is observed in profile line 50N between stations 90-115 at a depth of 1.5 m (Figure 50b). Depth of investigation decreases but resolution of the shallower layers improves at the higher antenna frequencies. This is seen in a comparison of the 50 and 100 MHz profiles along line 115E (Figure 51). Note the uplifting of the reflector at 1.5 m depth between stations 45-71 in the 50 MHz profile. Greater detail is apparent in the 100 MHz profile at this location, where the small, sharp hyperbolic reflections from individual sources can be identified.

Approximately 1 m depth of investigation was obtained with the 200 MHz antenna. The roughness of the shallow soil boundaries is observed in the data (Figure 52). The shallowest reflector imaged is at a depth of 0.3-0.4 m, and two deeper layers are detected at depths of 0.8 m and 0.9 m. An anomaly is apparent at a depth of 1.0 m in the 60E profile line at position 64.

Summary of Geophysical Results

Significant differences in the range and magnitude of soil conductivity and depths of investigation are observed between the sites at Fort Carson, Fort A. P. Hill, and JPG. A statistical comparison of the five 1-hectare sites based on analysis of the electrical conductivity data is given in Table 20. It emphasizes the similarity of the two sites at Fort A. P. Hill, as expected due to their proximity, and the variability in soil at Fort Carson. The contrast in average conductivity values is indicative of a sandier soil at Fort A. P. Hill and a higher clay content soil at Fort Carson, where the Seabee site soil has more clay than the Turkey Creek site. The soil at the JPG 1-ha site has a sand and clay content between that at Fort A. P. Hill and the Turkey Creek site at Fort Carson. Based on the average, median, and mode parameters, the soil at a given site is distributed uniformly over each site. The greatest variation in conductivity values occurs at Fort Carson, having standard deviation values of 6.2 and 11.0 for the Turkey Creek and Seabee sites, respectively. Table 21 provides a summary of typical background values and interpreted subsurface layer structure for the four geophysical surveys conducted. The following is a summary of geophysical findings at each 1-hectare site.

Fort Carson, Colorado

Soil conductivity is relatively high at Fort Carson, with the soil at the Seabee site having a higher moisture and clay content than at Turkey Creek. The background total magnetic field only varies 20–30 nT. Similarities in terms of number of stratigraphic layers identified and their depths are observed between the resistivity and GPR interpretations at both sites.

Seabee site. Four prominent interfaces were mapped within the upper 2 m of soil using GPR (depths of 0.08, 0.4, 1.2, and 1.6 m). The resistivity layer models

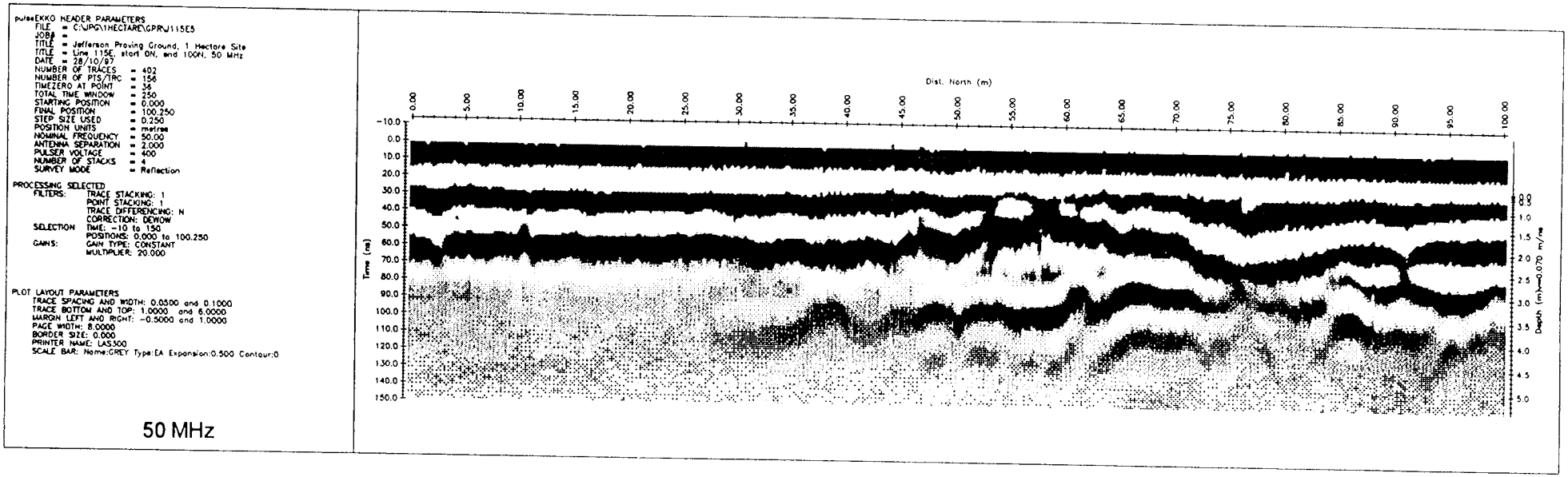

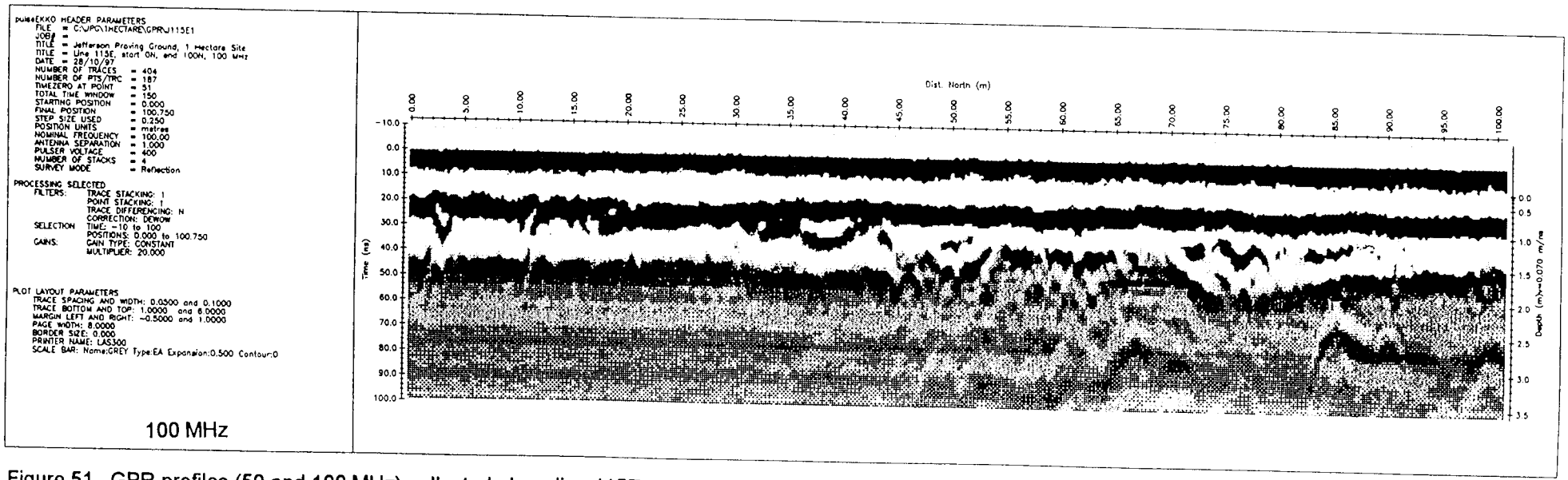

Figure 51. GPR profiles (50 and 100 MHz) collected along line 115E, 1-ha site, JPG

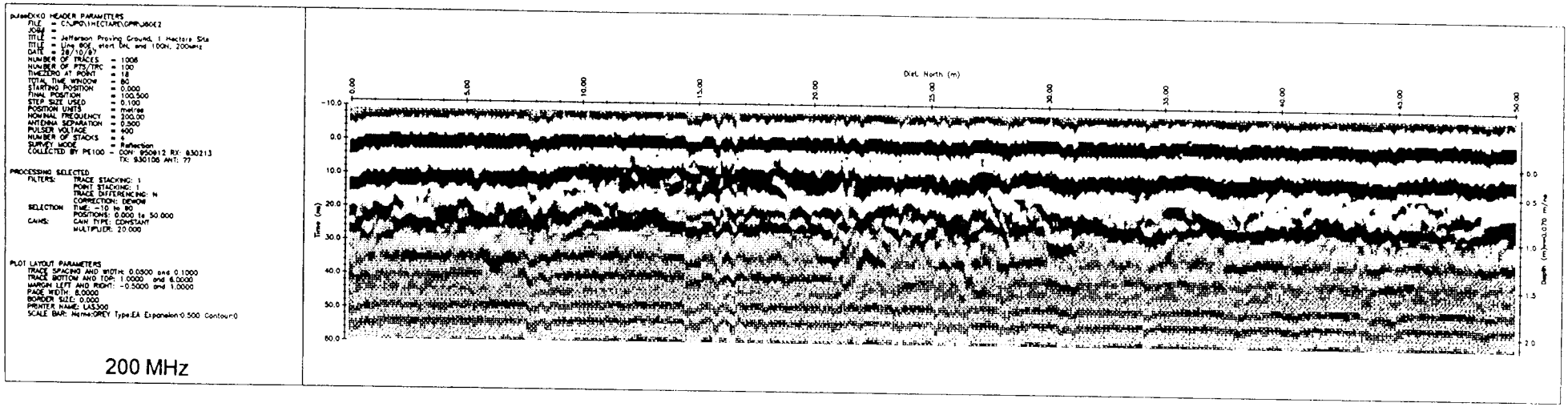

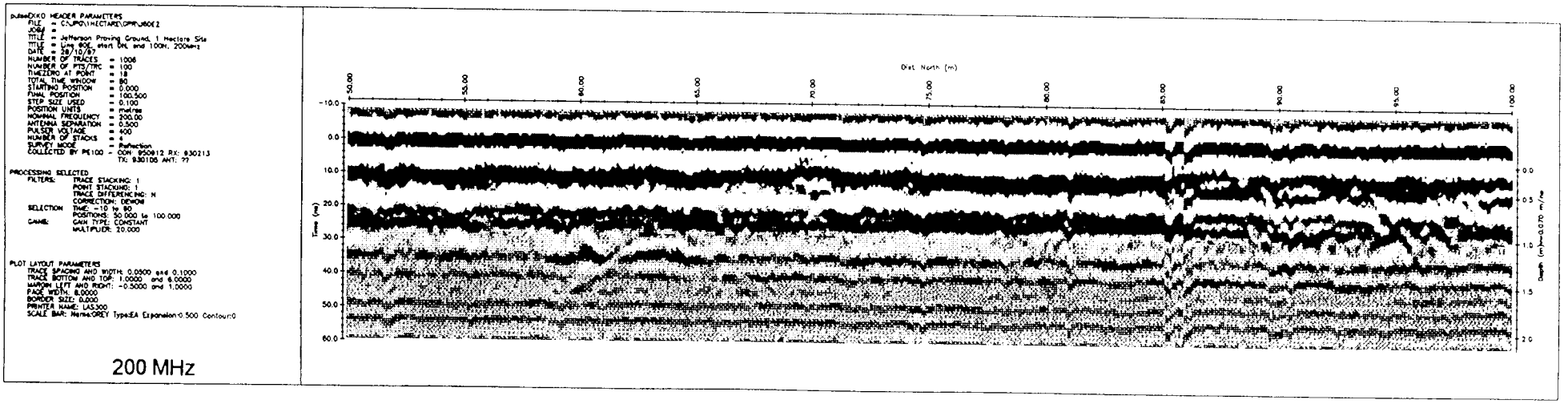

Figure 52. 200 MHz GPR profile collected along line 60E, 1-ha site, JPG

Table 20
Statistical Analysis of Conductivity Values for 1-Ha Sites (DARPA / JPG)

	Fort A. P. Hill, VA		Fort Carson, CO		Jefferson Proving Ground, IN
Statistical Parameter	**Firing Point 20**	**Firing Point 22**	**Seabee Site**	**Turkey Creek**	**1-Hectare Site**
Minimum (mS/m)	(-3.7)	(-20.5)	36.4	8.9	12.5
Maximum (mS/m)	20.9	15.1	91.6	43.7	25.4
Average (mS/m)	3.4	3.0	58.6	20.6	17.3
Variance $(mS/m)^2$	1.2	0.9	120.7	38.2	6.1
Standard deviation (mS/m)	1.1	0.9	11.0	6.2	2.5
Median (mS/m)	3.3	2.9	58.7	19.3	17.3
Mode (mS/m)	3.2	3.0	69.6	16.9	17.2

Table 21
Variation in Geophysical Background Measurements for 1-Ha Sites (DARPA / JPG)

	EM	Magnetometer	Electrical Resistivity			GPR	
	Conductivity (mS/m)	**Total Magnetic Field (nT)**	**Model Layers**	**Resistivity (Ω-m)**	**Depth to Half-space (m)**	**Prominent Reflectors**	**Maximum Depth of Investigation (m)**
Fort Carson							
Seabee	40–85	53,630–53,650	4	5–45	3–10	4	1.6
Turkey Creek	10–35	53,650–53,680	3	20–615	3–8	3	1.8
Fort A. P. Hill							
Firing Point 20	2–4	53,490–53,500	3–4	90–2,500	7–15	3	4
Firing Point 22	2–4	53,490–53,510	4	30–3,750	7–12	3	4
Jefferson Proving Ground							
1-Hectare Site	15–20	53,990–54,005	3–4	70–1300+	4.7–5.5	4	3.5

indicate an additional interface between 3 and 7 m depth. The high soil conductivity (40–85 mS/m) limited the GPR maximum depth of investigation to 1.6 m. Lower soil conductivity values are present in the central portion of the site and extend toward the southeast corner. The variability in soil conductivity is caused by changes in soil composition, mainly the amount of clay present, and moisture content. The EM and magnetometer data suggest a small, non-ferrous metallic object is buried at (113E, 77N) and a small, ferrous object is located at (5E, 8N).

Turkey Creek. Although soil conductivity (10–35 mS/m) is lower at Turkey Creek, the soil still was not favorable for collecting higher frequency (> 200 MHz) GPR data. However, three soil interfaces were identified at depths of 0.06, 0.3, and 1 m. The resistivity data suggest a deeper stratigraphic boundary between 3 and 4 m. Soil conductivity values decrease towards the east-northeast, which is likely caused by a reduction in clay content. Two small, non-ferrous metallic objects are thought to be buried at (73E, 64N) and (117E, 98N).

Fort A. P. Hill, Virginia

The soil at the two sites is characterized by very low electrical conductivity values (2–4 mS/m) which provided an excellent regime for performing GPR. However, the poor surface site conditions (holes, tire ruts, etc.) compromised the quality of the data. Strong reflections from as deep as 4 m were mapped with the lower GPR frequency. Both the electrical resistivity and GPR surveys identified distinct soil boundaries at similar depths within the upper 2 m of soil. Background total magnetic field readings varied 10–20 nT. The results of the geophysical surveys suggest that the sites have had considerable human activity.

Firing Point 20. Three subsurface boundaries were distinguishable at depths of 0.15, 1, and 2 m with the GPR and a deeper interface between 7 and 15 m depth was modeled based on the resistivity soundings. Three linear anomalies were coincident to the EM and magnetometer data ((20E, 65N–125E, 100N), (80E, 0N–115E, 85N), and (95E, 0N–120E, 85N)). No surface features were observed that would account for these anomalies, however some partially buried copper cables were found along the western portion of the site. These anomalies are probably a result of trenching activities associated with buried cables and/or other buried ferrous and non-ferrous metallic objects. One linear anomaly (0E, 80N–80E, 100N) was detected solely by the EM survey. A possible cause of this anomaly is soil disturbance generated by trenching and/or buried non-ferrous object(s). The northwestern and southwestern corners of the site appeared anomalous on both the EM and magnetic data plots; buried ferrous material could be present in these areas. Numerous small anomalies scattered across the site were evident in the EM data. Probable causes of these anomalies are small, shallow, non-ferrous objects.

Firing Point 22. There is some variation in the subsurface layer structure determined from the GPR and resistivity models. The GPR detects three continuous reflectors at depths of 0.1, 0.6, and 1.3 m, whereas the resistivity models also consist of four layers (including halfspace) but with interfaces at approximately 0.2, 2.7, and 7–12 m. A weak, linear anomaly (55E, 0N–85E, 80N) was detected by both the EM and magnetic surveys. There were no surface features which suggested a cause of the anomaly, but a backfilled trench containing small ferrous objects

could generate a similar response. Five prominent anomalies are present in both the EM and magnetic data: (15E, 75N), (25E, 5N), (72E, 100N), (120E, 15N), and (120E, 66N). The source of these anomalies is most likely shallow, ferrous objects. There were several small anomalies unique to either the EM or magnetometer data. Those anomalies present only in the EM data are probably caused by shallow, non-ferrous objects, whereas the magnetic anomalies are likely caused by shallow, ferrous objects.

JPG 1-hectare site

Analysis of the resistivity data suggests a three or four layer shallow earth model with a high-low-high resistivity pattern. The first layer is associated with a silt ranging in thickness from 0.2 to 0.8 m; the second layer a clay 4.2-5.2 m thick; and the lower-most layer limestone bedrock at a depth of 4.7-5.5 m. GPR profiles were collected using antenna frequencies of 50, 100 and 200 MHz. A maximum depth of investigation of 3.5 m was obtained with the 50 MHz antenna. The profiles showed relatively flat, continuous soil layers that extended across the site. An EM wave velocity of 0.7 m/ns was suitable for estimating depth of investigation. The near-surface soil has a background conductivity of 15-20 mS/m. Conductivity values increase across the site from north to south, with the most conductive region in the southeast corner. The magnetic data exhibit little variation over the site; a nominal background value is 54000 nT.

5 Summary

This report details the establishment and geophysical and geologic characterization of five 1-hectare UXO/landmine test sites: two at Fort Carson, Colorado, two at Fort A. P. Hill, Virginia, and one at Jefferson Proving Ground, Indiana. The purpose for characterizing the sites is to document them for comparison with other UXO/landmine test sites and to provide presite disturbance assessments of site heterogeneity (variability) and the presence of buried cultural features. General results of the site characterizations were made available to contractors for assessment and planning purposes prior to conducting the "backgrounds clutter data collection" geophysical surveys (initial contractor testing at Fort Carson and Fort A. P. Hill; contractor testing subsequent to Phase III TD at JPG).

The site selection objective was to achieve contrasting site conditions in terms of climate and soil types. Figure 1, in Chapter 1, indicates that selection of the four DARPA sites at two locations satisfies three of the four possibilities of the simple site classification scheme based on moist or dry climatic conditions and sand or clay soil type. The fourth possibility under this classification scheme is satisfied by the conditions at Jefferson Proving Ground, Indiana, location of the Congressionally-mandated UXO/landmine technology demonstrations. An indicator of the contrasting site conditions for the Fort Carson and Fort A. P. Hill sites is the soil conductivity values (summarized in Table 20, Chapter 4). The Seabee site has relatively high conductivity (40-85 mS/m), consistent with significant clay content in the soils, whereas the Turkey Creek site has a lower conductivity range (10-35 mS/m), consistent with a silty-sand with some clay content. The two sites at Fort A. P. Hill are virtually identical and have very low conductivity (2-4 mS/m), consistent with sandy soils with very low clay content.

In terms of geologic heterogeneity within each site, there are no indications of trends in the magnetic field across any of the sites (Figures 21, 27, 34, 40, 49). The geologic heterogeneity in bulk electrical conductivity of the upper 4 to 5 m of the sites can be assessed using Figures 20, 26, 33, 39 and 47. The conductivity maps for the Fort A. P. Hill sites show no site heterogeneity. In contrast, site heterogeneity is indicated in the conductivity maps for the Seabee and Turkey Creek sites at Fort Carson and in the JPG 1-ha site. The Seabee site does not have a systematic variation across the site, but is dominated by a low conductivity zone extending roughly from south to north that is surrounded by three large size, higher conductivity zones. The Turkey Creek site exhibits a systematic increase in conductivity from northeast to southwest across the site that is interrupted by a zone of higher conductivity in the southwest quadrant. At the JPG site, conductivity

values increase from north to south, with the exception in the northeast quadrant where conductivity values slightly lower than background are present.

The level of cultural background or clutter at the Fort Carson, Fort A. P. Hill, and JPG locations is dramatically different. At the Turkey Creek and Seabee sites (Fort Carson) and JPG site there are only one to two small, isolated anomalies which may indicate buried cultural features. For the Fort A. P. Hill sites, there are numerous small, isolated anomalous features, indicative of buried cultural features, as well as the linear anomalous features crossing the Firing Point 20 site (see Figures 32 through 34).

References

Altshuler, T. W., Andrews, A. M., Dugan, R. E., George, V., Mulqueen, M. P., and Sparrow, D. A. (1995). "Demonstrator performance at the unexploded ordnance technology demonstration at Jefferson Proving Ground (Phase I) and implications for UXO clearance," IDA Paper P-3114, Institute for Defense Analyses, Alexandria, VA.

Annan, A. P. (1992). *Ground penetrating radar workshop notes.* Sensors & Software, Inc., Mississauga, Ontario, Canada.

Baker, M. J. Inc. (1979). "Fort A. P. Hill, Virginia terrain analysis," Prepared for the Terrain Analysis Center, U.S. Army Engineer Topographic Laboratories, Fort Belvoir, VA.

Barrows, L., and Rocchio, J. E. (1990). "Magnetic surveying for buried metallic objects," *Ground Water Monitoring Review* 10(3), 204-11.

Bevan, B. W. (1983). "Electromagnetics for mapping buried earth features," *Journal of Field Archaeology* 10, 47-54.

Breiner, S. (1973). "Applications manual for portable magnetometers," Geometrics, Sunnyvale, CA.

Brown, G. S. (1990). "Clutter modeling for the real environment, What are the problems?," Proceedings of the Workshop on Detection, Discrimination, & Classification of Targets in Clutter, GACIAC PR 90-05, pp 271-275, GACIAC PR 90-05, IIT Research Institute, Chicago, IL.

Dobrin, M. B. (1976). *Introduction to geophysical prospecting.* 3rd ed., McGraw-Hill, New York.

Fenneman, N. M. (1938). *Physiography of the eastern United States.* McGraw-Hill, New York.

Geonics Limited (1984). "EM31 operating manual," Mississauga, Ontario, Canada.

George, V. (1996). "Backgrounds clutter data collection experiment test plan," Defense Advanced Research Projects Agency (unpublished, available by contacting Vivian George, "vgeorge@walcoff.com", Walcoff and Associates).

George, V. (1997). "The backgrounds clutter data collection experiment ," Defense Advanced Research Projects Agency (unpublished, available by contacting Vivian George, "vgeorge@walcoff.com", Walcoff and Associates).

Jenkins, E. D. (1964). "Ground water in Fountain and Jimmy Camp Valleys, El Paso County, Colorado," U.S. Geological Survey Water Supply Paper 1583, U.S. Government Printing Office, Washington.

Keller, G. V. and Frischknecht, F. C. (1982). *Electrical methods in geophysical prospecting.* Pergamon Press, New York.

Kreithen, D. D. and Crooks, S. M. (1990). "Improved clutter modeling and detection in high-resolution SAR imagery," Proceedings of the Workshop on Detection, Discrimination, & Classification of Targets in Clutter, GACIAC PR 90-05, pp 165-180, GACIAC, IIT Research Institute, Chicago, IL.

Leonard, G. J. (1984). "Assessment of water resources at Fort Carson Military Reservation near Colorado Springs, Colorado," U.S. Geological Survey Water Resources Investigations Report 83-4270, U.S. Government Printing Office, Washington.

Llopis, J. L. and Sharp, M. K. (1997). "A feasibility study on the use of water-borne ground penetrating radar to profile the bottom of the Kissimmee River, Florida," Draft Report, U.S. Army Engineer Waterways Experiment Station, Vicksburg, MS.

Llopis, J. L., Simms, J. E., Butler, D. K., Curtis, J. O., West, H. W., Arcone, S. A., and Yankielun, N. E. (1998). "Site characterization investigations in support of UXO technology demonstrations, Jefferson Proving Ground, Indiana," Technical Report GL-98-, U.S. Army Engineer Waterways Experiment Station, Vicksburg, MS.

McLaughlin, K. P. (1947). "Pennsylvanian stratigraphy of Colorado Springs Quadrangle", *Colorado Bulletin of the American Association of Petroleum Geologists* 31(11), 1936-1981.

Miller, C. A., Malone, C. R., and Blount, C. B. (1992). "Guide for the conduct of predeployment site characterization surveys for the AN/GSS-34 (V) Ported Coaxial Cable Sensor (PCCS)," Instruction Report EL-92-1, U.S. Army Engineer Waterways Experiment Station, Vicksburg, MS.

Mixon, R. B. and Newell, W. L. (1978). *The faulted coastal plain margin At Fredericksburg, Virginia.* Guidebook, Tenth Annual Virginia Geology Field Conference, 50 pages.

Onuschak, E. (1973). "Geologic studies, Coastal Plain of Virginia, Part Three: Pleistocene-Holocene environmental geology," Bulletin 83 (Part 3), Virginia Division of Mineral Resources, Charlottesville, Virginia, 106-153.

PRC Environmental Management, Inc. (1994). "Task 3: Preparation of demonstration site, Jefferson Proving Ground, Madison, Indiana."

——(1996). "Demonstration work plan, Phase III controlled site advanced technology demonstrations at Jefferson Proving Ground, Indiana."

Ray, L. L. (1974). "Geomorphology and Quaternary geology of the glaciated Ohio River Valley: A reconnaissance survey," U.S. Geological Survey, Professional Paper 826.

Schneider, A. F. (1966). *Natural features of Indiana*. "Physiography." Ed. Alton A. Lindsey, Indiana Academy of Science, Indianapolis, Indiana.

Simms, J. E. (1996). "Geophysical investigation at the Upatoi village archaeological site (9ME395), Fort Benning, Georgia," Draft Report, U.S. Army Engineer Waterways Experiment Station, Vicksburg, MS.

Simms, J. E., Butler, D. K., and Powers, M. H. (1995). "Full waveform inverse modeling of ground penetrating radar data: An initial approach," Miscellaneous Paper GL-95-4, U.S. Army Engineer Waterways Experiment Station, Vicksburg, MS.

Soil Conservation Service. (1981). "Soil survey of El Paso County Area, Colorado," U.S. Government Printing Office, Washington, 212 pages.

Sparrow, D. A., Andrews, A. M., and Dugan, R. E. (1995). "Evaluation of individual demonstrator performance at the unexploded advanced technology demonstration program at Jefferson Proving Ground (Phase I)," SFIM-AEC-ET-CR-95033, U.S. Army Environmental Center, Aberdeen Proving Ground, MD.

Telford, W. M., Geldhart, L. P., Sheriff, R. E., and Keys, D. A. (1973). *Applied geophysics*. Cambridge University Press, New York.

Ward, L. K. (1985). "Stratigraphy and characteristics mollusks of the Pamunkey Group (Lower Tertiary) and the Old Church Formation of the Chesapeake Group-Virginia Coastal Plain," U.S. Geological Survey Professional Paper 1346, U.S. Government Printing Office, Washington, 78 pages.

Wentworth, C. K. (1930). "Sand and gravel resources of the Coastal Plain of Virginia," Bulletin 32, Virginia Geological Survey. Charlottesville, 146 pages.